MODELING OF ENGINE-OUT HC EMISSIONS FOR PROTOTYPE PRODUCTION

by

Douglas A. Hamrin

B.S. Mechanical Engineering
Illinois Institute of Technology
(1992)

Submitted to the Department of Mechanical Engineering
in Partial Fulfillment of the Requirements
for the Degree of

MASTER OF SCIENCE IN MECHANICAL ENGINEERING

at the

MASSACHUSETTS INSTITUTE OF TECHNOLOGY

August, 1994

© Massachusetts Institute of Technology
All rights reserved

Signature of Author _____
Department of Mechanical Engineering
August 5, 1994

Certified by _____
John B. Heywood
Professor, Department of Mechanical Engineering
Thesis Advisor

Accepted by _____
Ain A. Sonin
Chairman, Department Graduate Committee

MASSACHUSETTS INSTITUTE
OF TECHNOLOGY

OCT 24 1994

LIBRARIES

ARCHIVES

MODELING OF ENGINE-OUT HC EMISSIONS FOR PROTOTYPE PRODUCTION ENGINES

by

Douglas A. Hamrin

Submitted to the Department of Mechanical Engineering on August 5, 1994
in partial fulfillment of the requirements for the Degree of
Master of Science in Mechanical Engineering

ABSTRACT

A model was developed to predict engine-out hydrocarbon emissions for spark-ignition engines. The model consists of a set of scaling laws that address the individual processes that contribute to HC emissions, whose independent variables are the critical engine design variables. Detailed models of the individual processes involved were used to parameterize the overall sequence of the processes through scaling relations and data fitting. The model was calibrated using production spark-ignition engine data at a fixed light load operating point. The data base consisted of two-valve and four-valve engine designs with variations in spark timing, valve timing, coolant temperature, crevice volume, and EGR. The results include engine-out HC emissions data for five different engines.

The hydrocarbon model provides insight into the individual phenomena involved in the total HC mechanism and how each individual process is affected by model inputs. The model results showed that the fuel sources (oil layers, deposits, and liquid fuel) and fuel-air sources (crevices, quench layers, and exhaust valve leakage) contributed approximately the same amount to the engine-out HC emissions. Typical in-cylinder oxidation levels were 68% (for fuel-air sources), with a retention in the cylinder of 22% of the HC and with exhaust port oxidation of 35%. The model predicted that the fuel source contribution to the engine-out HC emissions was most affected by changes in coolant temperature, compression ratio, EGR, and spark timing, whereas the contribution from the fuel-air sources was effected most by crevice volume, spark timing and compression ratio, and slightly by EGR, valve overlap and coolant temperature. The model was calibrated separately for three different engines to accommodate differences in engine design details and to determine the relative magnitudes of each of the major sources. The model was used to determine the magnitude of individual parameter changes that produced a 10% decrease in HC emissions.

Thesis Advisor:
John B. Heywood
Professor, Department of Mechanical Engineerings

ACKNOWLEDGMENTS

Throughout my brief time here at MIT many people have influenced my development as a student and as a person. I would like to thank the people who have influenced, guided, loved, helped, supported and made life enjoyable for me.

Without my family I would not be the person I am today. I would like to thank my parents, Wayne and Nancy Hamrin, for their love, support and encouragement through my entire life. Without them this would never have been possible. Also, I would like to thank my brothers Donn and Dave, and my sister Dawn for being there for me when I needed them.

Many people have helped guide this research. I would like to thank John Heywood for his guidance and technical expertise, which provided an excellent learning experience here at MIT. I will never forget his advice or comments. Many people in the lab provided useful insight for this research. I would like to thank Mike Norris, Kyoungdoug Min, and Jan-Roger Linna. I would like to thank Chrysler Corporation through MIT's Leaders for Manufacturing Program for funding this research and providing the necessary data needed to make it possible. I would like to thank Tom Asmus and Doug Wilmot for their help when I was working at Chrysler. Finally, I would like to thank Tom Milson, "computer genius"; without his suggestions and help I would have went crazy trying to extract the data from their computers.

During the years before and during my college career a few people have guided my future collegiate studies. Ms. Grandoine (arrogant high school teacher) told me, "You will never make it in college as an engineering student." It's good that I at least tried it out. Thank your for your advice. (NOT!) On a better note, I would like to sincerely thank Kevin Seidel for his "constant" guidance and advice regarding my college studies, without him I would not have had the career opportunities I have now. I would also like to thank all the faculty in the Mechanical Engineering Department at Illinois Institute of Technology who provided the engineering foundation I needed for my future. Never forget your roots.

I have had many memorable times during the last few years. Thanks to my officemates Sang-Myeong Han, Younggy Shin, Haissam Haidar (solitaire partner), Deayup Lee, and Mike Sampson. Thanks also to Pete Hinze, Gatis Bazbauers, Wolf Bauer, Goro Tamain, Tian Tian, Mike Norris, Janice Dearlove etc. for all the good times. Also thanks to Eric Deutsch and John Fox, the few crazy people in the lab who put life in perspective. I would also like to thank Michelle Hsu for her constant encouragement and being there when I needed her. Thanks also to Jim Nowicki, Bill Grassmyer, Kurt Roth, Brian Ippolitto, and Steve Cimaszewski for all the good times. I would also like to thank my friends from Chicago who where always there to hang out with: Jim Suttle, Mike Jelaca, Dave Larson, Mike Francis, and Todd Breadar. Finally, I would like to thank my friend Jim Shields, who always was there to keep my ego in check.

"meow meow" said the cat

DUG

TABLE OF CONTENTS

LIST OF TABLES

LIST OF FIGURES

CHAPTER 1: INTRODUCTION

1.1 Background

Since 1970 when the Clean Air Act was passed, automobile emissions regulations are become increasingly stringent. The hydrocarbon (HC) emission levels are scheduled to decrease further by approximately a factor of ten during the next 10 years. The current Federal HC emissions standard is 0.41 g/mile and will be reduced in California to 0.04 g/mile in 1998. Because of this legislation, reducing hydrocarbon emissions in spark-ignited engines has been a major subject of scientific research in both automobile companies and universities for several years.

The sources of hydrocarbon emissions in spark-ignited engines are well known. However, due to the complexity of the physics and chemistry governing several of the processes, the behavior of these sources is not well understood. These HC sources allow either just fuel or fuel-air mixture to escape the normal combustion process. The sources mechanisms of HC emissions are: 1) crevices 2) oil layers, 3) deposits, 4) quench layers, 5) liquid fuel, and 6) exhaust valve leakage. After escaping the combustion process, a fraction of these HC can be oxidized in the cylinder during the expansion and exhaust strokes, retained in the cylinder with the residual gases, or oxidized in the exhaust port, leaving the engine-out (before catalyst) HC emissions.

Two approaches have been used to develop an understanding of the physics involved in the mechanisms that contribute to hydrocarbon emissions: experimental studies and computer modeling. Experimental studies are very useful if they are properly

designed to isolate an individual phenomenon. In addition, computer models have been developed using the governing differential equations, but they currently require many assumptions that can limit their usefulness. Before developing a complex computer model, an alternative model can be developed that involves physically based scaling laws or relationships. Such models are developed using a framework structured to address the physics involved. Once scaling laws are complete, they are calibrated using real data. These types of models have been developed in the past to address such phenomena as residual gas fraction and spark-ignition engine friction [2][7]. The models are useful because they force the right questions to be asked to gain completeness. They also produce quantitative output that can lead to interesting trends and possibly guide future research.

1.2 Objective

The objective of this thesis is to develop a model using physically based scaling laws to predict engine-out (before catalyst) HC emissions. This will be accomplished by first developing a framework that outlines the processes and sources. Next, scaling laws will be developed for the major individual sources and mechanisms to combine into the framework. Finally, the model will be calibrated using real engine data including variations of crevice volumes, camshafts, compression ratios, and spark timings.

CHAPTER 2: HYDROCARBON MECHANISMS

This chapter discusses the spark-ignition engine HC emissions processes. The total process is separated into two sequential stages. First, there are several mechanisms which prevent a fraction of the HC inducted into the cylinder from burning during the normal combustion process of each cycle. These source mechanisms are summarized in Table 2.1. Second, to become part of the engine-out hydrocarbon emissions, the fuel that escaped the normal combustion process must remain unburned during the expansion and exhaust stroke, must exit the cylinder, and must remain unburned in the exhaust port and manifold. The sequence of these processes is illustrated in Figure 2.1.

Table 2.1 Summary of sources mechanisms that store fuel during the normal combustion process.

1. Crevices
2. Oil Layers
3. Bulk gas quenching
4. Deposits
5. Liquid fuel in the cylinder
6. Exhaust valve leakage

2.1 Sources of Unburned Hydrocarbons

2.1.1 Crevices

Hydrocarbons can escape the normal combustion process by flowing into crevice regions as the gas pressure in the cylinder rises during the compression and combustion processes. Figure 2.2 illustrates the crevices that are present in most spark-ignition

engines. A recent study indicates that crevice source hydrocarbons contribute to approximately 38% of the total engine-out HC emissions [1].

As the in-cylinder pressure rises, gases are compressed into the crevices until the maximum cylinder pressure is reached. Then, during the expansion and exhaust stroke, the pressure decreases and the gases expand and exit the crevices. The total crevice volume is typically 1-2 % of the clearance volume depending on the geometric details and component temperatures.

The gases that flow into the crevice are a combination of the following: unburned gas (fuel vapor, air and residual gas, and exhaust gas recirculation (EGR) if used), and burned gas. The fraction of each gas in the mixture is dependent on the location of the crevice relative to the flame during combustion. If the flame reaches a crevice region before the maximum pressure, burned gases will then flow into the crevice. The flame geometry primarily depends on the spark plug location. Namazian et al. [4] showed that for a circumferentially located plug, 60% of crevice gases were burned gases at maximum cylinder pressure, as opposed to a centrally located plug in which the flow into the headland crevice is essentially all unburned mixture. As for the other crevices such as the valve seat crevice and spark plug crevice, previous studies with a two-valve engine having an offset spark plug estimated the fraction of unburned gases in these crevices to be 33% and 50%, respectively.

The flows between the piston ring crevices are more complex because of substantial pressure differences across the rings for much of the engine cycle. The maximum mass trapped between the top two rings is about one-fifth of the maximum mass in the volume above and behind the top ring. During the engine cycle blow-by occurs, where a fraction of the gas flows past the piston ring, through the crevices, and down into the crankcase [4]. Blowby is small (about 1%)

The total mass in the crevice is dependent upon the crevice volume and density of the gas in the crevices. The pressure in the crevice region is usually assumed to be equal

to the in-cylinder pressure (except for the regions below the top ring). On the other hand, the temperature of the gases in the crevices is not equal to the in-cylinder gas temperature, because upon crevice entry they are rapidly cooled to close to crevice wall temperatures. For example, the temperature of the gases in the piston-ring-liner crevices depends on the temperature of the piston and of the liner, which changes with operating conditions, especially as the engine warms up from a cold start [21]. Also, as the engine warms-up, the crevice volumes decrease. For example, the piston expands as it warms up much more than the cylinder liner, so the piston crevice decreases in volume by an amount that depends on engine load.

2.1.2 Oil Layers

Lubricating oil is present on the cylinder liner to lubricate the piston rings and skirt, to reduce wear and friction. This oil layer, approximately a few microns thick, has the capability to absorb HC during the compression and combustion processes, and desorb HC during the expansion and exhaust processes. Thus the oil layer on the liner also contributes to HC emissions. In recent studies it was estimated that 10-25% of the engine-out HC emissions is contributed from oil layer absorption and desorption [1],[8]-[12].

The oil layer absorption and desorption of HC is governed by convection and diffusion, and Henry's Law is believed to control the oil and gas equilibrium at the interface. Henry's Law is a relationship between the partial pressure of the vapor component (p_f), the absorbed mole fraction of that component (x_f), and Henry's constant (H):

$$x_f = p_f/H$$

Experimental results show that Henry's constant exhibits an exponential relationship with oil temperature. Figure 2.3 illustrates that Henry's constant is very sensitive to the oil layer temperature.

Vapor absorption varies with temperature and pressure. The amount of vapor absorbed into the oil is significantly higher at lower oil temperatures and at higher gas pressures, which influences Henry's constant and each component's partial pressure, respectively. The temperature of the oil layer is essentially that of the cylinder liner temperature, which remains relatively constant during steady state engine operations. However, the cylinder liner temperature increases with increasing load, thus affecting the temperature of the oil layer.

Throughout the operating cycle in a spark-ignited engine, the oil layer is exposed to changes in pressure and temperature. During the intake stroke the oil layer is exposed to low temperatures and pressures relative to the rest of the cycle; thus little fuel is absorbed into the oil layer. During the compression stroke, the gas temperatures and pressures are increasing and the oil layer is covered by a portion of the piston. The exposed portion of the oil layer will absorb HC. Likewise, during the combustion process when temperatures and pressures are increasing rapidly, HC continue absorbing into the oil layer (possibly reaching a saturation limit) until the flame reaches the layer. After the HC have entered the oil layer they diffuse throughout the oil layer.

During the expansion and exhaust strokes the piston uncovers the oil layer, exposing it to decreasing temperatures and pressure and an almost zero concentration of HC in the burned gases. Thus, the hydrocarbons are desorbed out of the oil layer and diffuse into the cylinder gases. If they do not oxidize and they exit the cylinder, they will contribute to the unburned hydrocarbon emissions.

2.2.3 Liquid Fuel in the Cylinder

Liquid fuel in the cylinder also affects HC emissions. A recent study indicates that even in a warmed-up engine, liquid fuel contributes to 20% of engine-out HC emissions [1]. The amount of liquid fuel in the cylinder depends on injector type, injection strategy, and component temperatures.

Fuel is usually injected onto the intake valve and port walls, where a small amount of it evaporates before the valve opens. Upon intake valve opening, the rapid back flow of burned gases vaporizes much of the liquid fuel in the port [22]. However, the remaining liquid fuel entering the cylinder may either burn and become part of the combustion gases or escape the normal combustion process by entering deposits, oil layers, or crevices. When the fuel is injected onto the backside of an open valve, a larger amount of liquid fuel enters the cylinder and more liquid fuel is available to store in the sources, thus increasing hydrocarbon emissions. The fuel preparation procedure also can affect the amount of liquid fuel in the cylinder. Recent studies have compared the steady-state engine-out HC emissions of two types of fuel preparation systems: a conventional injector and a pre-vaporized gasoline injector. The results showed a 10-25% decrease in HC emissions for the pre-vaporized gasoline injector[10][6].

The liquid fuel effect is especially significant during start up. Boam et al. studied this phenomenon and found that for an engine starting at 20°C, only 20% of the metered fuel evaporated before reaching the inlet valve[10].

2.2.4 Flame Quenching

Flame quenching occurs when the flame which propagates across the cylinder is quenched on the cooled combustion chamber walls, leaving a layer of unburned mixture adjacent to the wall. After combustion, during the expansion stroke this layer rapidly diffuses into the burned gases and a large portion of layer is oxidized (during most operating conditions) [14]. The flame quenching effect can be significant when operating at lean conditions and dilute mixture conditions (with EGR). Recent studies indicate that about 5% of HC emissions is contributed by flame quenching [1].

2.2.5 Deposits

During normal engine operations deposits can build up over extended mileage. Deposits form on the intake valves, piston crown, and cylinder head. They are believed to absorb and desorb fuel components, with the amount depending on the operating conditions. When deposits are present on the backside of the intake valves, the injected fuel is absorbed into the deposits. This results in a lean charge in the cylinder during engine transients. Intake valve deposits do not significantly affect steady-state HC emissions. However, deposits on the piston crown and cylinder head can have an effect on HC emissions. During the compression and combustion process fuel can be absorbed in the deposits. In this way, the fuel escapes the normal combustion process and later desorbs during the expansion and exhaust stroke. Valtadoros et. al showed that in-cylinder deposits can increase HC emissions by 50-100% [15]. A recent study has estimated that 16% of the total HC emissions is contributed by deposit effects [1].

2.2.6 Exhaust Valve Leakage

As described in Table 2.1 exhaust valve leakage can contribute to unburned hydrocarbon emissions, when unburned mixture leaks through the valve seat into the exhaust port. Recent experiments with fast-response flame ionization HC detectors in the exhaust port of engines have shown that HC concentrations do increase periodically in the port while the valve is closed. Even though this phenomena is estimated to be small contribution (less than 7% of total HC emissions), it should not be neglected [23]. Exhaust valve leakage may have a larger effect on HC emission in poorly maintained older engines.

2.2 Oxidation and Retention in the Cylinder

After the end of the normal combustion process, the unburned HC that escaped burning can exit the regions where they have been stored and may either oxidize within

the cylinder, be retained in the residual gases, or be oxidized within the exhaust port and manifold. Each of these three mechanisms reduces the amount of unburned HC emitted by the engine.

2.2.1 In-Cylinder Oxidation

As described in Figure 2.1, after the combustion process ends the HC that escaped burning can oxidize in the hot burned gases. During the expansion and exhaust stroke, the bulk gas temperatures are high enough to oxidize HC provided enough oxygen is present and the HC diffuse into and mix with the hot burned gases. Because of the (short) time available in the cylinder, HC oxidation is not likely to occur at temperatures below 1000 K. [17]. After the exhaust valve opens, the blowdown process begins, in-cylinder gas pressures and temperatures decrease, and the in-cylinder oxidation is slowed down significantly [16].

Two different types of sources must be considered: sources that produce fuel-air mixture, and sources that produce fuel alone. Crevices and flame quenching represent fuel-air sources because they introduce unburned fuel-air mixture into the hot cylinder gases. This type of source has enough oxygen to burn up the HC. On the other hand, deposits, oil layers, and liquid fuel effects are fuel sources because they introduce only unburned fuel into the hot cylinder gases. This type of source is separated from the oxygen that was initially mixed with the fuel vapor. For this reason, the fuel sources are believed to oxidize significantly less than the fuel-air sources. The fraction oxidized in-cylinder also depends on the rate at which HC exit the source mechanisms, the time at which mixing with the burned gases occurs during the expansion and exhaust strokes, and the location of source within the cylinder. Recent studies have estimated that approximately two-thirds of the fuel/air sources HC oxidize and approximately one-third for the fuel sources [1].

2.2.2 HC Retention

The HC that survive in-cylinder oxidation can either be exhausted with exhaust gases or remain in the cylinder with the residual gases to become part of the cylinder charge in the next cycle. During the exhaust stroke, the piston is known to roll up the gases along the liner, forming a vortex [18]. The vortex presumably contains a large fraction of HC remaining from the piston crevice and oil layer. From geometric considerations, a fraction of HC is retained in the residual gases. Recent studies estimated for a typical load (1500 rpm, IMEP = 3.8 bar) one-third of the unoxidized HC are retained [1].

2.2.3 Exhaust Port Oxidation

With a warmed-up engine, the HC remaining in the exhaust gases can oxidize in the exhaust-port and to some extent in the manifold. During the exhaust process there is intense mixing and temperatures are high enough for some gaseous-phase HC to oxidize. Analytic and experimental studies show that for stoichiometric operation at part load about one-third of the HC will oxidize in the exhaust port and manifold [19][20].

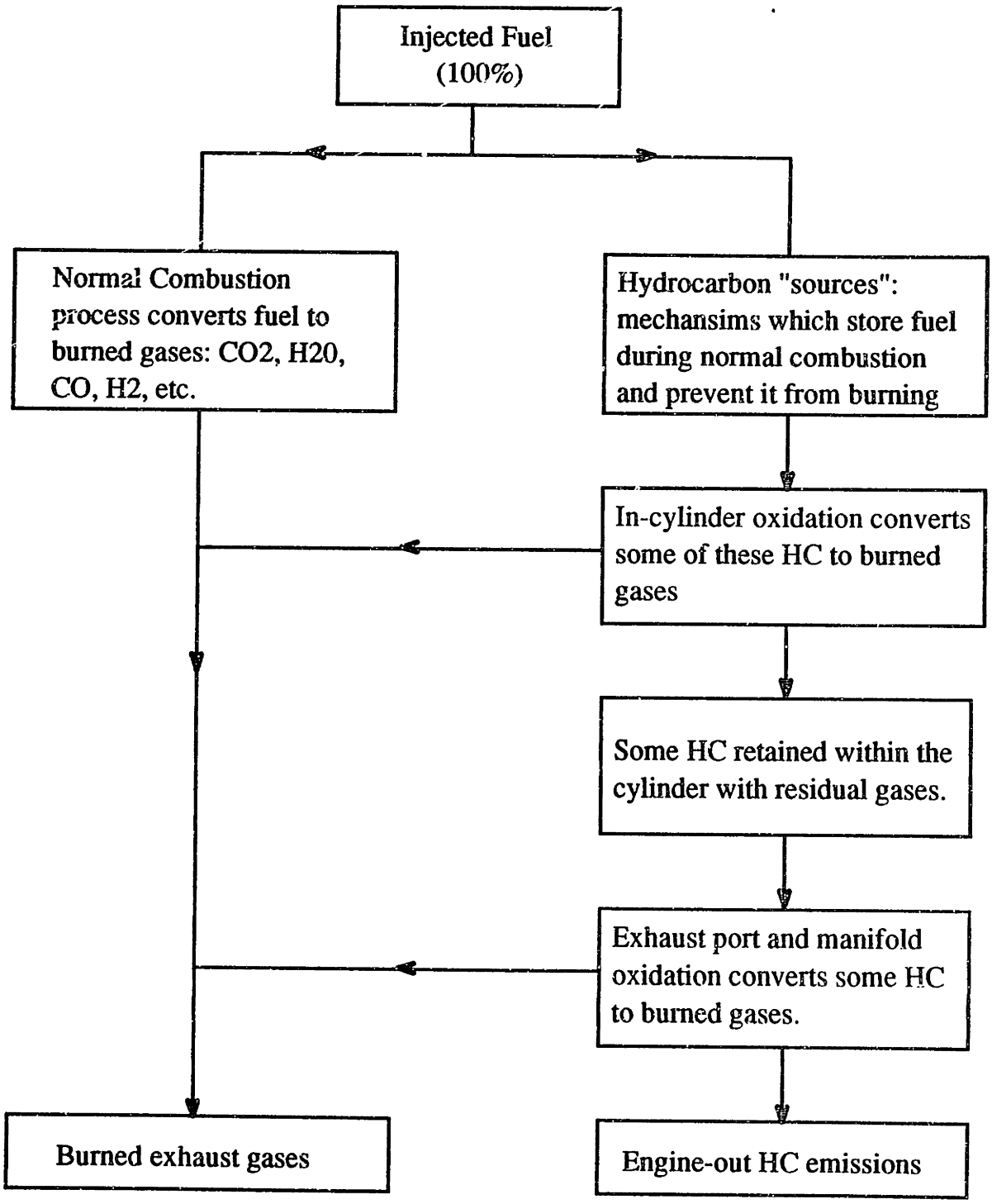

Figure 2.1 Schematic flow chart for the fuel which enters each cylinder each cycle.

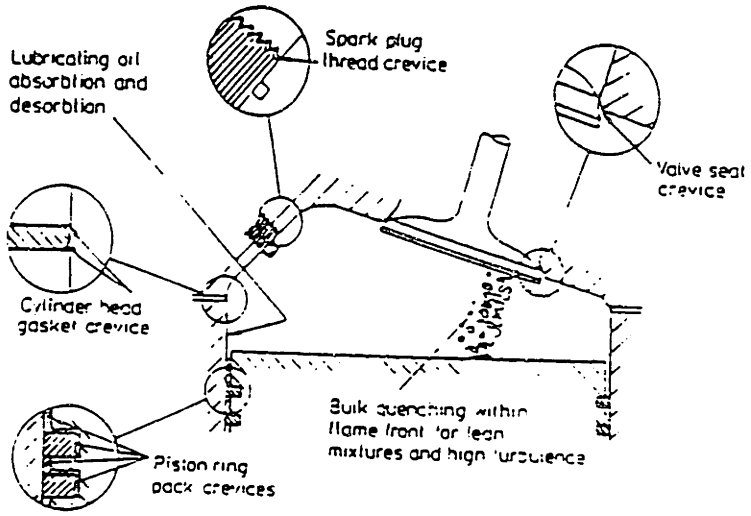

Figure 2.2 Schematic showing the different crevice volumes present in a typical spark-ignition engine.

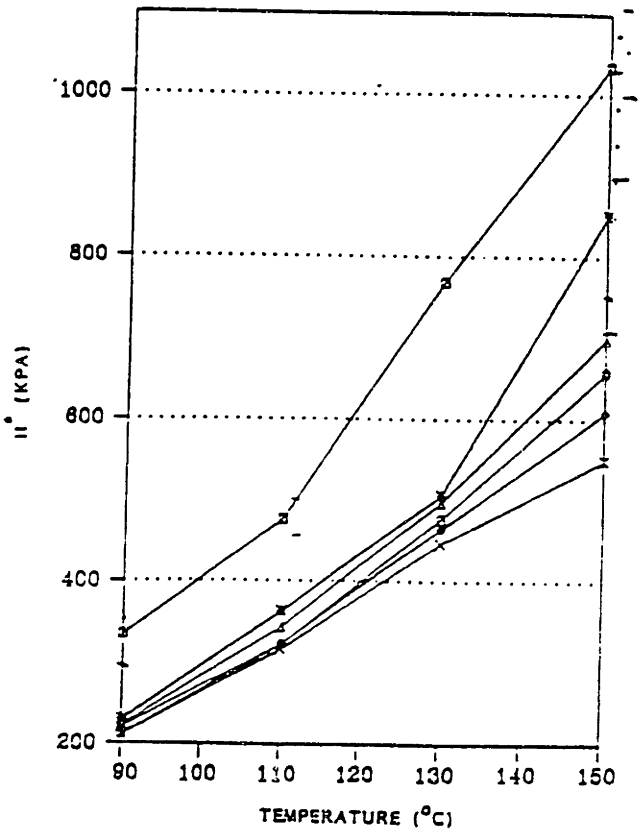

Figure 2.3 Experimental Data of Henry's Constant as a function of oil temperature for different lubricating oils [12].

CHAPTER 3: MODEL DEVELOPMENT

This chapter develops the framework used to connect together the mechanisms involved with spark-ignition engine-out hydrocarbon emissions. Also, physically based scaling laws will be developed for each major individual mechanism for the following operating conditions:

Speed = 1600 rpm Bmep = 241 kPa (35 psi)

This operating condition represents a large fraction of the Federal Test Procedure emissions testing.

3.1 Model Structure

The overall HC emissions process, as illustrated in Figure 2.1 and discussed in chapter 2, can be broken down into the following stages: (i) the source of hydrocarbon mechanisms by which HC escape the normal combustion process; (ii) the fraction of hydrocarbons that oxidize within the cylinder; (iii) the fraction retained in the cylinder; (iv) the fraction oxidized in the exhaust port and manifold. The combination of the above processes can be expressed in the following form:

$$HC_{engine-out} = \sum_i S_{HC,i}(1-f_{oxi\ cyl,i})(1-f_{ret\ cyl,i})(1-f_{oxi\ exh,i}) \qquad (1)$$

where,

$S_{HC,i}$ = individual hydrocarbon sources

$f_{oxi\ cyl,i}$ = fraction of sources i oxidized within the cylinder

$f_{ret\ cyl,i}$ = fraction of sources i retained in the cylinder

$f_{oxi\ exh,i}$ = fraction of sources i oxidized in the exhaust

3.2 Hydrocarbon Source Mechanism Model

The source mechanisms define the amount of hydrocarbons that do not burn during the normal combustion process. As described in Chapter 2, hydrocarbons escape combustion in the crevices, quench layers, exhaust valve leakage, deposits, liquid fuel, and the oil layer. Depending on the behavior of each source, either a mixture of fuel, air, residual gas, and burned gas, or just fuel is allowed to escape the normal combustion process. The source mechanism model was divided into two categories: fuel sources and fuel/air sources. Table 3.1 summarizes the sources and the corresponding category. Each source mechanism model will be described in detail in the following sections.

Table 3.1 Composition Separation of Hydrocarbon Sources

Fuel and Air Sources	Fuel Sources
Crevices	Oil Layers
Quench Layers	Deposits
Exhaust Valve Leakage	Liquid Fuel

3.2.1 Fuel-Air Source Mechanism Model

The fuel/air source model represents the crevices, quench layers, and exhaust valve leakage. The crevice source mechanism was chosen to represent this class of sources because, of the three sources, crevices are the largest contributor. Recent studies indicate the contribution to the unburned HC emission in a warmed up engine for each fuel/air source is as follows: 38% crevices, 5% quench layers, and 5% exhaust valve leakage [1]. The crevice source behavior has been successfully studied using both experiments and computer models and a good understanding of the physics involved has been developed. However, the physics governing the quench layers and the exhaust valve leakage is poorly understood.

To model the amount of hydrocarbons escaping combustion in the crevices, a scaling law was developed using: 1) the Ideal Gas Law, 2) the fuel-to-air ratio, and 3) the exhaust gas recirculation (EGR) and residual gas fractions. The development of each term will be discussed in the following paragraphs.

As described earlier, fuel/air mixture, residual gas, and EGR and to some extent burned gases flow into the headland crevice, valve seat crevice, head gasket crevice, and spark plug crevices during the compression and combustion process. The gas flow behavior into each crevice is different. The gases that flow into the head gasket crevice volume may or may not burn depending on the width of the entrance. If the entrance is larger than a certain size the flame can propagate into it, thus burning the hydrocarbons inside. The valve seat crevice volume is typically 5% of the headland crevice volume, and represents a small fraction of the engine-out hydrocarbon emissions. Therefore, it was neglected as a separate crevice. Similarly, the spark plug crevice was neglected because of its small size relative to total crevice volume. On the other hand, the headland crevice volume represents a large fraction of the total crevice volume. The gas flow behavior into the headland crevice volume is well understood; it therefore was chosen to represent the total crevice volume in this model.

The gas in the crevice was assumed to behave as an ideal gas. Solving the ideal gas law for the mass of gas in the crevice:

$$m_{gas} = \frac{p \cdot V_{crev} \cdot MW}{R \cdot T} \qquad (2)$$

where,

m_{gas} = mass of crevice gas

p = pressure

V_{crev} = crevice volume per cylinder

T = crevice gas temperature

R = Universal Gas constant

MW = molecular weight of crevice gas

The gas in the crevice is assumed to have cooled to near the crevice wall temperatures. For a typical part load-operating condition (1600 rpm, p_i = 0.4 atm), the crevice wall temperatures are lower than bulk gas temperatures during the majority of the engine cycle: the piston temperature is ~ 400 K, the cylinder wall temperatures ~ 360 K, and bulk gas temperatures range from ~400 K to ~2500 K [6]. The temperature of the crevice walls is influenced by speed, load and coolant temperature. Since this model was developed for only one speed and load, the temperature of the headland crevice walls was assumed to scale with the coolant temperature.

$$T_{crev} \propto T_{cool} \tag{3}$$

This assumption may need to be modified if other engine operating conditions are incorporated into the model.

Next, the maximum pressure of the gas in the crevice must be estimated. The maximum in-cylinder pressure was modeled as a function of indicated mean effective pressure (IMEP) at maximum brake torque (MBT) spark timing. Constant IMEP spark sweeps with a speed of 1600 rpm were performed using the MIT Cycle simulation for a typical production engine geometry. MBT was defined at the point of minimum fuel consumption. A least squares regression technique was used to fit the data illustrated in Figure 3.1. The relationship obtained is:

$$p_{max}(atm) = 1.2276 + 0.0568\ IMEP(kPa) \tag{4}$$

Correction equations have also been developed for spark timings other than MBT, coolant temperature variations, and compression ratio variations. See Appendix A for details.

The headland crevice volume was assumed to include the piston headland, and the volume above and behind the first ring. Figure 3.2 illustrates the headland crevice volume.

As discussed earlier, the gas mixture in the crevice is a combination of fuel/air mixture, residual gas, EGR, and burned mixture. The fraction of fuel/air mixture in the crevice was defined as:

$$f_1 = (1 - x_r - EGR) \tag{5}$$

where, x_r = residual gas fraction

EGR = exhaust gas recirculation fraction

The residual gas fraction (x_r) was estimated using a model developed by Fox [2]. This model will be discussed later when the residual HC model is developed. Next, a relationship for the fraction of fuel in the fuel and air mixture was derived as follows:

$$f_2 = \frac{1}{1 + A/F} \tag{6}$$

where, F = mass of fuel

A = mass of air

As previously discussed, the gas mixture in the headland crevice depends on the spark plug location. A typical two-valve engine has an off-center spark plug located, whereas, a four-valve engine has a centrally located spark plug. This geometric difference affects the amount of hydrocarbons flowing into the headland crevice region. The centrally located plug has practically all unburned mixture flowing into crevice. The offset spark plug has both burned and unburned mixture flowing into the headland crevice, because the flame arrives at a portion of the headland crevice before maximum pressure, thus allowing burned mixture to flow into the headland before maximum pressure is reached. Pervious studies compared the amount of unburned HC in the headland crevice for a centrally located spark plug and an edge located plug [4]. A normalized relationship relating spark plug location and engine bore was developed from these results:

$$f_{HC} = -0.429\left(\frac{2\ \text{Plug}}{B}\right) + 1.0 \tag{7}$$

where, Plug = spark plug position from bore center

B = bore

Figure 3.3 presents this relationship.

The previous relationships are now combined. The mass of fuel per cycle per cylinder is used to convert to an uHC emissions index. When unit conversions and constants are included, the following scaling law which relates the mass of the HC escaping combustion in the fuel-air source mechanisms is obtained:

$$S_{f\&a} = \frac{m_{HC,f\&a}}{m_f} = C \cdot 5443\left(\frac{p_{max}}{IMEP}\right)\left(\frac{V_{crev}}{V_d}\right)\left(\frac{1}{T_{cool}}\right)(1 - x_r - EGR) \times \left(\frac{1}{1+A/F}\right)\left(-0.429\left(\frac{2\,Plug}{B}\right)+1.0\right) \qquad (8)$$

where, m_f = mass of fuel per cylinder per cycle

V_d = displacement volume per cylinder

C = dimensionless constant of order unity

The fuel/air source mechanism scaling law assumes that the same amount of hydrocarbons flows in and out of the crevice volume; the blow-by phenomenon is neglected.

The hydrocarbon emissions are expressed as an emissions index, i.e. as a percentage of the amount of gasoline fuel that enters each cylinder during each cycle. The indicated fuel conversion efficiency was used to estimate the mass of fuel per cylinder per cycle. Combining this definition with the indicated mean effective pressure and then solving for mass of fuel:

$$m_f = \frac{IMEP \cdot V_d}{\eta_{f,i} \cdot Q_{HV}} \qquad (9)$$

where, m_f = mass of fuel per cylinder per cycle

IMEP = indicated mean effective pressure

V_d = displacement volume per cylinder

η_{fi} = indicated fuel conversion efficiency

Q_{HV} = heating valve of fuel

The indicated fuel conversion efficiency for a typical part load operating condition (1600 rpm, IMEP = 370 kPa) is approximately 0.35 [3]. The indicated fuel conversion efficiency and hence the mass of fuel per cycle changes with spark timing, compression ratio, EGR, and coolant temperature variations. A reference efficiency of 0.35 was used and correction equations were developed for these variations and are presented in Appendix A.

3.2.2 Fuel Source Hydrocarbon Mechanisms Model

The fuel source model represents oil layers, deposits, and liquid fuel. The oil layer source was chosen to represent the fuel source model because the liquid fuel effect is dependent on the injector type and injector strategy and is not well understood due the complexity involved. While, deposits have been a subject of recent research, their impact on HC emissions is poorly understood. Also deposits may behave analogously to oil films. As previously described, the oil layers absorb and desorb fuel during the operating cycle. Absorption and desorption are presumed to be functions of temperature, pressure, oil layer composition and thickness. Many modeling and experimental studies have recently been conducted which have led to an understanding of how the oil layer source impacts HC emissions.

As discussed earlier, the physics involved with oil layer absorption and desorption of fuel is governed by convection and diffusion, and Henry's law is believed to control the oil and fuel vapor equilibrium at the interface. The fuel source mechanism model was developed using a scaling law derived from Henry's law. The fuel source mechanism scaling relationship consists of two distinct terms derived from Henry's law: 1) a relationship for Henry's constant as a function of temperature, and 2) a relationship

for the partial pressure of fuel. The development of these terms will be discussed in the following paragraphs.

As described earlier, Henry's law is a relationship between the partial pressure of the fuel component (p_f), the absorbed mole fraction (x_f), and Henry's constant (H):

$$x_f = p_f / H \tag{10}$$

Expanding the partial pressure and the absorbed mole fraction from Henry's law and solving for the mass of hydrocarbons:

$$m_{HC} = p(F/A)\left(\frac{MW_{air}}{MW_{HC}}\right)\left(\frac{MW_{HC}}{MW_{oil}H}\right)m_{oil} \tag{11}$$

where,

m_{HC} = mass of hydrocarbons

F/A = fuel to air ratio

MW_i = molecular weight (air, hydrocarbons, and oil)

H = Henry's constant

p = total gas pressure in cylinder

m_{oil} = mass of oil layer

The mass of the oil on the cylinder liner over the entire stroke was estimated assuming a constant uniform oil layer thickness and a constant oil density:

$$m_{oil} = \rho_{oil}\pi\delta_{oil}BS \tag{12}$$

where,

ρ_{oil} = density of oil (~ 900 kg/m^3)

δ_{oil} = oil layer thickness (~ 3 μm)

B = engine bore

S = engine stroke

The partial pressure of hydrocarbons was assumed to be an average of the inlet pressure and the ideal maximum compression pressure defined by an isentropic compression relationship. The partial pressure is scaled as follows:

$$p \propto \frac{p_i + p_i r_c^{\gamma}}{2} \tag{13}$$

where, r_c = compression ratio

p_i = inlet pressure

A relationship was developed for the inlet pressure as a function of IMEP using the MIT cycle simulation. This is illustrated in Figure 3.4. The fitted correlation is given by:

$$p_i\,(\text{atm}) = 0.09875 + 0.00986\ \text{IMEP(kPa)} \qquad (14)$$

The inlet pressure also varies with changes in EGR, spark timing, coolant temperature, and compression ratio. Correction equations were incorporated into the model to adjust for such changes. See Appendix A for details.

Recent experiments were performed to quantify Henry's constant for different fuel in oil and oil combinations and they exhibited an exponential relationship with oil temperature. Figure 3.5 illustrates the relationship for a variable proportional to Henry's constant as a function of oil temperature in three different types of oil [12]. The data in Figure 3.5 was fitted and the slopes and intercepts were averaged resulting in the following relationship:

$$H^* \propto (10^{0.0082\,T_{oil}}) \qquad (15)$$

where $H^* = H(MW_{oil}/MW_{fuel})$

The oil temperature was assumed to be proportional to the coolant temperature at the operating condition of interest.

$$T_{oil} \propto T_{cool} \qquad (16)$$

Combining the previous equations, making the appropriate unit conversions, collecting the constants and dividing by the mass of fuel per cycle to convert to the HC emissions index results in the following scaling law for the fuel source mechanisms:

$$S_f = \frac{m_{HC,f}}{m_f} = C' \cdot 63024\left(\frac{1}{IMEP}\right)\left(\frac{F/A}{10^{0.0082\,T_{cool}}\,B}\right)\left(\frac{p_i + p_i r_c^{\gamma}}{2}\right) \qquad (17)$$

where C' = dimensionless constant of order unity.

The fuel source mechanism scaling law assumes uniform oil layer thickness, constant oil density, and the amount desorbed is proportional to the amount absorbed in equilibrium.

(note: the oil layer thickness, oil density, intercept for Henry's constant correlation, and other constants in the model do not affect the behavior of the model, because calibrating the model with a least squares regression will produce the same results regardless of the values of the constants.)

3.3 In-Cylinder Oxidation Hydrocarbon Model

When the hydrocarbons which have escaped the normal combustion process begin to exit the source regions, the burned gas temperature in the expansion stroke is high enough to oxidize a fraction of these hydrocarbons. The in-cylinder oxidation model was developed using recent model results of in-cylinder oxidation of headland crevice HC (a fuel-air source), because no detailed studies have addressed the fuel source in-cylinder oxidation.

Oxidation of HC exiting any crevice is dependent on the flow rate of gas out of the crevice, in-cylinder gas temperatures and pressures. Recent studies modeled the in-cylinder oxidation of headland crevice HC [5]. The results showed the following behavior which is presented in Figure 3.6. After combustion, as the expansion stroke begins all the exiting HC are completely oxidized. Then, a threshold is reached where there is a drastic reduction in the hydrocarbon oxidation at about 50 CA ATC, after which the oxidation steadily decreases. This threshold was used to structure the in-cylinder oxidation model in the form of a step threshold illustrated in Figure 3.7. The threshold location in the model (approx. 70 CA ATC for the data in Figure 3.6) represents the point at which 50% of exiting hydrocarbons remain unoxidized. The model assumes that the HC exiting the crevice before the threshold location oxidize completely; after the threshold, all the hydrocarbons remain unoxidized.

The threshold position is dependent on expansion stroke temperatures that can vary with changes in operating condition (i.e. spark timing). The in-cylinder oxidation model consists of scaling relationships to predict how the threshold moves. First, a

relationship was developed to determine the amount of gas remaining in the crevice regions at the threshold. This is given by the ratio of the pressure at the threshold to maximum cylinder pressure.

$$f_{HC,remaining} = \frac{p_{threshold}}{p_{max}} \tag{18}$$

where, $p_{threshold}$ = pressure at threshold location

p_{max} = maximum cylinder pressure

The pressure at the threshold is related to in-cylinder temperatures. However, in-cylinder oxidation is influenced by both the in-cylinder bulk gas temperatures and crevice wall temperatures, which are assumed to scale with coolant temperatures. Average temperatures were used to relate bulk gas and crevice wall temperatures as follows:

$$\bar{T} = \frac{T - T_{cool}}{\ln(T/T_{cool})} \tag{19}$$

where, $\bar{T}$ = log mean average temperature

The next task is to relate the pressure at the threshold location to the pressure and temperature at 70 CA ATC. A threshold temperature of 2100 K was taken from the in-cylinder bulk gas temperature at 70 CA ATC simulated by Min [5]. This temperature was averaged with the coolant temperature of 353 K used in the experiments performed by Min, resulting in an average threshold temperature of 980 K. This temperature is fixed but its timing in the expansion stroke varies with operating conditions such as spark timing, thus changing the threshold pressure. A scaling law was developed to shift the threshold by relating the temperature, pressure at 70 CA ATC and the threshold temperature to the threshold pressure. The scaling relationship assumed was:

$$p_{threshold} = p_{70\ CA\ ATC}\left(\frac{\bar{T}_{threshold}}{\bar{T}_{70\ CA\ ATC}}\right)^{n} \tag{20}$$

where, $p_{70\,CA\,ATC}$ = pressure at 70 crank angles ATC

$\overline{T}_{70\,CA\,ATC}$ = average temperature 70 crank angles ATC

$p_{threshold}$ = threshold pressure

$\overline{T}_{threshold}$ = average threshold temperature (980 K)

n = 3.0 (an empirically defined constant)

The exponent "n" was originally chosen to be 4.333 which would represent an isentropic expansion from the threshold temperature and pressure to the reference threshold temperature. However, when calibrating the model with such an exponent, the regression results were not consistent with the physics governing the entire hydrocarbon model structure (note: this will be discussed later in Chapter 4). 3.0 was chosen because it was the best fit to the physics. When calibrating the model with different values of "n", the behavior of the model changed. When increasing "n" from 3.0, the fuel-air sources HC predictions were reduced to levels which seemed unreasonable. In addition, when decreasing "n" from 3.0 the fuel sources HC predictions decreased.

The temperatures and pressures at 70 CA ATC were modeled as functions IMEP, EGR, spark timing relative to MBT compression ratio, and coolant temperature, using the MIT cycle simulation. Figure 3.8-3.10 illustrate the effects of these IMEP, EGR, and spark timing on these temperatures and pressures. The temperatures and pressures at 70 CA ATC as functions of IMEP are listed below:

$$p_{70\,CA\,ATC}\,(atm) = 0.209 + 0.0102\,IMEP\,(kPa) \qquad (21)$$

$$T_{70\,CA\,ATC}\,(K) = 1600 + 0.759\,IMEP\,(kPa) - 0.00051\,IMEP(kPa)^2 \qquad (22)$$

Normalized equations to adjust for changes in for spark timing, EGR compression ratio, and coolant temperature are used in the model and are presented in Appendix A.

Combining the previous equations results in the following relationship for the fraction of in-cylinder oxidation:

$$f_{oxi,cyl} = 1 - f_{HC,remaining} = 1 - \frac{p_{70\,CA\,ATC}}{p_{max}}\left(\frac{\overline{T}_{threshold}}{\overline{T}_{70\,CA\,ATC}}\right)^{3.0} \qquad (23)$$

3.4 Residual Hydrocarbon Model

The hydrocarbons remaining after the in-cylinder oxidation can either be exhausted out of the cylinder or be retained with the residual gases and participate in the next cycle. The fraction of hydrocarbons retained was assumed to be equal to the residual gas fraction. A residual gas model developed by Fox was used [2]. The model is based on the engine speed, valve overlap, inlet pressure, and fuel/air equivalence ratio. The model consists of two terms: First, an empirical expression for the overlap factor;

$$OF = \frac{1.45}{B}(107 + 7.8\Delta\Theta + \Delta\Theta^2)\frac{L_{v,max}D_v}{B^2} \qquad (24)$$

where, B = bore

$\Delta\Theta$ = valve overlap (valve event defined at 0.15 mm)

$L_{v,max}$ = average maximum valve lift (intake & exhaust)

D_v = average inner seat diameter (intake & exhaust)

Note: The overlap factor is multiplied by a factor of 2 for a four-valve engine. Second, an empirical expression for the residual gas fraction,

$$x_r = 1.266\frac{OF}{N}\left(\frac{p_i}{p_e}\right)^{-0.87}\sqrt{|p_e - p_i|} + 0.632\frac{\Phi(p_i/p_e)^{-0.74}}{r_c} \qquad (25)$$

where, p_i = inlet pressure

p_e = exhaust pressure

N = engine speed

r_c = compression ratio

Φ = fuel/air equivalence ratio

OF = overlap factor

Equations relating IMEP to inlet and exhaust pressure relationships were developed using the MIT cycle simulation. The equations are as follows:

$$p_i/p_e = (0.098745 + 0.000986\ IMEP)(0.016\ EGR + 1.00) \qquad (26)$$

$$\text{when } p_e = 1 \text{ atm}, \; p_e - p_i = 1 - p_i/p_e \tag{27}$$

Figure 3.11 illustrate this relationship. As discussed earlier, the inlet pressure varies with EGR, spark timing relative to MBT, compression ratio, and coolant temperature. Normalized relationships are presented in Appendix A.

3.5 Exhaust Hydrocarbon Oxidation Model.

The hydrocarbons that survive in-cylinder oxidation and exit the cylinder can be oxidized in the exhaust port and manifold. The mixing and oxidation processes that occur in the exhaust process are complex and are not completely understood. Previous studies have shown that exhaust hydrocarbon oxidation is dependent on the engine load, speed, coolant temperature and spark retard [20]. An empirical relationship was developed using the exhaust-port oxidation data from a typical two valve production engine. A least squares linear regression technique was used to fit the data to the above mentioned variables. The resulting relationship is given by,

$$f_{oxi,exh} = 0.866 - 0.0000148N - 0.0007IMEP - 0.00791Relsp - 0.0000255T_{cool} \tag{28}$$

This relationship was further modified to include the effects of EGR on exhaust port oxidation since EGR variations were not performed in the exhaust port oxidation experiments. As the EGR fraction increases, temperatures in the expansion stroke decrease which leads to reduced temperatures in the exhaust port. Previous studies performed cycle simulations to determine the effects of EGR and spark timing on exhaust gas temperature at a typical load condition (1400 rpm, BMEP = 325 kPa, and stiochometric operation). Figure 3.12 and Figure 3.13 present these relationships. Both sets of data were fit with respect to exhaust gas temperature. Then, the equations were set equal eliminating the exhaust gas temperature resulting in the following relationship:

$$Relsp_e = 0.829\frac{EGR\%}{100} \tag{29}$$

where, $Relsp_e$ = effective relative spark advance (spark -MBT) due to EGR

The effective relative spark advance should be added to the normal relative spark value to adjust for engine operation with EGR.

Also the flow speed in the exhaust port and manifold increases because the inlet pressure increases with increasing EGR fraction. This effect was included by multiplying the engine speed by the following factor to obtain an effective speed:

$$N_e = N\frac{EGR}{100} \tag{30}$$

where, N_e = effective increase in speed due to EGR

Next, compression ratio effects were incorporated into the exhaust oxidation model. As compression ratio increases the exhaust gas temperatures decrease because more energy is extracted from the combustion gases during the expansion stroke. Cycle simulations were performed to develop a relationship between exhaust gas temperature, compression ratio and spark advance. Figure 3.14 and Figure 3.15 presents the effects of compression ratio and spark advance on exhaust gas temperature. The spark advance data was fit linearly to the spark retard data points (negative spark timing). The compression ratio data was also fit linearly using a relative compression ratio of 9.0 because the data used to generate equation 28 was taken using this compression ratio. The equations of the two curve fits were set equal eliminating exhaust gas temperature resulting in the following relationship for an effective spark advance:

$$Relsp_{e'} = 3.323(r_c - 9.0) \tag{31}$$

where, $Relsp_{e'}$ = effective relative spark advance (spark-MBT) due to comp. ratio

A speed adjustment was made to account for the differences in the flow speed with changing compression ratio. As compression ratio increases the mass of fuel per cycle decreases because the engine becomes slightly more efficient. The normalized equations for mass of fuel per cycle with respect to changes in compression ratio illustrated in Appendix A were incorporated to make this flow adjustment. Since it is a normalized equation the reference compression ratio was changed to 9.0 with no effect

on the equation. This equation was incorporated as follows similar to the flow adjustments done for EGR.

$$N_{e'} = -0.0245N(r_c - 9.0) \qquad (32)$$

where, $N_{e'}$ = effective increase in speed due to compression ratio

The combination of the previous results in the fraction oxidized in the exhaust:

$$f_{oxi,exh} = 0.866 - 0.000148(N + N_e + N_{e'}) - 0.0007IMEP - 0.00791(Relsp + Relsp_e + Relsp_{e'}) - 0.0000255T_{cool} \qquad (33)$$

3.6 Four Valve Engine Adjustments

The model has been developed for a two-valve per cylinder spark-ignition engine, until now. Additional assumptions were needed to adjust the two-valve model to match four-valve engine data.

3.6.1 In-Cylinder Temperatures

A four-valve engine usually burns faster than a two-valve engine. A faster burn engine is believed to have lower expansion stroke temperatures, because more energy is extracted by the piston earlier in the expansion stroke process. The exact difference between the two engines' expansion stroke temperatures is difficult to estimate. Therefore, a non-linear least squares regression technique was performed on the two-valve HC model with four valve engine HC data to determine the difference.

3.6.2 Four Valve Exhaust Oxidation

The fraction of HC oxidation in the exhaust depends on the temperatures of the gas, the exhaust port and manifold. A four-valve engine typically has a larger amount of exhaust port and manifold surface. This leads to higher rates of heat transfer, which reduces the exhaust port and manifold gas temperatures. As discussed earlier, the expansion stroke temperatures are believed to be lower, which would also result in lower

exhaust gas temperatures. These phenomena together can reduce the fraction of HC oxidized in the exhaust system as compared to the two-valve engine. How much lower was determined by performing a non-linear regression technique against the two-valve model using four-valve engine data.

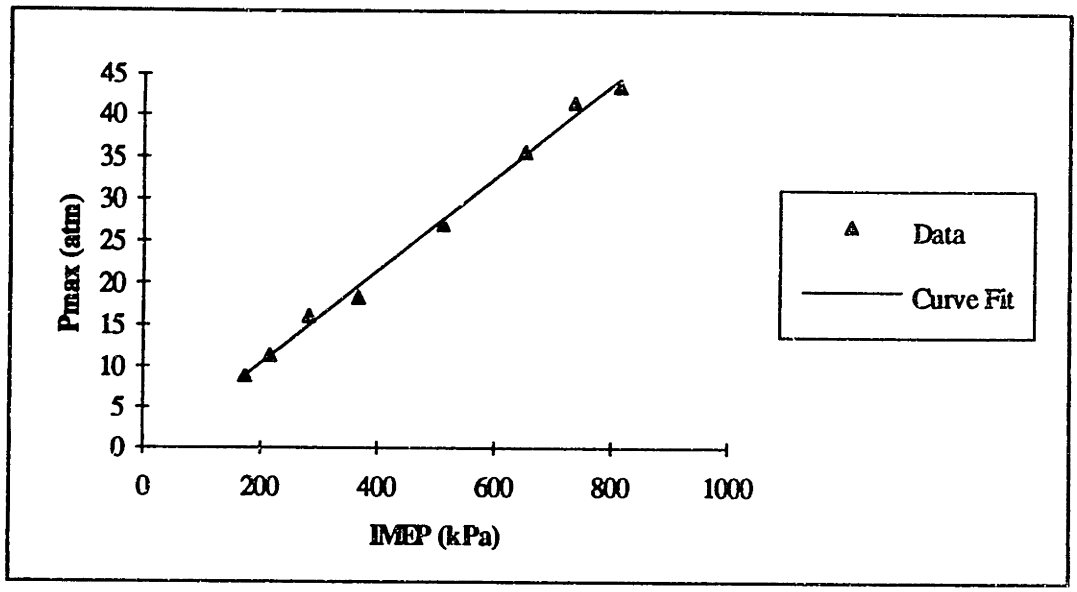

Figure 3.1 Maximum cylinder pressure (Pmax) versus indicated mean effective pressure (IMEP) simulated for a typical production spark-ignition engine. 1600 rev/min, MBT spark timing, stoichiometric operation.

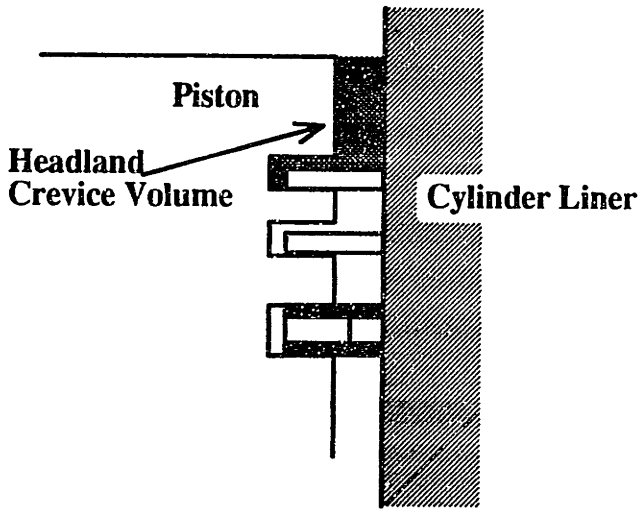

Figure 3.2 Schematic of headland crevice volume.

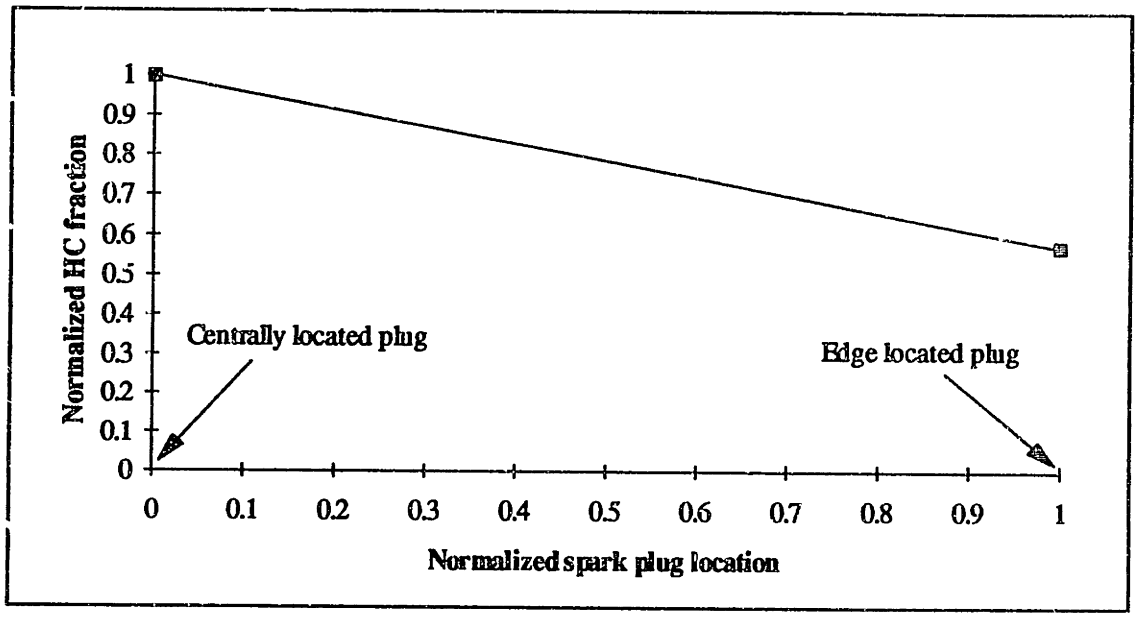

Figure 3.3 Normalized HC fraction in HC crevice versus normalized spark plug location for typical spark ignition engines, where zero normalized location indicates a centrally located plug and one normalized location indicates an edge located spark plug.

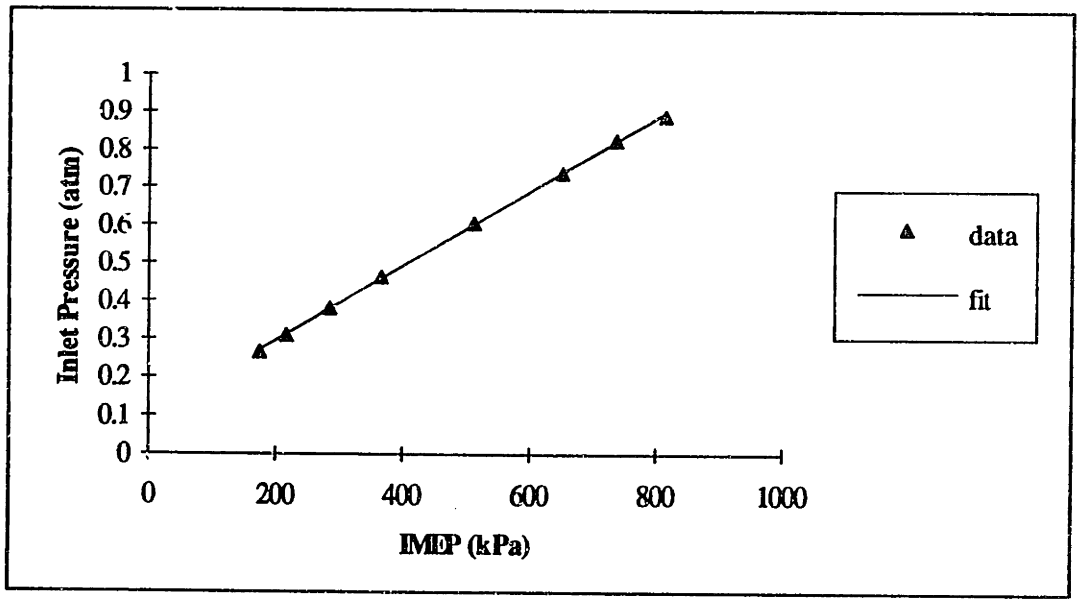

Figure 3.4 Inlet pressure versus indicated mean pressure for a typical spark-ignition engine. 1600 rev/min, MBT spark timing, and stoichiometric operation.

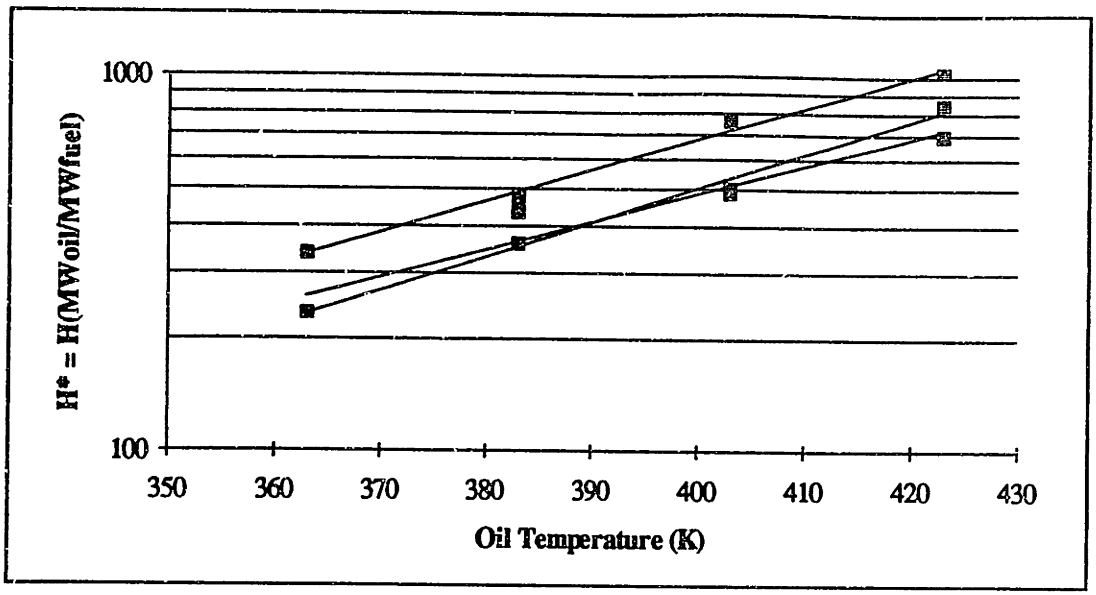

Figure 3.5 H* (proportional to Henry's constant) versus oil temperature for isooctane desolved in three different lubricating oils [12].

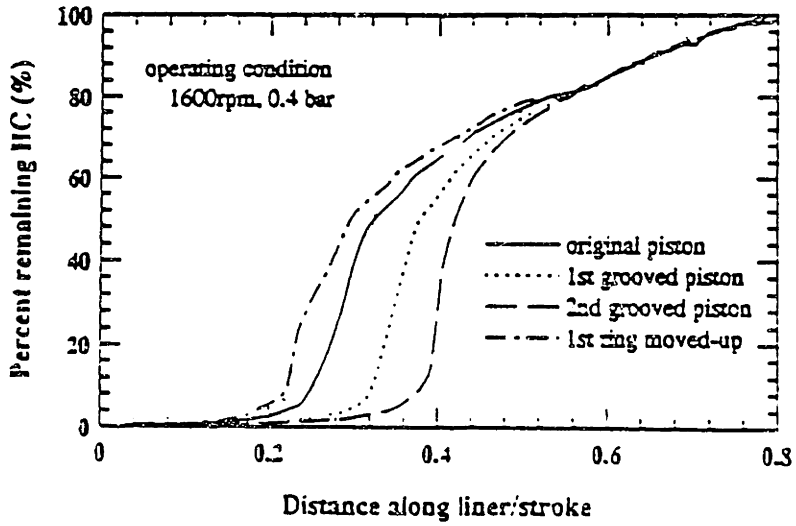

Figure 3.6 Percentage HC remaining from four different grooved pistons versus normalized distance [5].

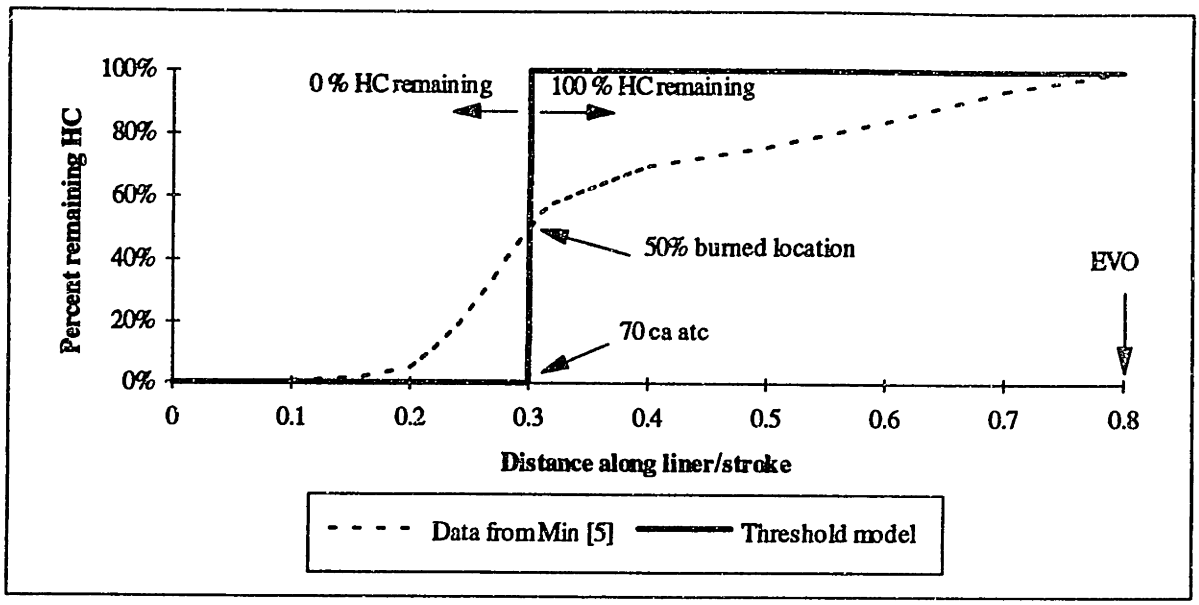

Figure 3.7 Schematic of oxidation model developed from Min results for the originally grooved piston [5]. 1600 rpm, 0.4 bar, and stoichiometric operation.

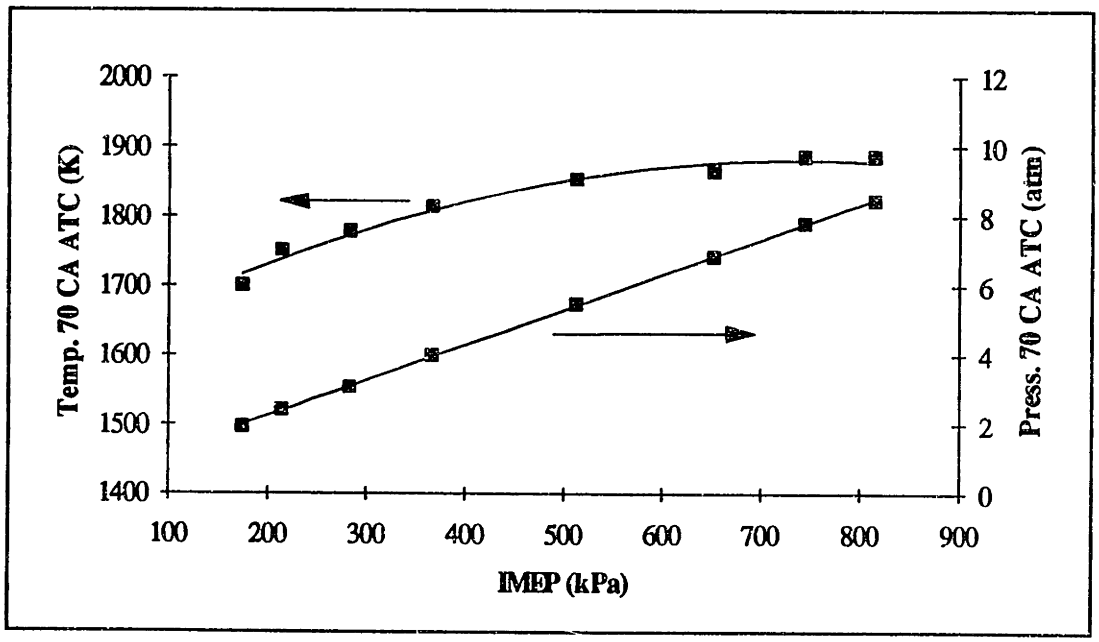

Figure 3.8 In-cylinder temperature and pressure at 70 CA ATC as a function of indicated mean effective pressure simulated for a typical spark-ignition engine. 1600 rpm, MBT spark timing, and stoichiometric operation.

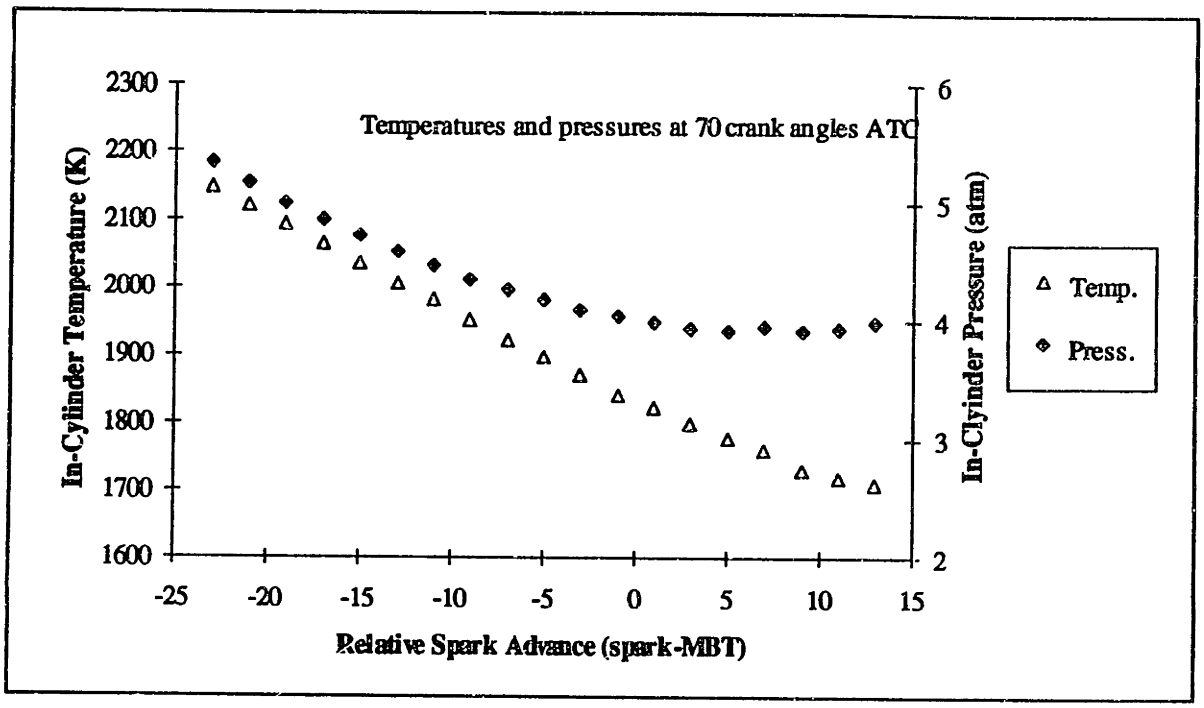

Figure 3.9 In-cylinder pressures and temperatures at 70 CA ATC for constant BMEP spark sweep (MBT spark timing = 0). 1600 rev/min, BMEP = 241 kPa, stoichiometric operation.

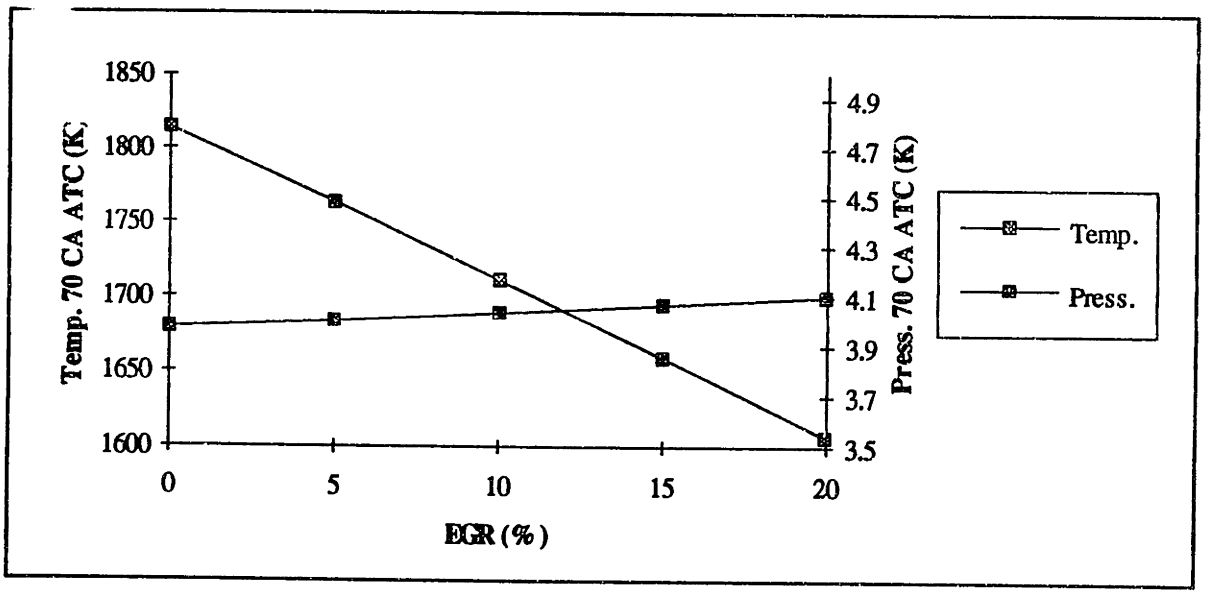

Figure 3.10 Effect of EGR on temperature and pressure at 70 CA ATC simulated for a typical spark ignition engine at 1600 rpm, BMEP = 241 kPa, MBT spark timing, and stoichiometric operation.

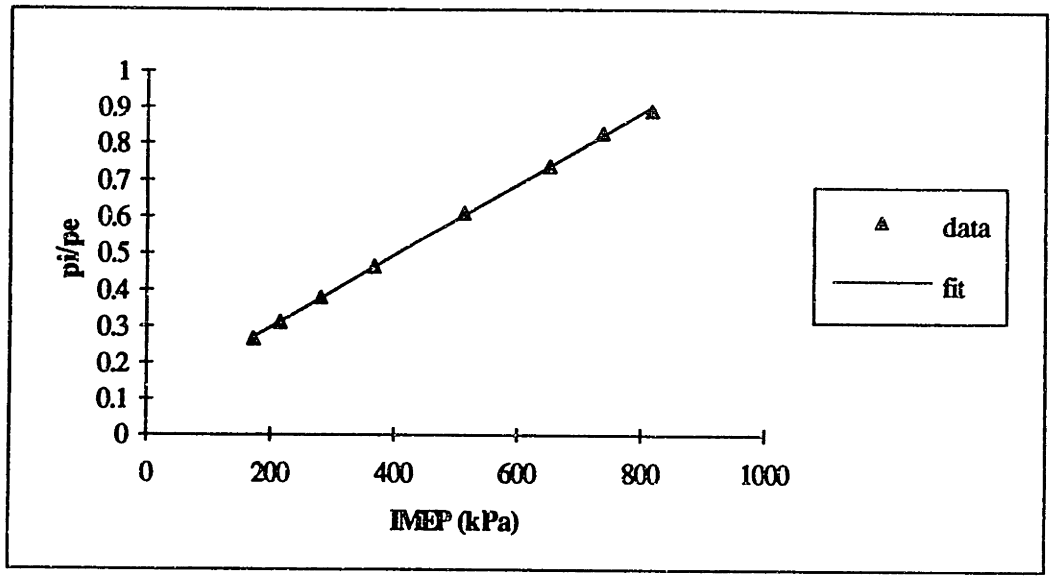

Figure 3.11 Ratio of inlet pressure to exhaust manifold pressure versus indicated mean effective pressure for a simulated spark-ignition engine. 1600 rpm, MBT spark timing, and stoichiometric operation.

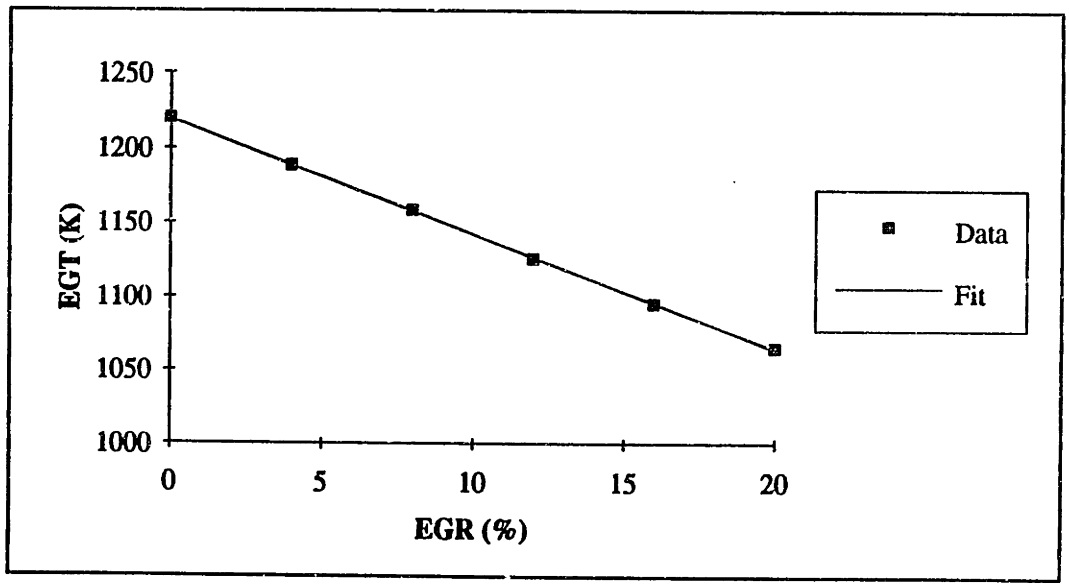

Figure 3.12 EGR effects on exhaust gas temperature simulated for a typical spark ignition engine. 1400 rev/min, BMEP = 325 kPa, burn duration of 60 CA, and stoichiometric operation [24].

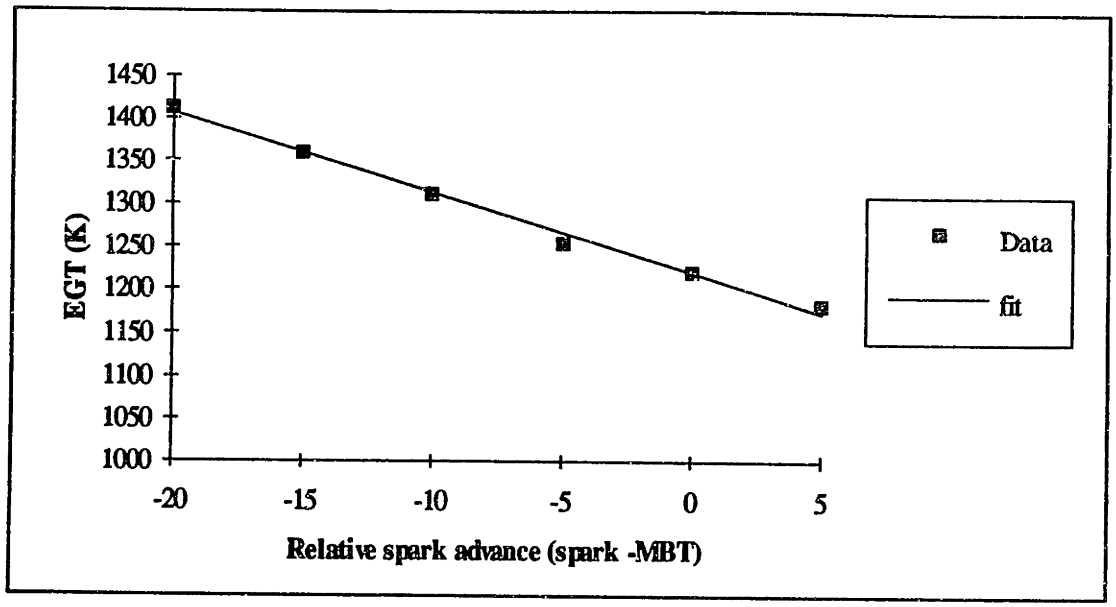

Figure 3.13 Spark advance effects on exhaust gas temperature for a typical spark ignition engine. 1400 rev/min, BMEP = 325 kPa, burn duration of 60 CA, and stoichiometric operation [24].

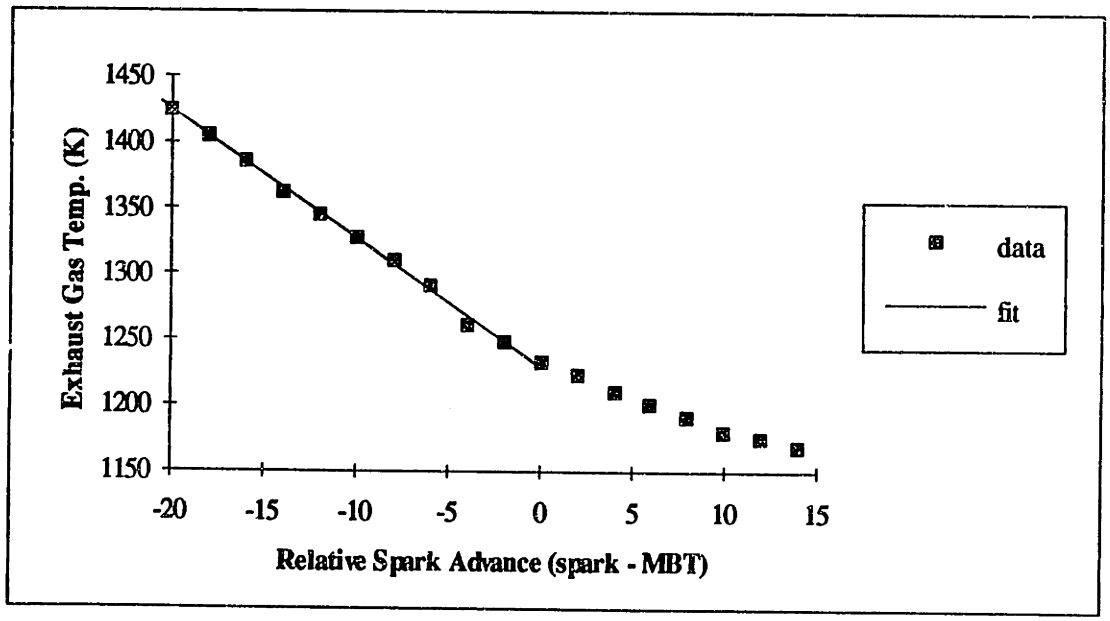

Figure 3.14 Effect of spark timing on mean exhaust gas temperature for a typical spark ignition engine at 1600 rpm, BMEP = 241 kPa, MBT spark timing, and stoichiometric operation. Zero relative spark advance indicates MBT timing

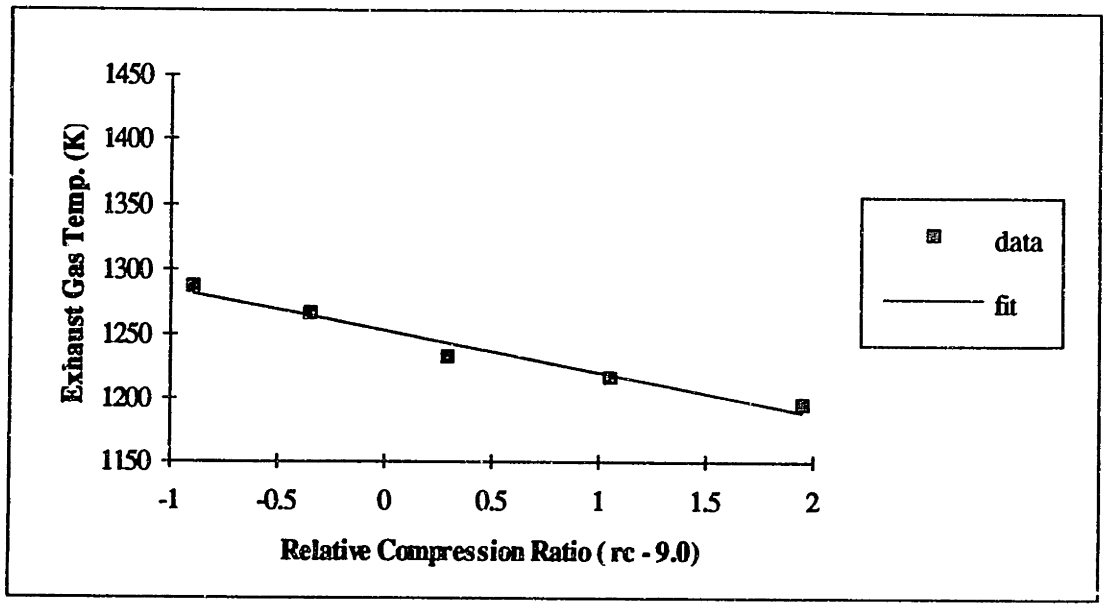

Figure 3.15 Effect of spark timing compression ratio on exhaust gas temperature for a typical spark ignition engine at 1600 rpm, BMEP = 241 kPa, MBT spark timing, and stoichiometric operation. Zero relative compression ratio indicates a 9.0 compression ratio.

CHAPTER 4: MODEL CALIBRATION

4.1 Spark-Ignition Data

After the scaling laws were developed and combined in the HC framework, the model was calibrated using spark-ignition engine data. Data from five production engines was used for this purpose. Table 4.1 presents the spark-ignition engines:

Table 4.1 List of Spark Ignition Engines in Data Base

3.3 L - 6 cylinder - 2 valve
2.5 L - 4 cylinder - 2 valve
2.2 L - 4 cylinder - 2 valve
2.0 L - 4 cylinder SOHC - 4 valve
3.5 L - 6 cylinder SOHC - 4 valve

The data obtained for the 3.3L, 3.5L and 2.0L consisted of variations in compression, ratios, camshafts (valve lift heights, and overlap duration), crevice volumes, spark timing, and EGR%. The data obtained for the 2.5L and 2.2L engines were limited to spark timing variations. A description of each engine's geometric variables is located in Appendix B.

As discussed earlier, the model was developed for one operating condition:

Speed = 1600 rpm BMEP = 241 kPa (35 psi)

This particular speed and load was chosen because it represents a significant fraction of the operating time during the Federal Test Procedure driving cycle. In the model, the load was represented by the indicated mean effective pressure (IMEP). The data base did not include friction data for each engine. Thus, a friction model developed by Patton

was used to estimate the engine friction to calculate the IMEP for each engine [7]. The friction model was based on operating conditions, engine geometry, and camshaft design. The BMEP values for each engine were adjusted as follows:

$$IMEP = BMEP + FMEP$$

Table 4.2 indicates the friction estimates for each engine design.

Table 4.2 Friction estimates for engine data base.

Engine Displacement	Compression Ratio	Camshaft	FMEP (kPa)
3.3L	8.9	Cam #1	143.4
3.3L	8.5	Cam #1	142.7
3.3L	8.2	Cam #1	142.1
3.3L	7.9	Cam #1	141.5
3.3L	7.2	Cam #1	140.1
3.3L	8.9	Cam #2	143.9
3.3L	8.4	Cam #2	143.1
3.3L	8.5	Cam #3	144.5
2.0L	8.8	Cam #4	143.2
2.0L	9.3	Cam #4	144.0
2.5L	9.5	Cam #5	151.4
2.2L	9.0	Cam #5	150.6
3.5L	9.9	Cam #6	143.3

4.2 Model Calibration

The model was calibrated in two phases. In the first phase, the model was calibrated using two-valve engine data (i.e. 3.3L, 2.2L, and 2.5L). The second phase was required to incorporate the differences between the two and four-valve engines and also to accommodate different engine designs. The different designs were assumed to affect the fraction oxidized in the exhaust and in-cylinder.

After each calibration of the model, the model behavior was examined to determine if the physics of the model was retained. In some cases, the constants did not retain the sign needed to maintain the physics incorporated into the model. For example,

if the fuel source constant was negative it is acting as a sink instead of a source. Also, when examining the behavior of the in-cylinder oxidation model, it was noticed that the model predicted values larger than 100% for some initial model regressions, which is not physically possible.

The first calibration was performed using a least squares linear regression in EXCEL and setting the regression intercept to zero. Four terms in the model were initially calibrated using the two-valve engine data. The terms in model are as follows:

$$HC_{engine-out} = C_1 S_{f\&a}(1-f_{ret,cyl})(1-f_{oxi,exh}) - C_2 S_{f\&a} f_{oxi,cyl}(1-f_{ret,cyl})(1-f_{oxi,exh})$$
$$+C_3 S_f(1-f_{ret,cyl})(1-f_{oxi,exh}) - C_4 f_{oxi,cyl} S_f(1-f_{ret,cyl})(1-f_{oxi,exh})$$

where, C_1 = calibration constant for fuel-air sources
C_2 = calibration constant for in-cylinder oxidation of fuel-air sources
C_3 = calibration constant for fuel sources
C_4 = calibration constant for in-cylinder oxidation of fuel sources

Calibrating with the four constants did not produce reasonable results. The constants did not retain the signs to reflect the physics involved with each term. The calibration constant involving the in-cylinder oxidation of the fuel sources was believed to be the problem.

Little is known about the behavior of the in-cylinder oxidation of the fuel sources. Different in-cylinder oxidation scenarios were therefore attempted, however, without success. The final calibration was performed assuming that the in-cylinder oxidation of the fuel sources was zero (C_4 = 0.0), because the in-cylinder oxidation of the fuel sources is believed to be significantly lower than the fuel-air source in-cylinder oxidation. The resulting calibration constants are as follows:

$$C_1 = 0.717 \quad C_2 = 0.635$$
$$C_3 = 0.747 \quad C_4 = 0.000$$

The regression coefficient was 0.82. Figure 4.1 presents the actual data with the predicted data, where the solid line indicates a perfect correlation. Some of the variation

in the predicted values is due to unmodeled phenomena in some of the engines, which affects engine out hydrocarbon emissions. Figure 4.2 presents actual 3.3L engine data with respect to the predicted values for two different engine make-ups: a change in compression ratio (8.4 to 8.9), a change in the camshaft overlap factor (34 to 36 crank angles), and a change in headland crevice volume (0.899 to 0.810 cubic centimeters). Figure 4.3 compares 3.3L engine data with model predictions for two different compression ratios: 8.9 and 7.5. Figure 4.4 and Figure 4.5 compare the model predictions with 2.5L and 2.2L engines respectively. The first regression results matched the data for the 3.3L engine data relatively well. The model slightly over predicted the 2.5L and 2.2L engine data.

Next, the model was calibrated to match other engine data which may have different scaling proportions with the model due to engine design differences. Separate calibrations were performed for the 2.0L because the two-valve model under predicted the data by approximately 2. The model under predicted the 3.5L engine data by a small amount. A second calibration was performed to see the effect on the 3.5L model. Three coefficients were chosen for the terms affected by the different engine designs and number of valves per cylinder.

$$HC_{engine-out} = C_5 C_1 S_{f\&a}(1-f_{ret,cyl})(1-C_6 f_{oxi,exh}) - C_7 C_2 S_{f\&a} f_{oxi,cyl}(1-f_{ret,cyl})(1-C_6 f_{oxi,exh}) + C_3 S_f (1-f_{ret,cyl})(1-C_6 f_{oxi,exh})$$

where, C_5 = calibration constant for the fuel-air source
C_6 = calibration constant for exhaust port oxidation
C_7 = calibration constant for in-cylinder oxidation of fuel-air sources

The calibrations were performed on three coefficients in the model using a non-linear regression technique in SAS. The three calibration coefficients calculated in the previous regression were held constant, which allowed comparisons to be made between the

engines with respect to the magnitude of the fuel-air sources and to the fraction oxidized in-cylinder and the exhaust port. A constant was initially included on the fuel source term for the second calibration, but the non-linear regression technique did not converge to a solution that retained the physics of the model. The values calculated by the non-linear regression for the 2.0L and 3.5L engines are as follows:

2.0L engine: $C_5 = 1.392$ $C_6 = 0.480$ $C_7 = 1.030$

3.5L engine: $C_5 = 1.049$ $C_6 = 1.097$ $C_7 = 0.947$

These constants represent values relative to the first calibration. For example, the exhaust oxidation constant (C_6) for the 2.0L engine predicts that the exhaust oxidation is 48% of the first calibration set of engines. Modest changes are needed to calibrate the model for the 3.5L engine, while larger changes are needed to calibrate for 2.0L engine, especially for the exhaust oxidation (C_6). Figure 4.6 and Figure 4.7 present the model predictions with and without a second model calibration for the 2.0L and the 3.5L engines, respectively.

If the magnitudes of the constants are compared, the second calibration predicts that the fuel-air sources are more important relative to the 3.3L engine. The exhaust oxidation is reduced for the 2.0L engine, and does not change significantly for the 3.5L engine. The in-cylinder oxidation is slightly less for the 3.5L engine engines relative to the 3.3L engine.

How can these differences be explained? It is believed that these constants address not only the mechanisms built into the model, but also include phenomena that depend on engine design details which are not included in the model. Each engine has a different coolant system design that directly affects the component temperatures. The engine component temperatures affect the crevice volumes as discussed in Chapter 3. Since the model uses cold crevice volume as an input, the fuel-air source model constant

presumably scales the model to hot crevice volumes which are smaller than cold crevice volumes in the headland region. Thus, if component temperatures are varied from engine to engine the scaling will change. Also, the 2.0L engine has siamesed bores which could lead to warmer "lower" bore temperatures and increased bore distortion; these phenomena have opposite effects on HC emissions. Increased lower bore temperatures are believed to reduce HC emissions because of decreased oil layer HC absorption and increased oxidation of fuel-air sources. However, bore distortion is believed to increase HC emissions because of a possible increase in the oil layer thickness. It is also believed that 4-valve engines have more exhaust valve leakage due to clamping loads close to valve seats. The combination of these effects and others which were not quantified separately are combined in the 2nd regression coefficients.

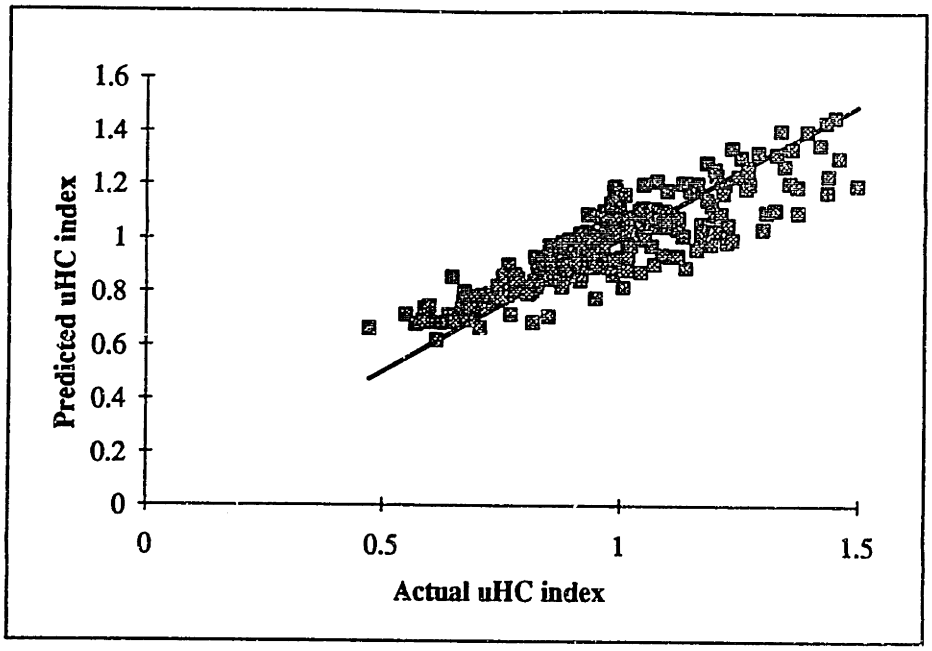

Figure 4.1 3.3L model calibration comparing the model fit to a perfect model correlation. The solid line represents perfect correlation with the data. The regression coefficient is 0.82

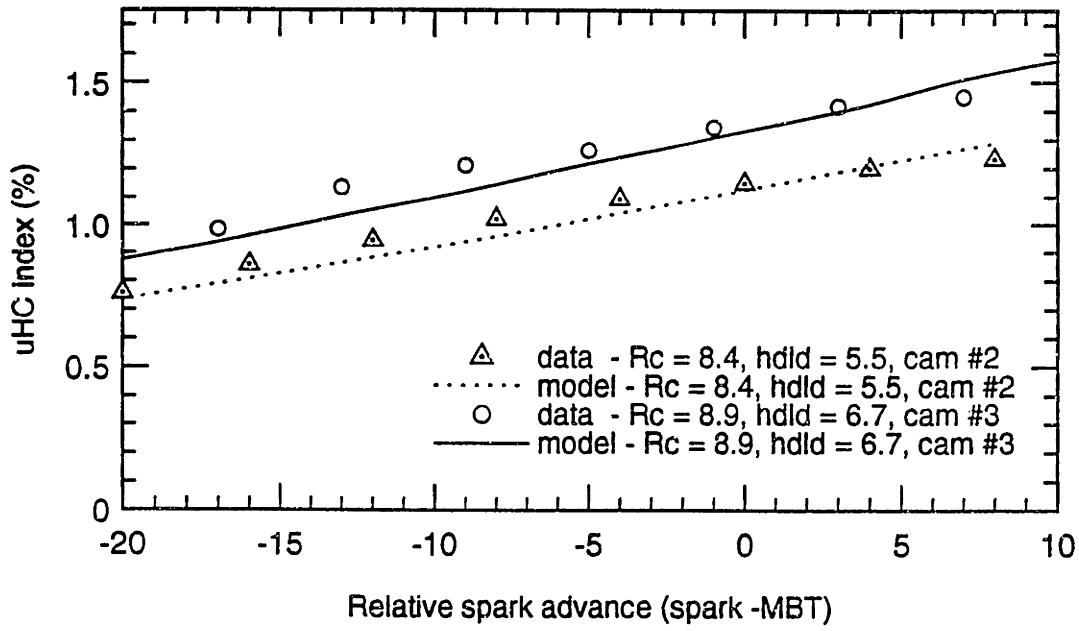

Figure 4.2 Model comparison to 3.3L engine data for a change in compression ratio from 8.4 to 8.9, valve overlap from 34 to 36 CA and headland height from 5.5 to 6.7 mm, which corresponds to a crevice volume of 0.81 to .90 cc, respectively.

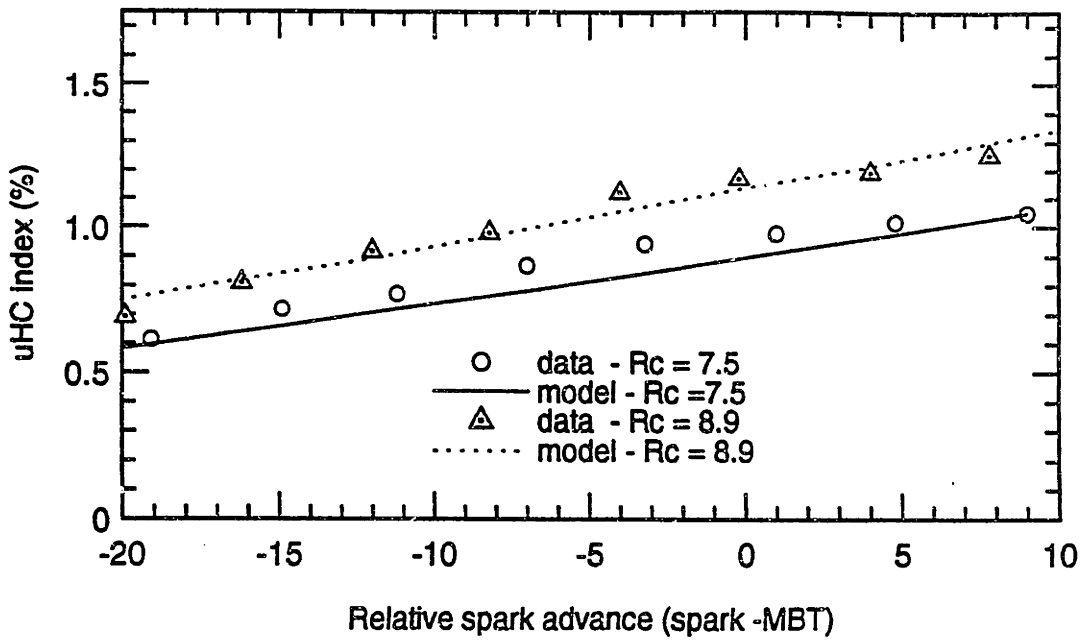

Figure 4.3 Model comparison to 3.3L engine data for a change in compression ratio from 7.5 to 8.9.

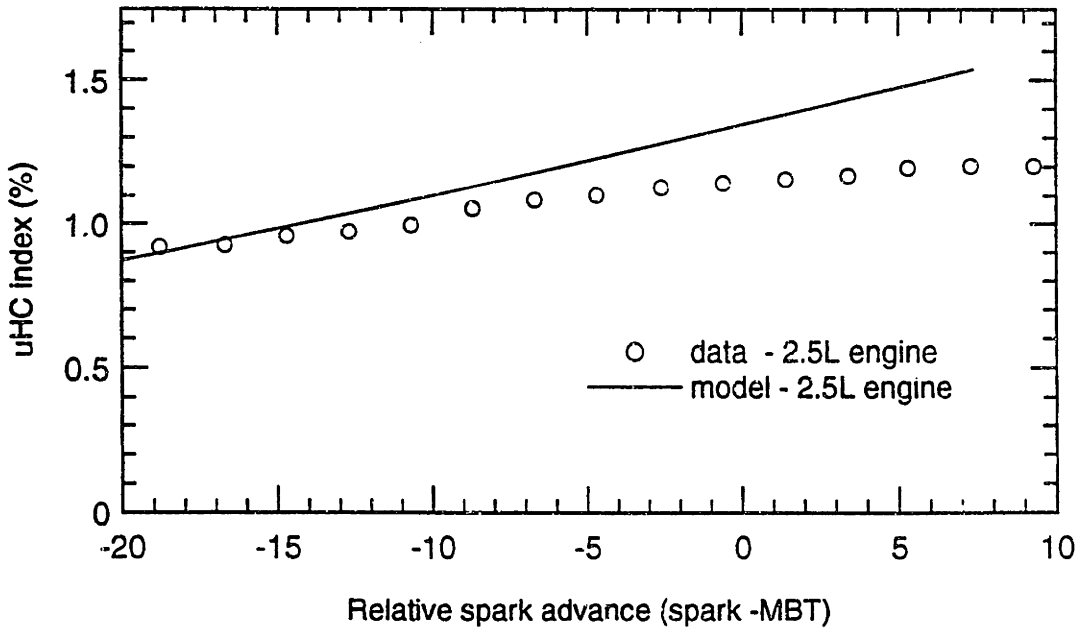

Figure 4.4 Model comparison to 2.5L engine data

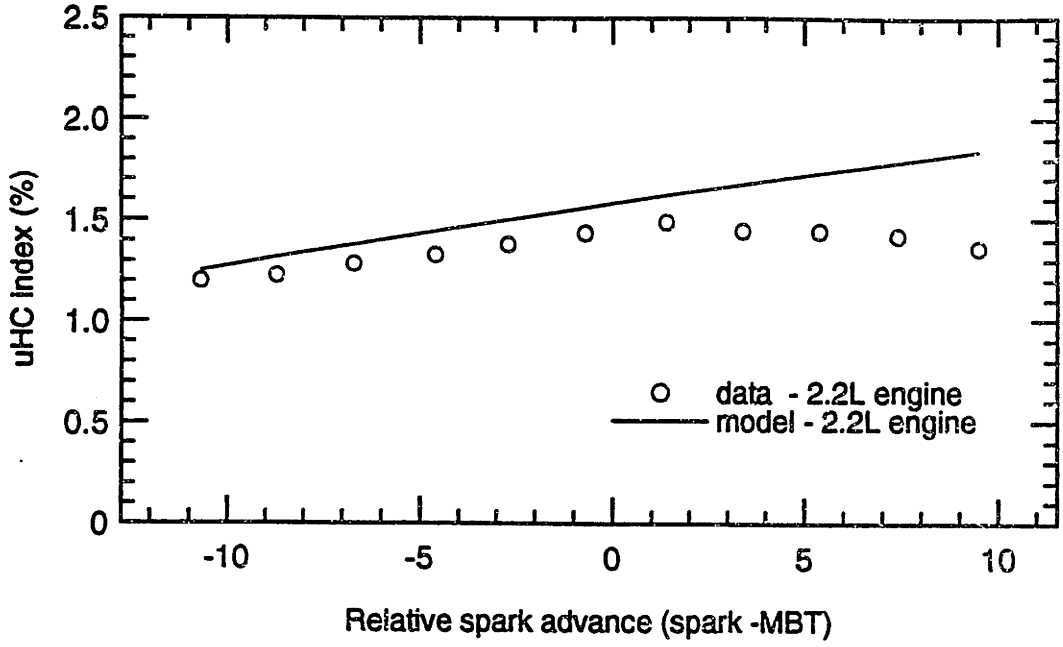

Figure 4.5 Model comparison to 2.2L engine data.

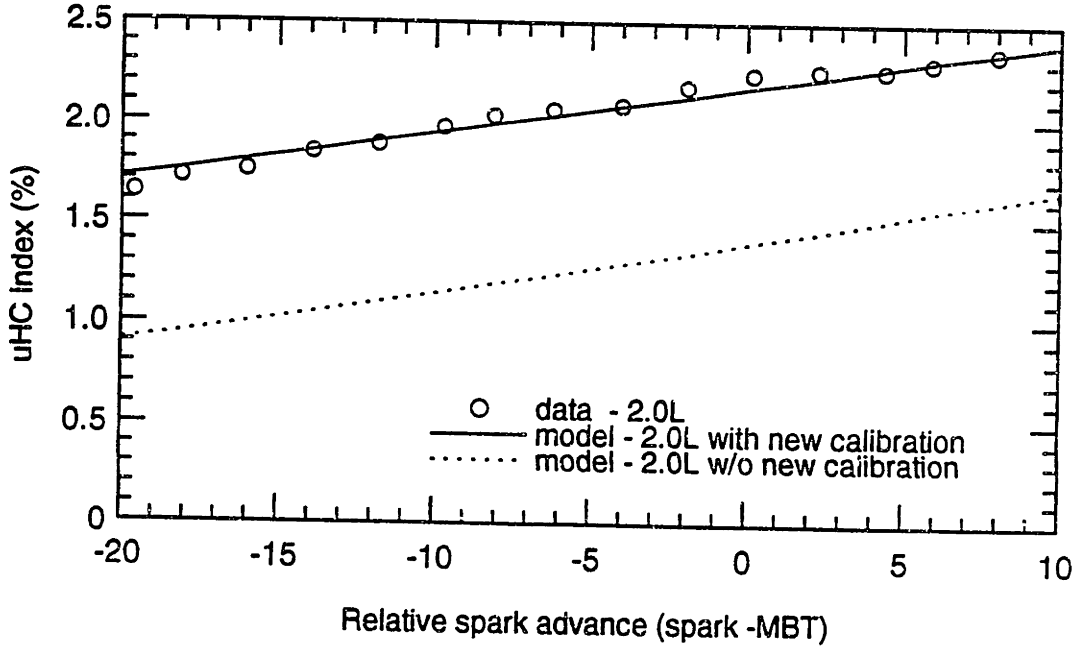

Figure 4.6 Model comparison to 2.0L engine data with first model calibration and with second model calibration.

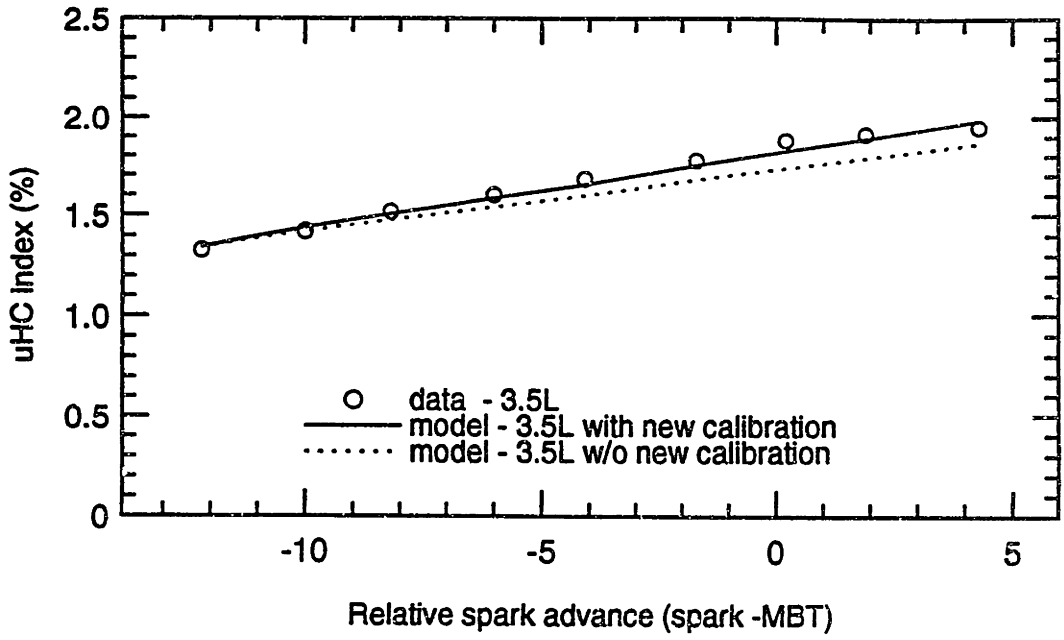

Figure 4.7 Model comparison to 3.5L engine data with first model calibration and with second model calibration.

CHAPTER 5: MODEL RESULTS AND CONCLUSIONS

5.1 Comparison of Model to Engine Data for Parameter Variations

The geometric parameters and operating conditions in the model were varied to observe their effect on engine-out HC emissions. Also, the trends were compared with the engine data used to calibrate the model. The data base consisted of many parameter changes and lacked the systematic and precise equipment variation needed to isolate individual parameter effects on HC emissions. Regardless, the trends were compared for the best systematic variations in the data base with respect to crevice volume, compression ratio, and EGR%. Spark timing variations are illustrated in Chapter 4, and show consistent trends with the data.

The model trends were compared with compression ratio changes in the 3.3L engine. The 3.3L engine data base consists of four different compression ratio changes at MBT spark timing. Figure 5.1 compares the model predictions with the engine data. From the figure, one can see that there are large variations in the engine data, but the model predicts the basic trend observed in the data.

Next, the model trends were compared to crevice volume changes for three different engines. Figure 5.2 compares the model predictions with the 3.3L, the 2.0L, and the 3.5L engines crevice volume changes at MBT spark timing. The model predicts the trends well.

Finally, the model was compared to engine data for EGR variations. The 3.3L data base consisted of four EGR conditions 5, 10, 15, and 20% at MBT spark timing. Figure 5.3 compares the model predictions with the engine data. The model predictions

are consistently lower for all EGR data points, but the trend is of the correct magnitude except for high EGR conditions where poor combustion stability is believed to be responsible for the faster increase in HC emissions after 15% EGR.

5.2 Parameter Variation

The HC model was broken-down to observe the behavior of each component of the total HC mechanism. It is acknowledged that several of the model assumptions are speculative. Regardless, the model provides useful insight into the likely behavior of each mechanism.

The model behavior was evaluated at constant speed and load for one set of engine geometric parameters. Table 5.1 presents the operating conditions and engine geometric parameters.

Table 5.1 Operating Conditions and Engine Geometry Used for Parameter Variation.

IMEP = 380 kPa
Speed = 1600 rpm
Crevice Volume = 0.81 cc
Compression Ratio = 8.9
Bore = 93 mm
Stroke = 81 mm
Intake Valve Diameter = 45.5 mm
Exhaust Valve Diameter = 37.5 mm
Maximum Intake Valve Lift = 10.16 mm
Maximum Exhaust Valve Lift = 10.16 mm
Valve Overlap = 38 CA
Number of Cylinders = 6
Displacement Volume = 3.3 L
Fuel-to-Air Ratio = stoichiometric
Coolant Temperature = 370 K
Number of Valves per cylinder = 2.
Spark Plug Offset = 17.0 mm

5.2.1 Spark Timing Effects on Engine-Out HC Emissions

During engine operation spark timing is retarded from MBT to reduce HC and NO_x emissions. The HC emissions trends are well known for spark timing variations relative to MBT, but the behavior of each contributing mechanism can provide further insight to this phenomenon. The model was broken up into the individual mechanisms to observe the behavior. Spark timing was normalized to the MBT spark timing (spark - MBT) for a constant IMEP spark sweep, where a negative spark timing designates spark retard and a positive spark timing designates spark advance from MBT. Figure 5.4a and b describe the behavior for the fuel-air and fuel source mechanism. The figures quantify the amount of each source remaining after each mechanism: in-cylinder oxidation, retained HC, and exhaust oxidation. (note: the fuel source model assumes no in-cylinder oxidation.)

In Figure 5.4a, the amount of HC escaping combustion in the fuel-air sources decreases with increased spark retard because of the decreasing maximum cylinder pressure. In Figure 5.4b, the amount of HC escaping combustion in the fuel sources remains relatively constant. Figure 5.4c presents the behavior of the fraction of in-cylinder oxidation, the fraction of exhaust-port oxidation, and the fraction of HC remaining in the cylinder. The amount of in-cylinder oxidation decreases for increasing spark retard, opposite to what one might expect. As discussed earlier, the in-cylinder temperatures and pressures in the expansion stroke decrease for increased spark retard. However, the maximum cylinder pressure per cycle is also decreasing, thus forcing less HC in the fuel-air sources. The maximum cylinder pressure effect apparently offsets the effect of decreasing temperatures and pressures in the expansion stroke. Next, the exhaust port-oxidation increases due to increasing exhaust temperatures with increased spark retard. Finally, the residual fraction remains essentially constant.

The relative contribution of the fuel-air and fuel sources are presented in Figure 5.4d and e. Each figure shows that the fuel-air sources contribute slightly more to the HC

emissions at MBT timing (or at "zero" relative spark advance). However, both the fuel-air and fuel sources contribute approximately the same amount to the total engine-out HC emissions for the entire set of spark timings.

5.2.2 Compression Ratio Effects on Engine-Out HC Emissions

The compression ratio changes from engine to engine to achieve an optimum design with regards to efficiency and emissions. However, there is a trade off between the two requirements, because with increasing compression ratio, the engine efficiency improves but the HC emissions tend to increase.

In Figure 5.5a the behavior of the fuel-air source mechanisms are affected. This is because the maximum cylinder pressure is increasing for increasing compression ratio. Figure 5.5b shows that the behavior of the fuel source model is affected because the compression stroke pressures will be greater for larger compression ratios, thus forcing more HC in the fuel sources. Figure 5.5c shows that the in-cylinder oxidation increases slightly due to increasing expansion stroke temperatures. This occurs because engines become slightly more efficient and extract more energy from the combustion gases as the compression ratio increases, thus reducing the expansion stroke temperatures. The exhaust oxidation decreases because, the exhaust gas temperatures decrease with increased compression ratio. The residual HC fraction decreases slightly for increasing compression ratio. Figures 5.5d and e shows that fuel-air sources contribute slightly more to the total engine-out HC emissions for compression ratio changes.

5.2.3 Crevice Volume Effects on Engine-Out HC Emissions

The crevice volume from engine to engine varies depending on the engine design. Typical spark-ignition production engines range from 0.6 to 1.2 cc per cylinder. This volume can be reduced to decrease engine-out HC emissions. Figures 5.6a and b show the fuel-air source HC increase with increasing crevice volume, but there is no effect on

the fuel source mechanism. Figure 5.6c shows that the crevice volume has no effect on the in-cylinder oxidation, exhaust oxidation and residual HC fraction. Figures 5.6d and e illustrate that the fuel sources contribute less than the fuel-air sources to the engine-out HC emissions for large crevice volumes.

5.2.4 Coolant Temperature Effect on Engine-Out HC Emissions

The model was developed assuming that the coolant temperature scales with engine component temperatures for a single speed and load condition. The engine coolant temperature affects the engine component temperatures depending upon the engine design, which has an affect on the amount of HC escaping combustion in both the fuel and fuel-air source.

The coolant temperature was varied from 355 K to 390 K. In Figure 5.7a, the total HC escaping combustion in the fuel-air source decrease with an increase in coolant temperature due to the decreasing headland crevice gas density. The fuel source HC escaping combustion decreases with increasing coolant temperature, as observed in Figure 5.7b. The oil layer absorbs less HC with increasing oil layer temperature, which is influenced by an exponential relationship with Henry's Constant. Figure 5.7c shows that the in-cylinder oxidation increases slightly, and the residual HC fraction and exhaust oxidation remains relatively constant. Figure 5.7d show that the overall effect on HC emissions decreases with increasing coolant temperature. Figure 5.7e shows that as the coolant temperature increase the fuel source contribution decreases below the fuel-air source contribution for increased coolant temperatures.

5.2.5 Valve Overlap Effect on Engine-Out HC emissions.

The valve overlap is defined as the time from intake valve opening to exhaust valve closing. This time usually ranges from 25 to 40 CA depending on the engine design. The

valve overlap affects the fraction of the residual gases remaining in the cylinder that become part of the next cycle. Included in this fraction are hydrocarbons.

This parameter was varied, producing slight decreases in the overall HC emissions. The valve overlap produced a small change in the fuel-air sources. Figure 5.8a shows that for an increase in valve overlap the HC escaping combustion in the fuel-air sources will decreases slightly. This is due to an increasing fraction of residual gases in fuel-air sources. In Figure 5.8b, the fuel sources mechanism remains constant for all valve overlaps. The in-cylinder oxidation and exhaust oxidation remains unaffected, while the residual gas fraction increases, as seen in Figure 5.8c. In Figure 5.8d, The engine-out HC emissions decreases slightly for increasing valve overlap because a larger fraction of HC are retained in the cylinder with the residual gases. Figure 5.8e shows that the fuel-air sources contribute slightly more to the engine-out HC emissions than the fuel sources.

5.2.6 EGR Effects on Engine-Out HC Emissions

EGR is used in spark-ignition engines to reduce NO_X emissions. However, it has a reverse effect on HC emissions. Figure 5.9a shows that the HC escaping combustion in the fuel-air sources decreases slightly, due to an increased fraction of EGR gases in these sources. Figure 5.9b shows that the HC escaping combustion in the fuel sources increases with increasing EGR, due to an increase in the inlet pressure. This increases the pressure in the compression stroke, which forces more fuel in the fuel sources. In Figure 5.9c, the in-cylinder oxidation reduces slightly due to temperature decreases in the expansion stroke. Also, the exhaust oxidation decreases because of decreasing temperatures, while the residual gas fraction decreases slightly because of an increase in inlet pressure. The overall engine-out HC emissions increase with increasing amounts of EGR, with both sources contributed approximately the same amount as observed in Figure 5.9e.

5.3 Engine Design Recommendations for Low Engine-Out HC Emissions

In previous sections, the model parameters were varied to observe their effect on engine-out HC emissions. Now, the model will be used to predict a 10% reduction in HC emissions for separate changes in each parameter. All the parameters discussed in section 5.1 will be reviewed except EGR because it causes and increase in HC emissions. The engine design described in Table 5.1 will be used as reference (except a 9.5 compression ratio and valve overlap of 25 CA will be used). Table 5.2 presents the changes in each parameter needed to reduce HC emissions by 10%.

Table 5.2 Model Predictions for a 10% decrease in engine-out HC emissions for the 3.3L engine. 1600 rpm, IMEP = 380 kPa, and stoichiometric operation.

Parameter	Original Value	Value to produce a 10% decrease in HC emissions
Crevice Volume	0.81 cc (hdld = 5.5mm)	0.66 cc (hdld = 3.6 mm)
Valve Overlap	25 CA	43 CA
Compression Ratio	9.5	8.8
Coolant Temperature	370 K	375 K
Spark Timing	MBT	retard 6 CA

When all these five effects are combined the model predicts that the engine-out HC emissions reduces from 1.31% to 0.75% (uHC emissions index), which is a 43 % reduction.

5.4 Discussion

The intention of this work was to develop a model to predict engine-out HC emissions for spark-ignition engines. The model incorporates physically based scaling laws for the processes involved in producing HC emissions. The model was calibrated

using spark-ignition engine data from current production engines. Additional calibrations were needed to accommodate different engine designs. The data correlated relatively well with the model.

Comparing the model with the individual variable trends observed in actual data was difficult due to limited sets of such data. However, the model fit the data well for the crevice volume and the compression ratio variations and followed the correct trend for variations in EGR.

5.5 Summary and Conclusions

1. A set of scaling laws was developed to predict engine-out HC emissions for spark-ignition engines at a typical part load operating condition, by addressing the physics of the major mechanism that contribute.

2. The model was calibrated against data from five different engines to determine the relative magnitude of each of the major sources. The calibration constants for the fuel-air HC sources were predicted to be approximately 1.39 higher than the two valve engine constants for the 2.0L engine. Other changes made to the calibration constants to adjust for 4-valve engines were small except for the exhaust oxidation which decreased to 48% of the two valve model for the 2.0L engine.

3. The model predicts that the three processes: 1) in-cylinder oxidation, 2) retention, and 3) exhaust oxidation reduce the fraction of fuel-air source engine-out HC emissions overall by 84% at 1600 rpm, IMEP = 380 kPa, MBT spark timing, and stoichiometric operation. The in-cylinder oxidation makes up about two-thirds of this reduction. Also in-cylinder oxidation only appears to be significant for the fuel-air source mechanisms.

4. The model predicts that the fraction of HC oxidized in-cylinder decreases with increased spark retard. Even though the expansion stroke temperatures are increasing, the maximum pressure decreases, which affects the amount of gases exiting the crevice regions in the expansion stroke. Thus, the fraction oxidized in-cylinder is limited by gas flow out of the crevice during the expansions stroke.

5. The model predicts that the engine-out HC emissions contributed from the fuel sources can be decreased by increasing the coolant temperature, decreasing the compression ratio and increasing the valve overlap and the spark retard. On the other hand, the contribution from the fuel-air sources can be reduced by decreasing crevice volume, increasing the valve overlap, and increasing spark retard. The overall engine-out emissions could be reduced by increasing the coolant temperature, valve overlap, and spark retard and decreasing the crevice volume and compression ratio.

6. The engine-out hydrocarbon emissions increase for increasing amounts of EGR for the same load conditions. The model predicts the fuel-air source hydrocarbons decrease slightly because an increased fraction of EGR gases are stored. The fuel sources HC increase because of an increase in inlet pressure. To reduce HC emissions for EGR operating conditions the fuel source mechanism must be reduced. The model predicts that this could be accomplished by increasing the coolant temperature, thus reducing HC emissions contributed from the fuel source mechanism.

7. The model predicts that the fuel source mechanisms increase with increasing EGR, while the fuel-air sources remain relatively constant. The fuel-air sources remain relatively unaffected because the maximum cylinder pressure does not change for increasing EGR. The fuel sources increase because the inlet pressure is increasing which directly influences the magnitude of this sources

8. For an increase in compression ratio at the same load conditions, the model predicts that both the fuel and fuel-air source increase at appoximately the same rate. The total HC emissions increase 0.2 per unit increase in compression ratio.

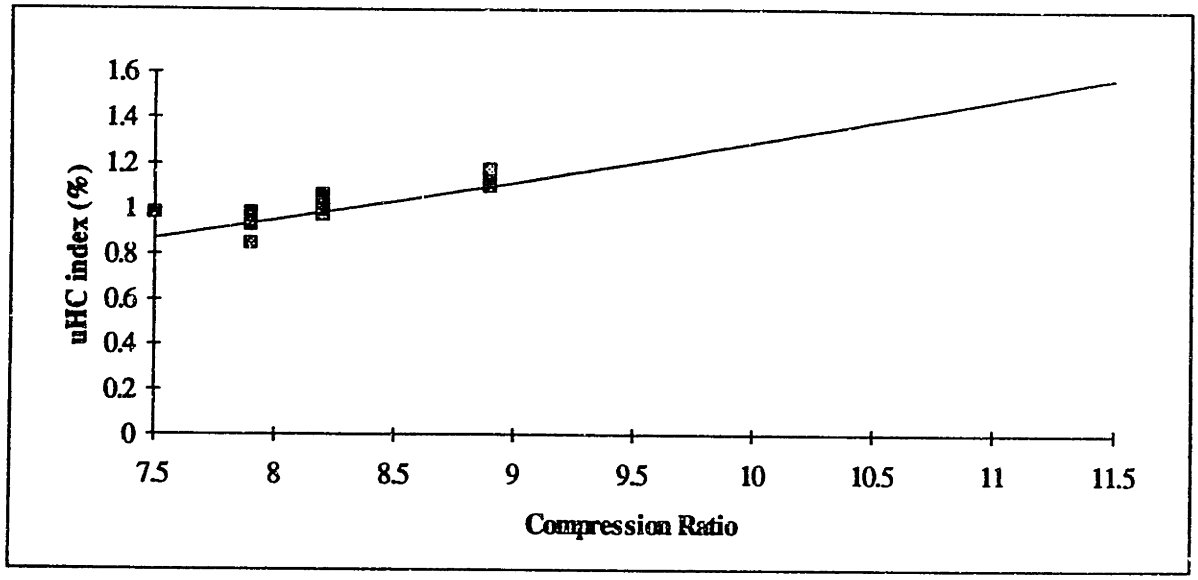

Figure 5.1 Model compression ratio trends compared to 3.3L engine data.
1600 rpm, BMEP = 241 kPa

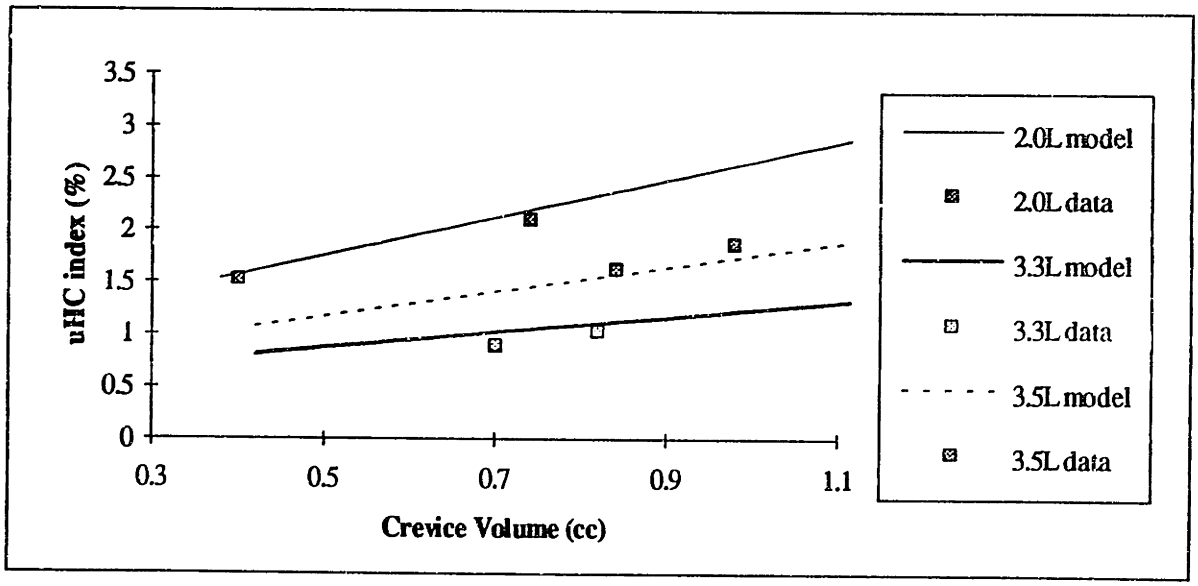

Figure 5.2 Model crevice volume trends compared to 3.3L engine data.
1600 rpm, BMEP = 241 kPa

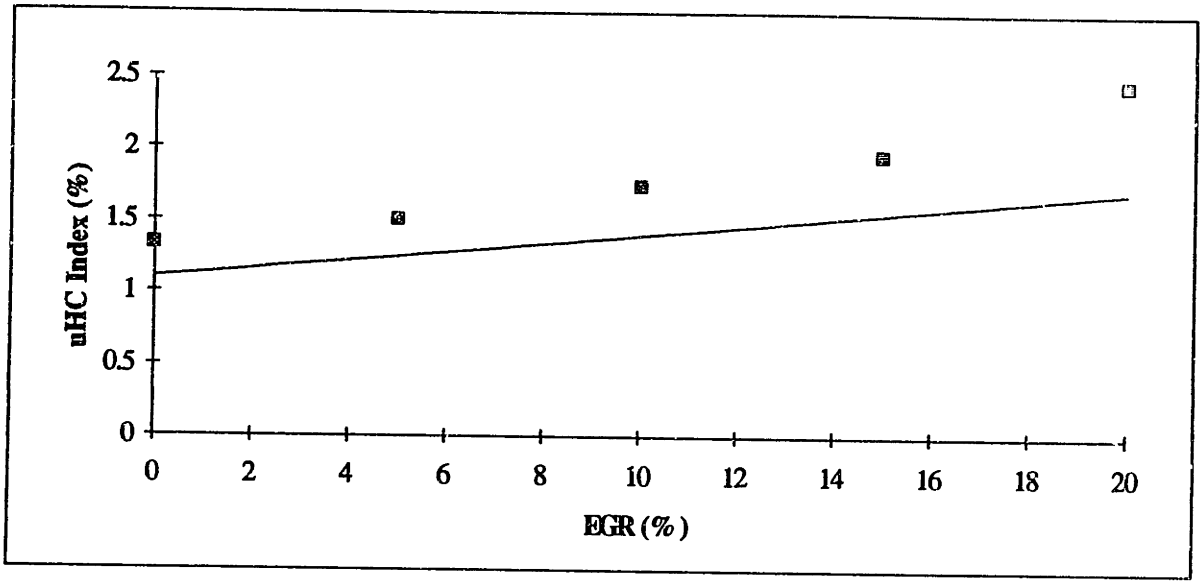

Figure 5.3 Model EGR trends compared to 3.3L engine data.
1600 rpm, BMEP =241 kPa

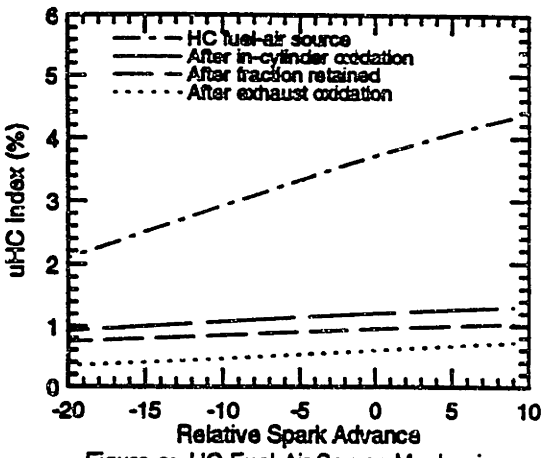

Figure a: HC Fuel-Air Source Mechanism

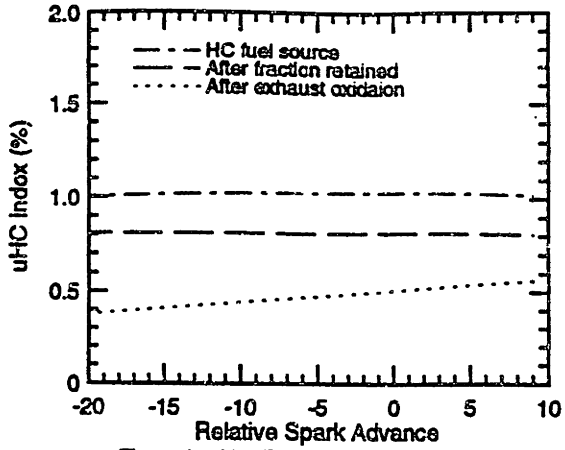

Figure b: HC Fuel Source Mechansims

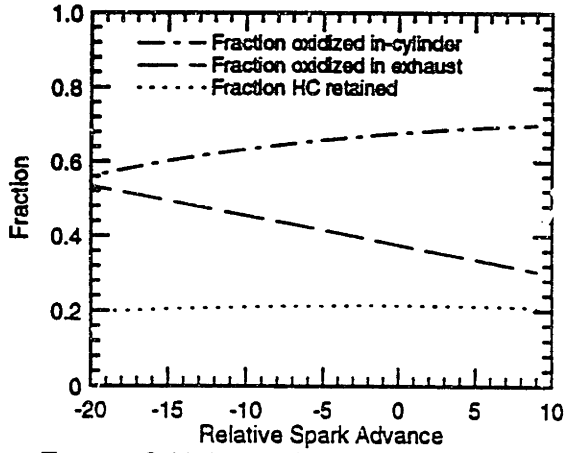

Figure c: Oxidation and Residual Mechanism Behavior

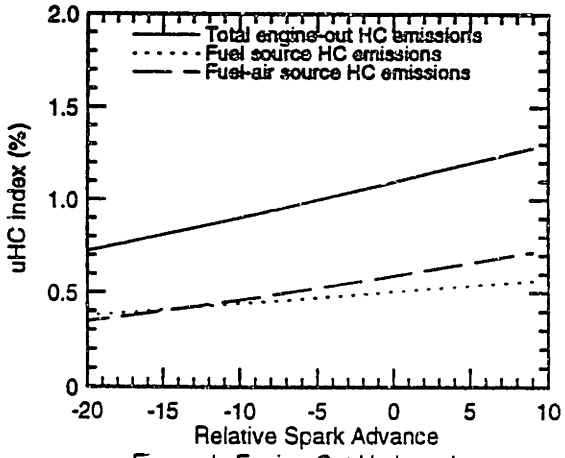

Figure d: Engine-Out Hydrocarbons

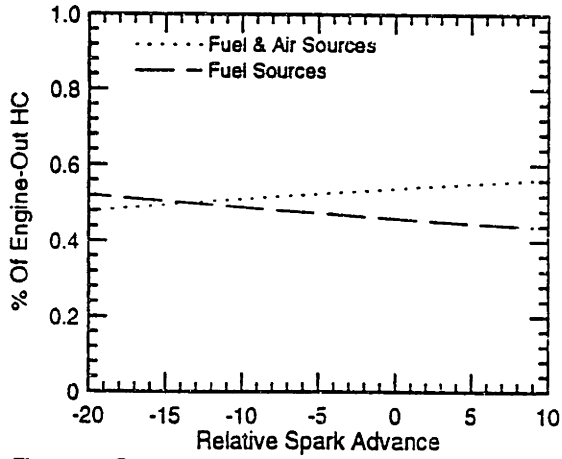

Figure e: Percentage Contribution to Eng-out HC Emissions

Figure 5.4 Spark timing relative to MBT (spark-MBT) effects on engine-out HC emissions for a 3.3L engine. (a) Fuel-air source process break-up, (b) Fuel source process break-up, (c) oxidation and residual model behavior, (d) total engine-out HC emissions, (e) percentage contribution from fuel and fuel-air sources to total HC emissions.

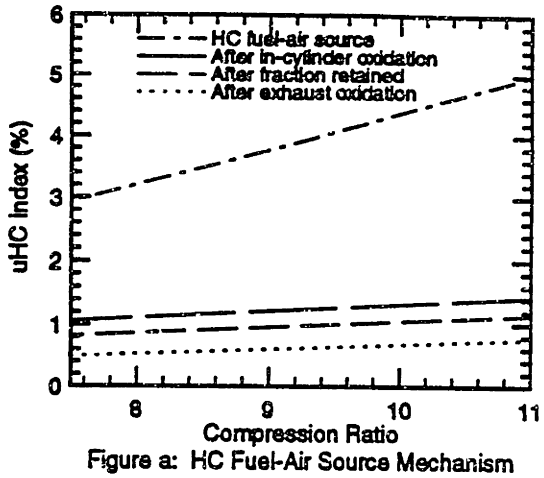

Figure a: HC Fuel-Air Source Mechanism

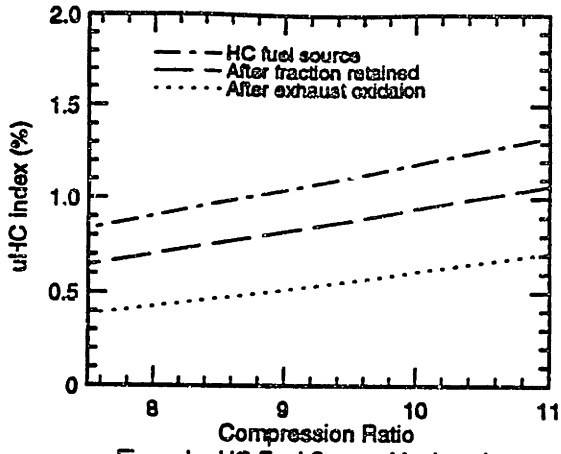

Figure b: HC Fuel Source Mechansims

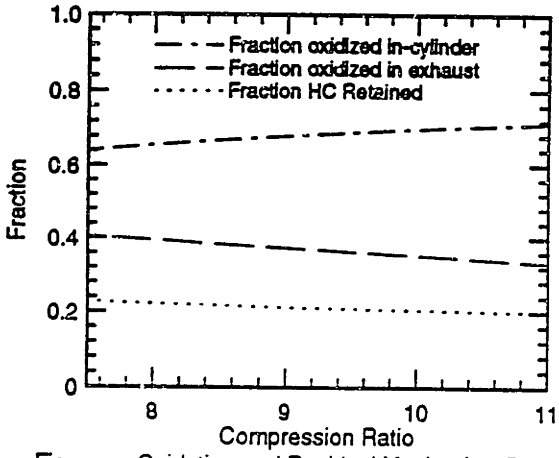

Figure c: Oxidation and Residual Mechanism Behavior

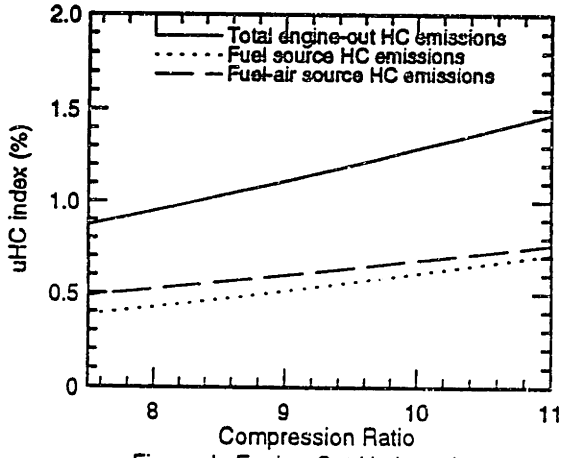

Figure d: Engine-Out Hydrocarbons

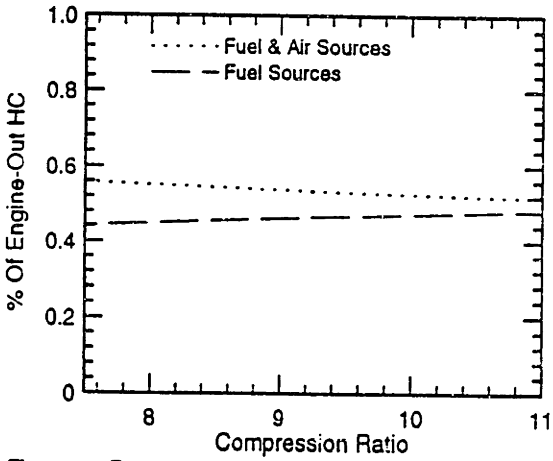

Figure e: Percentage Contribution to Eng-out HC Emissions

Figure 5.5 Compression ratio effects on engine-out HC emissions for a 3.3L engine. (a) Fuel-air source process break-up, (b) Fuel source process break-up, (c) oxidation and residual model behavior, (d) total engine-out HC emissions, (e) percentage contribution from fuel and fuel-air sources to total HC emissions.

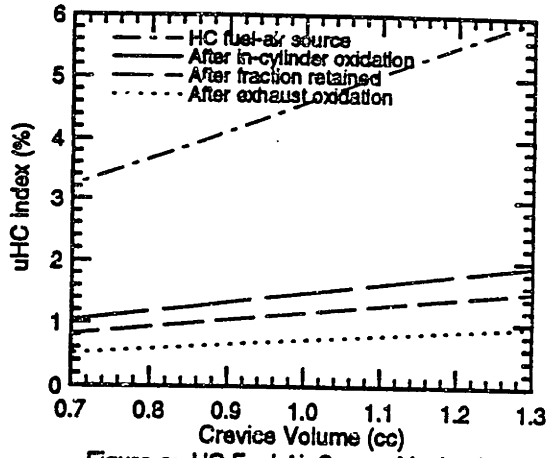

Figure a: HC Fuel-Air Source Mechanism

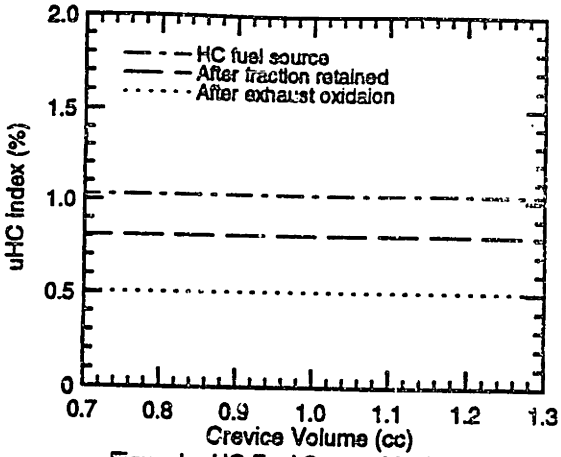

Figure b: HC Fuel Source Mechansims

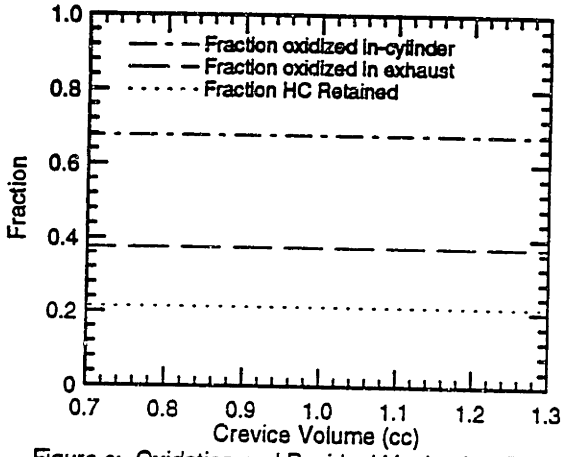

Figure c: Oxidation and Residual Mechanism Behavior

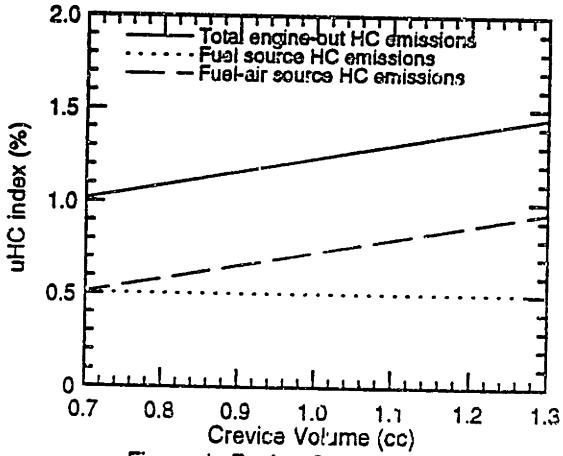

Figure d: Engine-Out Hydrocarbons

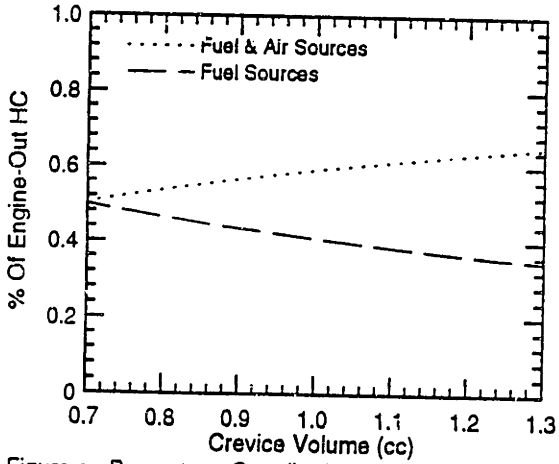

Figure e: Percentage Contribution to Eng-out HC Emissions

Figure 5.6 Crevice volume effects on engine-out HC emissions model for a 3.3L engine. (a) Fuel-air source process break-up, (b) Fuel source process break-up, (c) oxidation and residual model behavior, (d) total engine-out HC emissions, (e) percentage contribution from fuel and fuel-air sources to total HC emissions.

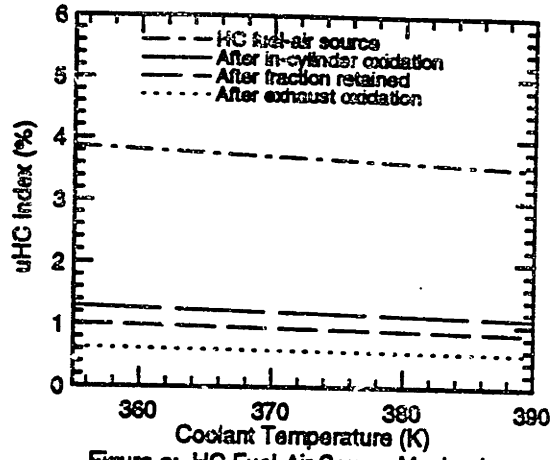

Figure a: HC Fuel-Air Source Mechanism

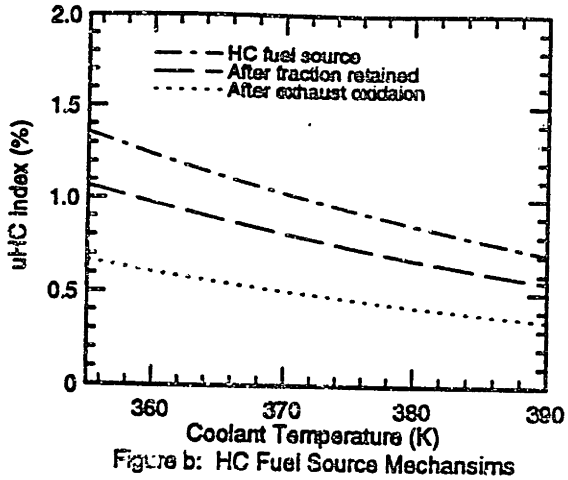

Figure b: HC Fuel Source Mechansims

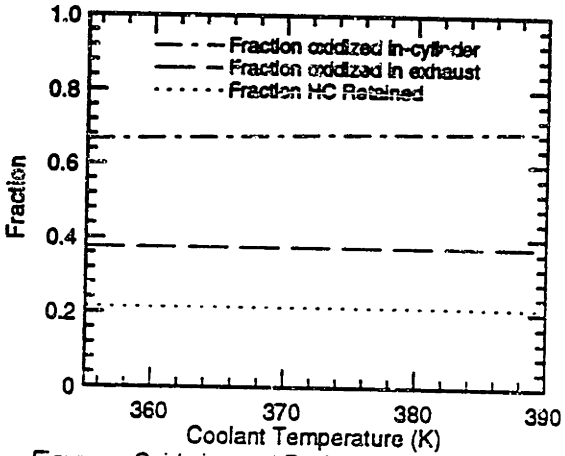

Figure c: Oxidation and Residual Mechanism Behavior

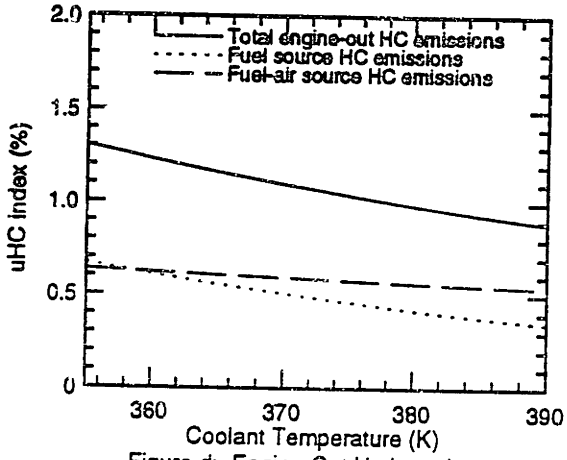

Figure d: Engine-Out Hydrocarbons

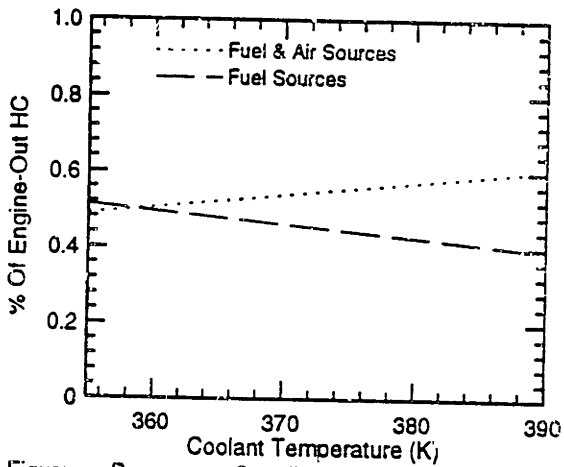

Figure e: Percentage Contribution to Eng-out HC Emissions

Figure 5.7 Coolant temperature effects on engine-out HC emissions model for a 3.3L engine. (a) Fuel-air source process break-up, (b) Fuel source process break-up, (c) oxidation and residual model behavior, (d) total engine-out HC emissions, (e) percentage contribution from fuel and fuel-air sources to total HC emissions.

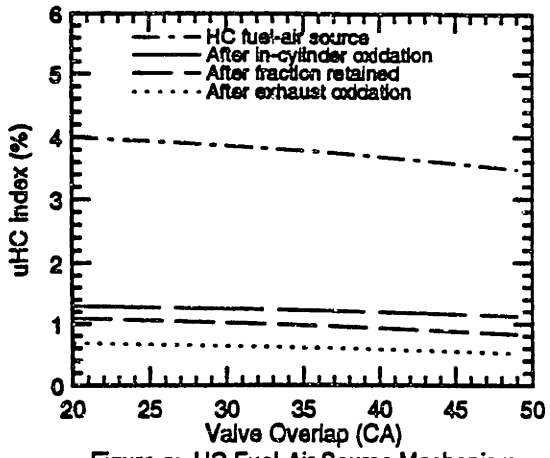

Figure a: HC Fuel-Air Source Mechanism

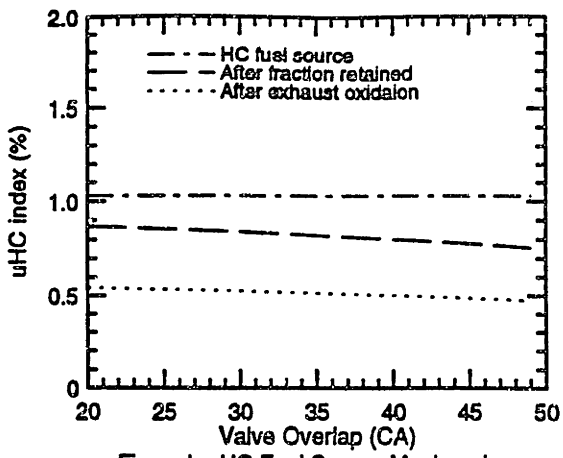

Figure b: HC Fuel Source Mechansims

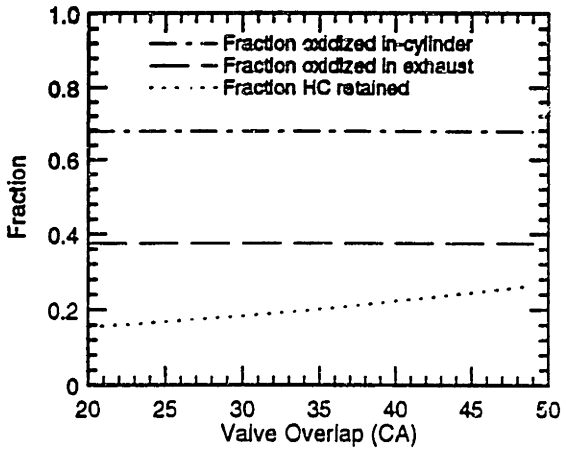

Figure c: Oxidation and Residual Mechanism Behavior

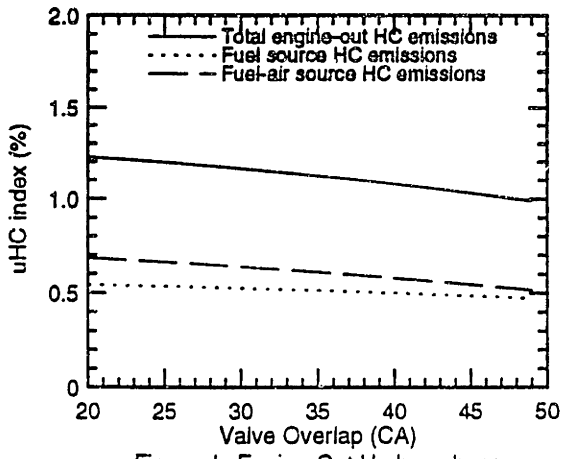

Figure d: Engine-Out Hydrocarbons

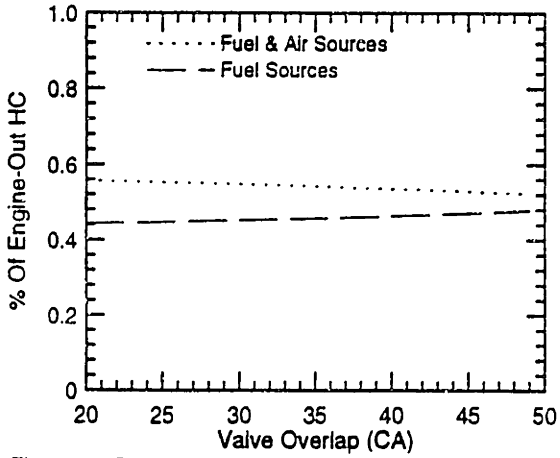

Figure e: Percentage Contribution to Eng-out HC Emissions

Figure 5.8 Valve overlap effects on engine-out HC emissions model for a 3.3L engine. (a) Fuel-air source process break-up, (b) Fuel source process break-up, (c) oxidation and residual model behavior, (d) total engine-out HC emissions, (e) percentage contribution from fuel and fuel-air sources to total HC emissions.

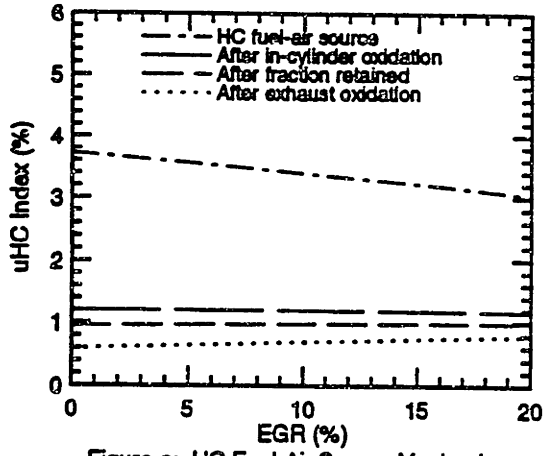

Figure a: HC Fuel-Air Source Mechanism

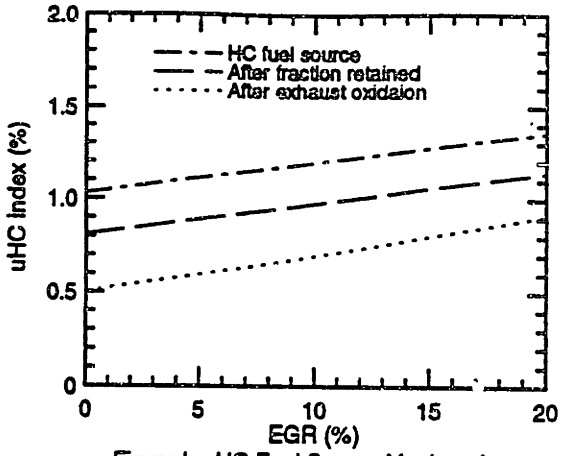

Figure b: HC Fuel Source Mechansims

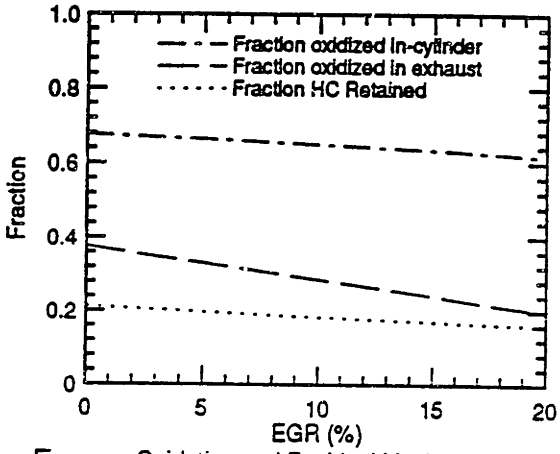

Figure c: Oxidation and Residual Mechanism Behavior

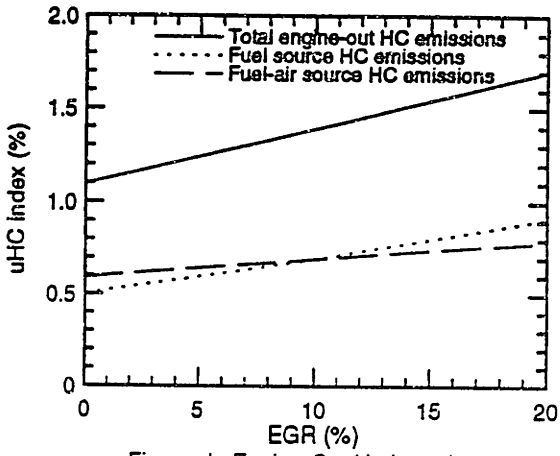

Figure d: Engine-Out Hydrocarbons

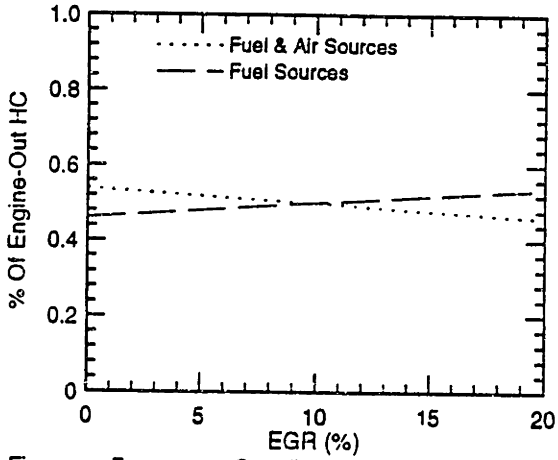

Figure e: Percentage Contribution to Eng-out HC Emissions

Figure 5.9 EGR effects on engine-out HC emissions model for a 3.3L engine. (a) Fuel-air source process break-up, (b) Fuel source process break-up, (c) oxidation and residual model behavior, (d) total engine-out HC emissions, (e) percentage contribution from fuel and fuel-air sources to total HC emissions.

REFERENCES

[1] Cheng. W.K., Hamrin, D., Heywood, J.B., Hochgreb, S., Min, K.D., and Norris, M., "An Overview of Hydrocarbon Emissions Mechanisms in Spark-Ignition Engines, " SAE paper 932708, 1993.

[2] Fox, J.W., Cheng, W.K., Heywood, J.B., "A Model for Predicting Residual Gas Fraction in Spark-Ignition Engines," SAE paper 931025, 1993.

[3] Heywood, J.B., Internal Combustion Engine Fundamentals,, McGraw-Hill, Inc., New York, 1988.

[4] Namazian, M., and Heywood, J.B., "Flow in the Piston-Cylinder-Ring Crevices of a Spark-Ignition Engine: Effect on Hydrocarbon Emissions, Efficiency and Power," SAE paper 820088, 1982.

[5] Min, K.D., and Cheng, W.K., "In-Cylinder Oxidation of Piston-Crevice Hydrocarbon in SI Engines," 3rd International Symposium of Diagnostics and Modeling of Combustion in Internal Combustion Engines (COMODIA), 1994.

[6] Min, K.D., "The Effects of Crevices on the Engine-Out Hydrocarbon Emissions in Spark-Ignition Engines", Ph.D. Thesis, Department of Mechanical Engineering, Massachusetts Institute of Technology, 1994.

[7] Patton, K.J., "Development and Evaluation of a Performance and Efficiency Model for Spark-Ignition Engines", S.M. Thesis, Deparatment of Mechanical Engineering, Massachusetts Institute of Technology, 1985.

[8] Ishizawa, S. and Takagi, Y., "A Study of HC Emissions from a Spark Ignition Engine" (The Influence of Fuel Absorbed in to Cylinder Lubricating Oil Film), JSME International Journal, Vol. 30, No. 260. 1987.

[9] Gatellier, B., Trapy, J., Herrier D., Quenlin, J.M., and Galliot, F., " Hydrocarbon Emissions of SI Engines as Influenced by Fuel Absorption-Desorption in Oil Films," SAE paper 920095, 1992.

[10] Boam, D.J., Finlay, I.C., Biddulph, T.W., Ma, T., Lee, R., Richardson, S.H., Bloomfield, J., Green, J.A., Wallace, S., and Woods, W.A., "The Sources of Unburnt Hydrocarbon Emissions from Spark Ignition Engines During Cold Satarts and Warm-Up," IMechE paper C448/064, Institution of Mechanical Engineers Conference Proceedings, 1992.

[11] Dent, J.C. and Lakshminarayanan, P.A., "A Model for Absorption and Desorption of Fuel Vapour by Cylinder Lubricating Oil Films and Its Contribution to Hydrocarbon Emissions," SAE paper 830652, 1983.

[12] Schramm, J. and Sorenson, S.C., "Effects of Lubricating Oil on Hydrocarbon Emissions in an SI Engine," SAE 890622, 1989.

[13] Yang, J., Kaiser, E.W., Siegl, W.O., and Anderson, R.W., "Effects of Port-Injection Timing and Fuel Droplet Size on Total and Speciated Exhaust Hydrocarbon Emissions," SAE paper 930711, 1993.

[14] LoRusso, J.A., Kaiser, E.W., and Lavoie, G.A., " In-Cylinder Measurements of Wall Layer Hydrocarbons in A Spark Ignited Engine," Combustion Science and Technology, Vol. 33, pp 75-112, 1983.

[15] Valtadoros, T.H., Wong, V.W., and Heywood, J.B., "Fuel Additive Effects on Deposits Build-Up and Engine Operating Characteristics," ACS Preprints, Vol. 36, No. 1, Symposium on Fuel Composition/Deposits Formation Tendencies, Division of Petroleum Chemistry, American Chemical Society, Atlanta, April 14-19, 1991.

[16] Weiss, P. and Keck, J.C., "Fast Sampling Valve Measurements of Hydrocarbons in the Cylinder of a CFR Engine," SAE paper 810149, 1981

[17] Tamura, T. and Hochgreb, S., "Chemical Kinetic Modeling of the Oxidation of Unburned Hydrocarbons," SAE paper 922235, 1992.

[18] Tabaczynski, R.J., Hoult, D.P., and Keck, J.C., "High Reynolds Number Flow in a Moving Corner," J. Fluid Mech, 42, pp. 249-255, 1970.

[19] Caton, J.A., Heywood, J.B., and Medillo, J.V., "Hydrocarbon Oxidation in a Spark Ignition Engine Exhaust Port," Combustion Science & Technology, Vol. 37, Nos. 3 & 4, pp. 153-169, 1984.

[20] Drobot, K., "Hydrocarbon Oxidation in the Exhaust Port and Runner of a Spark Ignition Engine," S.M. Thesis, Department of Mechanical Engineering Massachusetts Institute of Technology, 1994.

[21] Kaplan, J.A. and Heywood, J.B., "Modeling the Spark Ignition Engine Warm-Up Process to Predict Component Temperatures and Hydrocarbon Emissions," SAE paper 910302, 1991.

[22] Cheng, C-O., Cheng, W.K., Heywood, J.B., Maroteaux, D., and Collings., N., "Intake Port Phenomena in a Spark-Ignition Engine at Part Load," SAE paper 912401, 1991.

[23] Meernik, P., and Alkidas, A., "Impact of Exhaust Valve Leakage on Engine-Out Hydrocarbon," SAE paper 932752, 1993.

[24] Heywood, J. B., Higgins, J. M., Watts, P. A. and Tabaczynski, R. J., "Development and Use of a Cycle Simulation to Predict SI Engine Efficiency and NO_X Emissions", SAE paper 790291, 1979.

APPENDIX A: NORMALIZED MODELS

Normalized models were developed to describe behavior that occurs during constant load spark loops (BMEP = 241 kPa). The models are used as multipliers of the base values that are functions of IMEP. Cycle simulations were performed to obtain data for operating conditions such as spark timing, EGR and compression ratio. Then the following parameters were normalized reference values for these operating conditions.

1. temperature at 70 CA ATC
2. pressure at 70 CA ATC
3. inlet pressure
4. mass of fuel per cycle
5. maximum cylinder pressure

A.1 Effect of Changes in Spark Timing from MBT Timing

The parameters were normalized to their value at maximum brake torque (MBT) spark timing. MBT was defined at the point of minimum mass of fuel per cycle at fixed BMEP. Each parameter was normalized as follows with spark timing in degree crank angles:

$$\text{Relative Spark} = \text{Spark Timing} - \text{MBT Timing}$$

$$\text{Parameter} = \frac{\text{Parameter}}{\text{Parameter@ MBT}}$$

Figure A.1, A.2 and A.3 presents the normalized models:

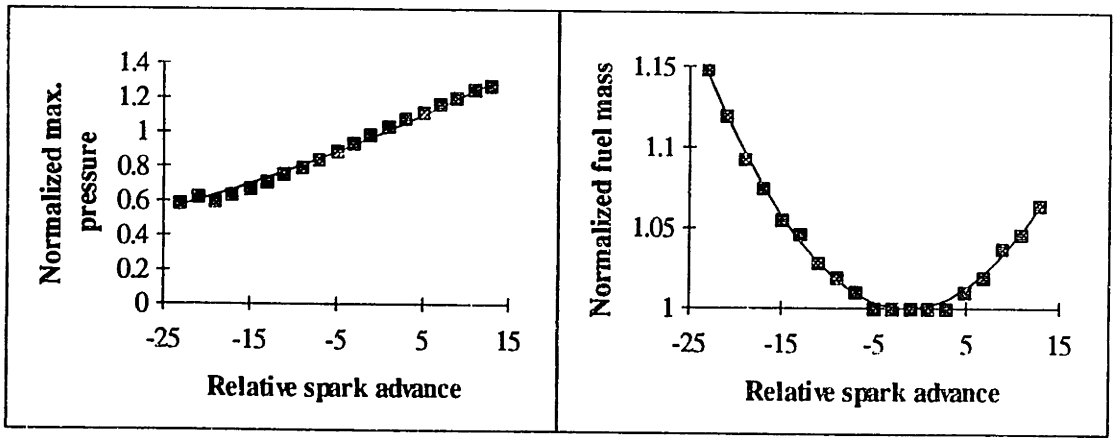

Figure A.1 Normalized models of maximum cylinder pressure and mass of fuel per cycle with respect to relative spark advance. Data generated from the MIT cycle simulation at BMEP = 241 kPa, 1600 rpm , and stoichiometric operation.

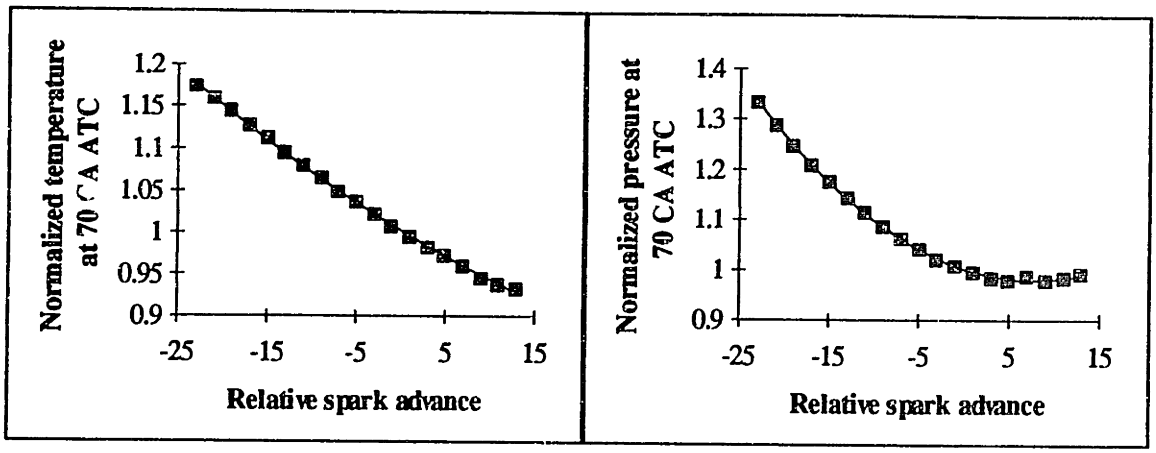

Figure A.2 Normalized models of temperatures and pressures at 70 CA ATC with respect to relative spark advance. Data generated from the MIT cycle simulation at BMEP = 241 kPa, 1600 rpm , and stoichiometric operation.

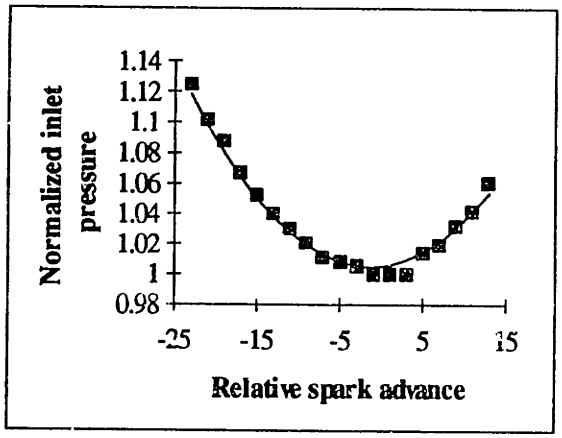

Figure A.3 Normalized model of the inlet pressure with respect to relative spark advance. Data generated from the MIT cycle simulation at BMEP = 241 kPa, 1600 rpm , and stoichiometric operation.

Normalized model equations as functions of relative spark timing are listed below.

$$m_{f,ns} = \frac{m_f}{m_f @ MBT} = 1.00 + 7.18\times10^{-4}\,\text{Relspark} + 2.96\times10^{-4}\,\text{Relspark}^2$$

$$p_{max,ns} = \frac{p_{max}}{p_{max} @ MBT} = 1.00 + 0.0208\,\text{Relspark} + 7.34\times10^{-4}\,\text{Relspark}^2$$

$$T_{70\ CA\ ATC,ns} = \frac{T_{70\ CA\ ATC}}{T_{70\ CA\ ATC} @ MBT} = 1.00 - 5.53\times10^{-3}\,\text{Relspark} + 8.84\times10^{-4}\,\text{Relspark}^2$$

$$p_{70\ CA\ ATC,ns} = \frac{p_{70\ CA\ ATC}}{p_{70\ CA\ ATC} @ MBT} = 1.00 - 4.84\times10^{-3}\,\text{Relspark} + 3.53\times10^{-4}\,\text{Relspark}^2$$

$$p_{i,ns} = \frac{p_{inlet}}{p_{inlet}@MBT} = 1.00 + 6.1\times10^{-4}\,\text{Relspark} + 2.41\times10^{-4}\,\text{Relspark}^2$$

where,

$m_{f,ns}$ = mass of fuel per cycle normalized to MBT timing
$p_{max,ns}$ = maximum cylinder pressure normalized to MBT timing
$T_{70\ CA\ ATC,ns}$ = temperature at 70 CA ATC normalized to MBT timing
$p_{70\ CA\ ATC,ns}$ = pressure 70 CA ATC normalized to MBT timing
$p_{i,ns}$ = inlet pressure normalized to MBT timing
Relspark = spark - MBT timing

A.2 Effect of EGR

Normalized equations were developed to model the behavior of inlet pressure temperature at 70 CA ATC and pressure at 70 CA ATC with respect to EGR. As mentioned before these model are multiplied by the equation that determines the magnitude of each quantity at a given load to adjust for EGR conditions. The parameters were normalized as follows:

$$\text{Normalized Parameter} = \frac{\text{Parameter}}{\text{Parameter@ Zero EGR}}$$

Figures A.4 and 5 presents the normalized relationships:

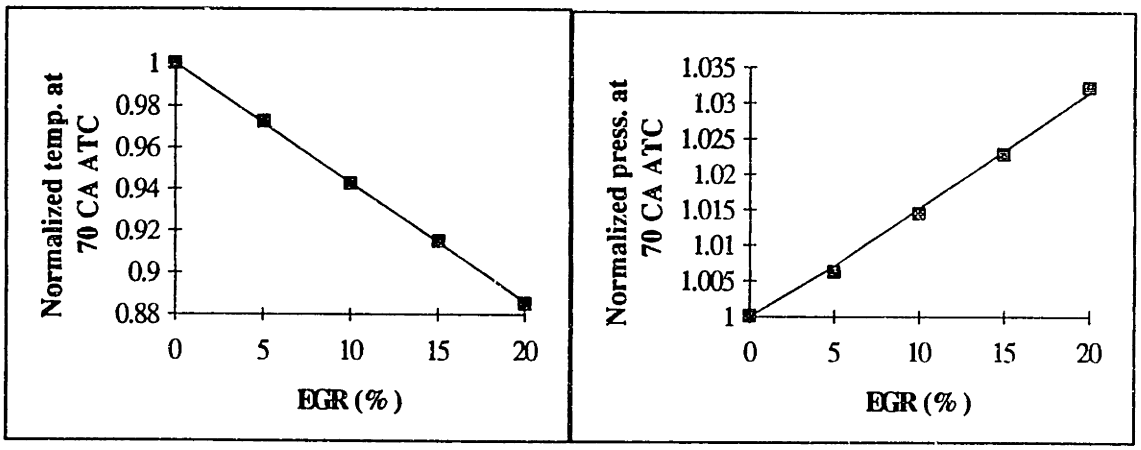

Figure A.4 Normalized model of the temperature and pressure at 70 CA ATC as a function of EGR at MBT spark timing. Data generated from the MIT cycle simulation at BMEP = 241 kPa, 1600 rpm , and stoichiometric operation.

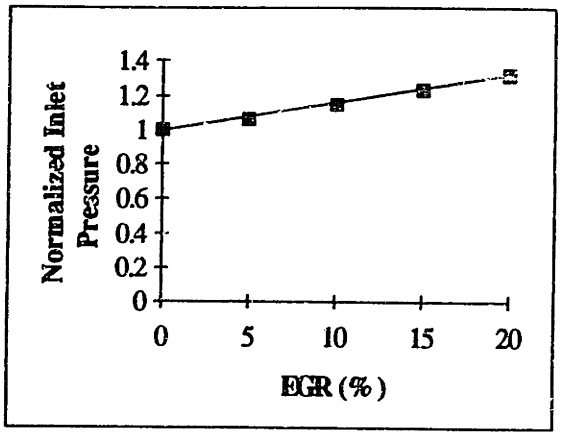

Figure A.5 Normalized model of the inlet pressure as a function of EGR at MBT spark timing. Data generated from the MIT cycle simulation at BMEP = 241 kPa, 1600 rpm, and stoichiometric operation.

Normalized model equations with respect to EGR (in %) are listed below.

$$p_{i,negr} = \frac{p_{inlet}}{p_{inlet}@\ \text{"0" EGR}} = 0.016EGR + 1.00$$

$$T_{70\ CA\ ATC,negr} = \frac{T_{70\ CA\ ATC}}{T_{70\ CA\ ATC}@\ \text{"0" EGR}} = -0.0057EGR + 1.00$$

$$p_{70\ CA\ ATC,negr} = \frac{p_{70\ CA\ ATC}}{p_{70\ CA\ ATC}@\ \text{"0" EGR}} = 0.0016EGR + 1.00$$

where, $T_{70\ CA\ ATC,negr}$ = temperature at 70 CA ATC normalized to zero EGR
$p_{70\ CA\ ATC,negr}$ = pressure at 70 CA ATC normalized to zero EGR
$p_{i,negr}$ = inlet pressure normalized to zero EGR at MBT

A.3 Effect of Changes in Compression Ratio

Normalized equations were developed to model the behavior of maximum cylinder pressure, mass of fuel per cycle, temperature at 70 CA ATC, pressure at 70 CA ATC, and inlet pressure with respect to compression ratio. The models were normalized to a compression ratio of 9.3 (i.e. "0" on graph indicates a compression ration of 9.3). As mentioned before these models are multiplied by the equation that determines the value of each quantity at a given load. The parameters were normalized as follows:

$$\text{Normalized Parameter} = \frac{\text{Parameter}}{\text{Parameter}@\ r_c = 9.3}$$

Figure A.6 - A.8 present normalized as a function of relative compression ratio change for maximum cylinder pressure, mass of fuel per cycle, temperatures at 70 CA ATC, pressure at 70 CA ATC, and inlet pressure.

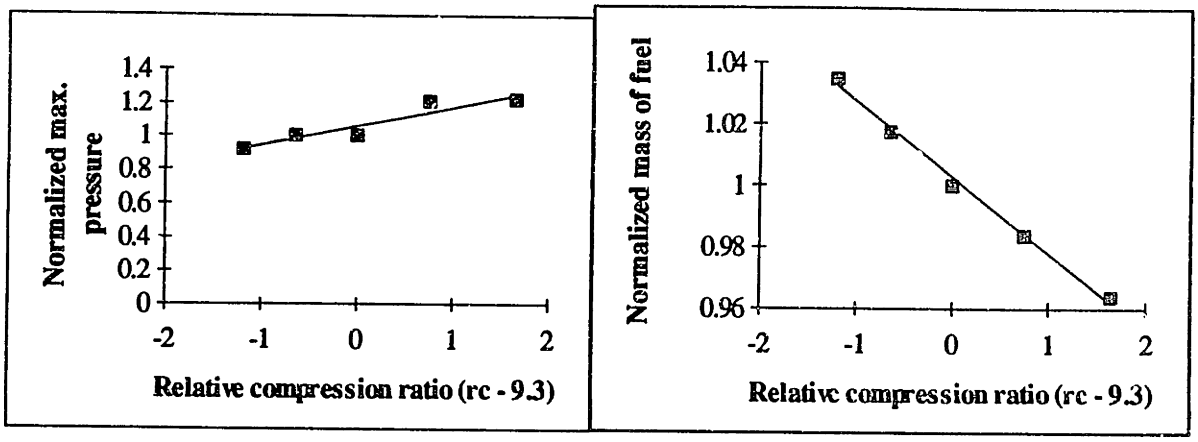

Figure A.6 Normalized models of the maximum cylinder pressure and mass of fuel per cycle as a function of a relative compression ratio of 9.3 at MBT spark timing. The data was generated from the MIT cycle simulation at BMEP = 241 kPa, 1600 rpm, and stoichiometric operation.

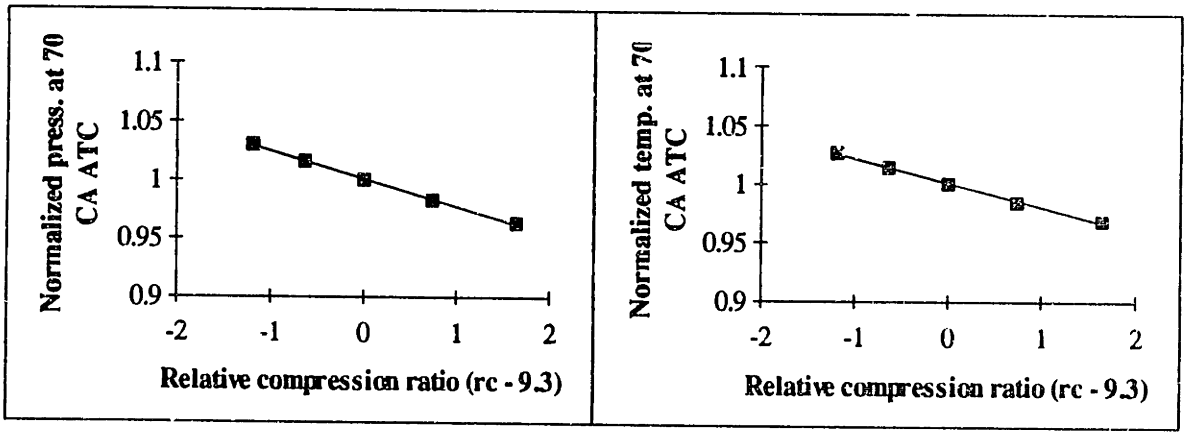

Figure A.7 Normalized models of the temperature and pressure at 70 CA ATC as a function of a relative compression ratio of 9.3 at MBT spark timing. The data was generated from the MIT cycle simulation at BMEP = 241 kPa, 1600 rpm, and stoichiometric operation.

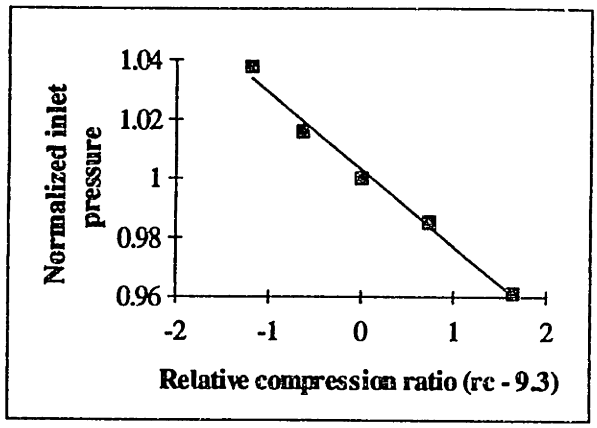

Figure A.8 Normalized model of the inlet pressure as a function of a relative compression ratio of 9.3 at MBT spark timing. The data was generated from the MIT cycle simulation at BMEP = 241 kPa, 1600 rpm, and stoichiometric operation.

Normalized model equations with respect to compression ratio are listed below.

$$p_{max,nrc} = 0.1155(r_c - 9.3) + 1.0591$$

$$m_{f,nrc} = -0.02481(r_c - 9.3) + 1.0027$$

$$T_{70\ CA\ ATC,nrc} = -0.02073(r_c - 9.3) + 1.0014$$

$$p_{70\ CA\ ATC,nrc} = -0.0236(r_c - 9.3) + 1.0012$$

$$p_{inlet,nrc} = -0.02589(r_c - 9.3) + 1.0030$$

where, $m_{f,nrc}$= mass of fuel per cycle normalized to compression ratio
$p_{max,nrc}$ = maximum cylinder pressure normalized to compression ratio
$T_{70\ CA\ ATC,nrc}$= temp. at 70 CA ATC normalized to compression ratio
$p_{70\ CA\ ATC,nrc}$ = pressure at 70 CA ATC normalized to compression ratio
$p_{i,nrc}$ = inlet pressure normalized to compression ratio

A.4 Effect of Coolant Temperature Changes

Normalized equations were developed to model the behavior of mass of fuel per cycle, inlet pressure, temperature at 70 CA ATC, and pressure at 70 CA ATC. The maximum cylinder pressure remained constant for coolant temperature variations. This reference value was chosen arbitrarily so the data could be normalized. Cycle simulations did not have a coolant temperature input. Thus the component temperatures were varied assuming that the coolant temperature was directly proportional. A reference coolant temperature of 365 K was chosen and the models were normalized to this value. The models were normalized as follows.

$$\text{Normalized Parameter} = \frac{\text{Parameter}}{\text{Parameter@ } T_{cool} = 365 \text{ K}}$$

Figure A.9 and A.10 present the normalized models.

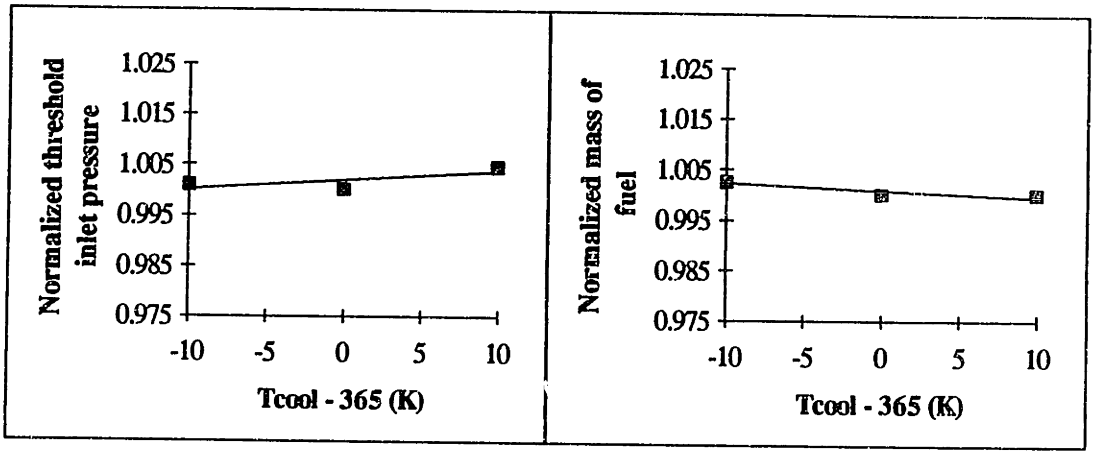

Figure A.9 Normalized models of the inlet pressure and mass of fuel per cycle as a function of a reference coolant temperature of 365 K at MBT spark timing. The data was generated from the MIT cycle simulation at BMEP = 241 kPa, 1600 rpm, and stoichiometric operation.

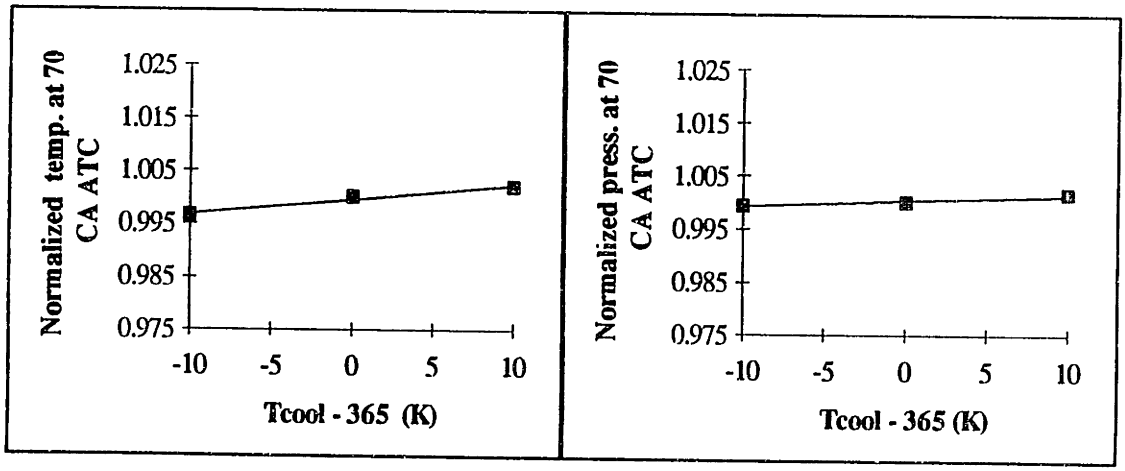

Figure A.10 Normalized models of the temperature and pressure at 70 CA ATC as a function of a reference coolant temperature of 365 K at MBT spark timing. The data was generated from the MIT cycle simulation at BMEP = 241 kPa, 1600 rpm, and stoichiometric operation.

Normalized model equations with respect to coolant temperature are listed below.

$$m_{f,ncool} = -0.00014(T_{cool} - 365) + 1.001$$

$$p_{i,ncool} = 0.000183(T_{cool} - 365) + 1.002$$

$$T_{70\ CA\ ATC,ncool} = 0.000276(T_{cool} - 365) + 1.000$$

$$p_{70\ CA\ ATC,ncool} = 0.000101(T_{cool} - 365) + 1.001$$

where, $m_{f,ncool}$= mass of fuel per cycle normalized to coolant temperature
$p_{i,ncool}$ = inlet pressure normalized to coolant temperature
$T_{70\ CA\ ATC,ncool}$ = temperature at 70 CA ATC normalized to coolant temperature
$p_{70\ CA\ ATC,ncool}$ = pressure at 70 CA ATC normalized to coolant temperature

APPENDIX B: SUMMARY OF ENGINE GEOMETRIC DATA

Table B.1 Engine Geometric Data

Number of Cylinders	6	4	4	4	6
Displacement Volume (L)	3.3	2.0	2.2	2.5	3.5
Bore (mm)	93	87.5	87.5	87.5	96
Stroke (mm)	81	83	92	104	81
Compression Ratio	7.5 - 8.9	8.3 - 9.3	8.9	9	9.9
Number of Valves per Cylinder	2	4	2	2	4
Valve Diameters					
Intake (mm)	45.5	35.5	40.6	40.6	35
Exhaust (mm)	37.5	30.5	35.4	35.4	29
Maximum Lift					
Intake (mm)	10.16 - 10.20	8.49	10.92	10.92	8.15
Exhaust (mm)	10.16 - 10.20	8.59	10.92	10.92	6.53
Valve Overlap (CA)	34 - 38	25	32	32	23
Crevice Volume (cc)	0.677 - 0.899	0.406 - 0.820	1.241	1.241	0.847 - 0.984
Spark Plug Offset (mm)	17	1	16	16	1

APPENDIX C: TOTAL HC EMISSIONS MODEL

C.1 Model Structure

$$HC_{engine-out} = C_1 C_5 S_{HC,fuel-air}(1-f_{ret,cyl})(1-C_6 f_{oxi,exh}) - C_2 C_5 C_7 S_{HC,fuel-air} f_{oxi,cyl}(1-f_{ret,cyl})(1-C_6 f_{oxi,exh}) + C_3 S_{HC,fuel}(1-f_{ret,cyl})(1-C_6 f_{oxi,exh})$$

C.2 Model Equations

C.2.1 Fuel-Air Source Term

$$S_{HC,fuel-air} = 5443\left(\frac{p_{max}}{IMEP}\right)\left(\frac{V_{crev}}{V_d}\right)\left(\frac{1}{T_{cool}}\right)(1-x_r-EGR)\left(\frac{1}{1+A/F}\right)\left(-0.429\left(\frac{2\ Plug}{B}\right)+1.0\right)\left(\frac{p_{max,nor}}{m_{f,nor}}\right)$$

where, $p_{max,nor}$ = normalized maximum cylinder pressure equations
$m_{f,nor}$ = normalized mass of fuel per cycle equaitons
p_{max} (atm) = 1.2276 + 0.0568 IMEP (kPa)

The normalized equations for compression ratio, spark timing, EGR, and coolant temperature are summarized in Appendix A.

C.2.2 Fuel Source Term

$$S_{HC,fuel} = 63024\left(\frac{1}{IMEP}\right)\left(\frac{F/A}{10^{0.0082\,T_{cool}}B}\right)\left(\frac{p_i + p_i r_c^{\gamma}}{2}\right)\frac{p_{i,nor}}{m_{f,nor}}$$

where, $p_{i,nor}$ = normalized inlet pressure equations
p_i (atm) = 0.09875 + 0.00986 IMEP (kPa)

The normalized equations for compression ratio, spark timing, EGR, and coolant temperature are summarized in Appendix A.

C.2.3 In-Cylinder Oxidation Term

$$f_{oxi,cyl} = 1 - \frac{p_{70\ CA\ ATC}}{p_{max}}\left(\frac{980(T_{70\ CA\ ATC}T_{70\ CA\ ATC,nor} - T_{cool})}{\ln(T_{70\ CA\ ATC}T_{70\ CA\ ATC,nor}/T_{cool})}\right)^{3.0}\frac{p_{70\ CA\ ATC,nor}}{p_{max,nor}}$$

where, $T_{70\ CA\ ATC}$ = temperature at 70 CA ATC
$T_{70\ CA\ ATC,nor}$ = normalized temperature at 70 CA ATC equations
$p_{70\ CA\ ATC}$ = pressure at 70 CA ATC
$p_{70\ CA\ ATC,nor}$ = normalized pressure at 70 CA ATC equations

$$P_{70\,CA\,ATC}\,(atm) = 0.209 + 0.0102\,IMEP\,(kPa)$$
$$T_{70\,CA\,ATC}\,(atm) = 1600 + 0.759\,IMEP - 0.00051\,IMEP\,(kPa)^2$$

The normalized equations for compression ratio, spark timing, EGR, and coolant temperature are summarized in Appendix A.

C.2.4 Residual HC Term

$$OF = \frac{1.45}{B}(107 + 7.8\Delta\Theta + \Delta\Theta^2)\frac{L_{v,max}D_v}{B^2}$$

$$x_r = f_{ret,cyl} = 1.266\frac{OF}{N}\left(\frac{p_i p_{i,nor}}{p_e}\right)^{-0.87}\sqrt{|p_e - p_i p_{i,nor}|} + 0.632\frac{\Phi(p_i p_{i,nor}/p_e)^{-0.74}}{r_c}$$

C.2.5 Exhaust Oxidation Term

$$f_{oxi,exh} = 0.866 - 0.000148(N + N_e + N_{e'}) - 0.0007IMEP$$
$$-0.00791(Relsp + Relsp_e + Relsp_{e'}) - 0.0000255T_{cool}$$

$$N_{e'} = -0.0245(r_c - 9.0)N \qquad Relsp_{e'} = 3.323(r_c - 9.0)$$

$$N_e = N\frac{EGR\%}{100} \qquad Relsp_e = 0.829\frac{EGR\%}{100}$$

C.3 Regression Constant Summary

Table C.1 Summary of Regression Constants

Engine	C1	C2	C3	C4	C5	C6	C7
3.3L	0.717	0.635	0.747	0.000	1.0	1.0	1.0
2.5L	0.717	0.635	0.747	0.000	1.0	1.0	1.0
2.2L	0.717	0.635	0.747	0.000	1.0	1.0	1.0
2.0L	0.717	0.635	0.747	0.000	1.392	0.480	1.030
3.5L	0.717	0.635	0.747	0.000	1.049	1.058	0.947

C.4 Summary of Model Input Variables

Table C.2 Model Input Summary

Input	Units	Notes
Number of Cylinders		
Compression Ratio		
Displacement Volume	liters	
Bore	millimeters	
Stroke	millimeters	
Crevice Volume	cubic centimeters	
Number of Valves per cylinder		
Intake Valve Diameter	millimeters	
Exhaust Valve Diameter	millimeters	
Intake Valve Max. Lift	millimeters	
Exhaust Valve Max. Lift	millimeters	
Valve Overlap	crank angles	events defined at 0.15mm lift
Coolant Temperature	millimeters	
Spark Plug Offset	millimeters	Measured from bore center

APPENDIX D: HC MODEL - FORTRAN PROGRAM

MODEL CONSTANTS ----> INPUT FILE = 'CON2'

```
 &MODCON
      C1 = 0.474
      C2 = 0.363
      C3 = 0.859
      C5 = 1.0
      C6 = 1.0
      C7 = 1.0
/
```

ENGINE SET-UP ----> INPUT FILE = 'ENGINE.INP'

```
 &INPUT
      CYL = 6.
      VD = 3.3
      RC = 8.9
      B = 93.
      S = 81.
      PLUG = 17.0
      NUMV=2.
      IVALDIA = 45.5
      EVALDIA = 37.5
      IMAXLIF = 10.16
      EMAXLIF = 10.16
      VO = 38.
      CREVVOL = 0.810
      EGR = 0.0
      TCOOL = 370.
      RELSPRKO = 0.0
/
```

FORTRAN PROGRAM

```
CCCCCCCCCCCCCCCCCCCCCCCCCCCCCCCCCCCCCCCCCCCCCCCCCCCCCCCCCCCCCCCCCCCCCCCCCCCCCCC
C
C     ENGINE-OUT HYDROCARBON EMISSIONS MODEL
C     MASSACHUSETTES INSTITUTE OF TECHNOLOGY
C     WRITTEN BY: DOUGLAS A. HAMRIN - MASTER'S OF SCIENCE IN
C                 MECHANICAL ENGINEERING THESIS @ MIT
C     DATE: AUGUST 5, 1994
C
CCCCCCCCCCCCCCCCCCCCCCCCCCCCCCCCCCCCCCCCCCCCCCCCCCCCCCCCCCCCCCCCCCCCCCCCCCCCCCC
C
C     THIS PROGRAM READS MODEL CONSTANTS FROM A FILE NAMED "CON2"
C     THE ENGINE CHARACTERISTICS CAN EITHER BE READ FROM
C     THE FILE "ENGINE.INP" DIRECTLY OR ENTERED MANUALLY.  BOTH
C     INPUT FILES MUST REMAIN IN THE ORGINAL FORMAT.
C
CCCCCCCCCCCCCCCCCCCCCCCCC  INPUT LIST  CCCCCCCCCCCCCCCCCCCCCCCCCCCCCCC
C
C     VD = DISPLACEMENT (liters)
C     CYL = NUMBER OF CYLINDERS
C     B = BORE (mm)
C     S = STROKE (mm)
C     RC = COMPRESSION RATIO
C     PLUG = SPARK PLUG OFFSET FROM BORE CENTER (mm)
C     IMAXLIF = MAXIMUM INTAKE VALVE LIFT (mm)
```

```
C      EMAXLIF = MAXIMUM EXHAUST VALVE LIFT (mm)
C      IVALDIA = INTAKE VALVE DIAMETER (mm)
C      EVALDIA = EXHAUST VALVE DIAMETER (mm)
C      EGR = EXHAUST GAS RECIRCULATION
C      TCOOL = COOALNT TEMPERATURE (kelvin)
C      CREVVOL = CREVICE VOLUME (mm)
C      VO = VALVE OVERLAP (IVO TO EVC) (CA)
C      RELSPRKO = RELATIVE SPARK TIMING TO MBT (SPARK - MBT) (CA)
C
CCCCCCCCCCCCCCCCCCCCCCCCCCCCCCCCCCCCCCCCCCCCCCCCCCCCCCCCCCCCCCCCCCCCCCCCCCC
C
       IMPLICIT REAL (A-Z)
       REAL VAR(50),POSTOXI(50),XR2(50),EXHMOD2(50),FASBPO(50)
      & ,FSBRES(50),FASAPO(50),FASARES(50),FSARES(50),FASOUT(50)
      & ,FS(50),UHCI(50),FAS(50)
       INTEGER ANS1,ANS2,ANS3,FLAG,J
       CHARACTER VARNAM1*35,VARNAM2*5,FILEOUT*8
       COMMON/GEOM/B,VD,CYL,RC,CREVVOL,PLUG
       COMMON/VALVE/IVALDIA,EVALDIA IMAXLIF,EMAXLIF,VO,NUMV
       COMMON/OPER/SPEED,TCOOL,EGR,RELSPRKO
       COMMON/MOD/FASMOD,FSMOD,XR,OXIMOD,EXHMOD,UHCI
       COMMON/MOD2/XR2,EXHMOD2
       COMMON/BREAK/FAS,FASOXI,FASOUT,FASAPO,FASARES,FASBPO,POSTOXI,
      &    FS,FSARES,FSBRES,J
       COMMON/CON/C1,C2,C3,C5,C6,C7
       NAMELIST/INPUT/CREVVOL,RC,B,S,IVALDIA,EVALDIA,IMAXLIF,EMAXLIF,
      &   VO,CYL,VD,TCOOL,NUMV,PLUG,EGR,RELSPRKO
       NAMELIST/MODCON/C1,C2,C3,C5,C6,C7
       OPEN(UNIT=6, STATUS ='UNKNOWN', FILE='ENGINE.INP')
       OPEN(UNIT=7, STATUS ='UNKNOWN', FILE='CON2')
       FLAG = 0
CCCCCCCCCCCCCCCCCCCCCCCCCCCCCCCCCCCCCCCCCCCCCCCCCCCCCCCCCCCCCCCCCCCCCCCCCCC
C
C      THIS SECTION READS IN THE ENGINE INPUT
C      THERE ARE TWO OPTIONS
C      1.     TEST A SINGLE TEST POINT
C      2.     VARY A MODEL INPUT PARAMETER
C
CCCCCCCCCCCCCCCCCCCCCCCCCCCCCCCCCCCCCCCCCCCCCCCCCCCCCCCCCCCCCCCCCCCCCCCCCCC
C
       WRITE(*,*) 'USE INPUT FILE FOR ENGINE GEOMETRY AND CONDITIONS ?'
       WRITE(*,*) 'ENTER "1" ----> YES OR "2" ----> NO'
       READ(*,*) ANS1
       READ(7,MODCON)
       IF (ANS1 .EQ. 1) THEN
             READ (6,INPUT)
       END IF
       WRITE(*,*) 'ENTER "1" FOR ONE TEST POINT'
       WRITE(*,*) 'ENTER "2" FOR MODEL INPUT VARIATION'
       READ(*,*) ANS2
C
CCCCCCCCCCCCCCCCCCCCCCCCCCCCCCCCCCCCCCCCCCCCCCCCCCCCCCCCCCCCCCCCCCCCCCCCCCC
C
C            MANUAL INPUT
C
CCCCCCCCCCCCCCCCCCCCCCCCCCCCCCCCCCCCCCCCCCCCCCCCCCCCCCCCCCCCCCCCCCCCCCCCCCC
C
       IF (ANS1 .EQ. 2) THEN
       WRITE(*,*)'ENTER ENGINE DISPLACEMENT IN liters '
       READ(*,*) VD
       WRITE(*,*)'ENTER NUMBER OF CYLINDERS'
       READ(*,*)CYL
       WRITE(*,*)'ENTER NUMBER OF VALVES PER CYLINDER'
       READ(*,*) NUMV
```

```
      WRITE(*,*)'ENTER BORE AND STROKE IN mm '
      READ(*,*) B,S
      WRITE(*,*)'ENTER COMPRESSION RATIO '
      READ(*,*) RC
      WRITE(*,*) 'ENTER CREVICE VOLUME IN cc '
      READ(*,*) CREVVOL
      WRITE(*,*) 'ENTER SPARK PLUG OFFSET FROM BORE CENTER IN mm '
      READ(*,*) PLUG
      WRITE(*,*) 'ENTER VALVE OVERLAP IN CA DEG.'
      READ(*,*) VO
      WRITE(*,*)'ENTER INTAKE & EXHAUST VALVE INNER SEAT DIA. IN mm'
      READ(*,*) IVALDIA,EVALDIA
      WRITE(*,*)'ENTER INTAKE AND EXHAUST VALVE MAXIMUM LIFT IN mm '
      READ(*,*) IMAXLIF,EMAXLIF
      WRITE(*,*) 'ENTER COOLANT TEMPERATURE IN K '
      READ(*,*) TCOOL
      WRITE(*,*) 'ENTER EGR AMOUNT (10% ENTER 0.1) '
      READ(*,*) EGR
      END IF
CCCCCCCCCCCCCCCCCCCCCCCCCCCCCCCCCCCCCCCCCCCCCCCCCCCCCCCCCCCCCCCCCCCCCCCCCC
C
C     SINGLE INPUT PARAMETER OUTPUT
C
CCCCCCCCCCCCCCCCCCCCCCCCCCCCCCCCCCCCCCCCCCCCCCCCCCCCCCCCCCCCCCCCCCCCCCCCCC
C
C     EXHMOD2(J) = DUMMY VARIABLE USED FOR COMPUTING EASE
C     XR2(J) = DUMMY VARIBLE FOR USED COMPUTING EASE
C
C     SUBROUTINE MODEL - PERFOMRS HC MODEL CALULATIONS
C     SUBROUTINE BREAKDOWN - BREAKSDOWN THE MODEL TO OBSERVE THE
C           BEHAVIOR OF THE INDIVIDUAL HC MECHANISMS.
C
      IF (ANS2 .EQ. 1) THEN
            CALL MODEL
            J=1
            EXHMOD2(J)=EXHMOD
            XR2(J) = XR
            CALL BREAKDOWN
C
CCCCCCCCCCCCC  SINGLE TEST POINT OUTPUT  CCCCCCCCCCCCCCCCCCCCCCCCCCCC
C
      WRITE(*,1000) CYL,VD,NUMV,RC,B,S,PLUG,CREVVOL,VO,TCOOL,RELSPRKO,
     & EGR*100,IVALDIA,EVALDIA,IMAXLIF,EMAXLIF
      WRITE(*,*)
      WRITE(*,*)
      WRITE(*,1007)
      WRITE(*,1008)
      WRITE(*,1015) POSTOXI(J)*100,XR2(J)*100,EXHMOD2(J)*C6*100
      WRITE(*,1020) FASBPO(J),FSBRES(J),FASAPO(J),FSBRES(J),FASARES(J)
     &  ,FSARES(J),FASOUT(J),FS(J),UHCI(J)
      WRITE(*,3000)
C
CCCCCCCCCCCCC  WRITE TO OUTPUT FILE OPTION  CCCCCCCCCCCCCCCCCCCCCCCC
C
      WRITE(*,*) 'DO YOU WANT TO WRITE THE OUTPUT TO A FILE'
      WRITE(*,*) 'TYPE "1" FOR YES OR "2" FOR NO'
      READ(*,*) ANS3
      IF (ANS3 .EQ. 1) THEN
      WRITE(*,*) 'ENTER FILE NAME MAXIMUM OF 8 CHARACTERS'
      READ(*,'(A8)') FILEOUT
      OPEN (UNIT = 8, STATUS = 'UNKNOWN', FILE = FILEOUT)
      WRITE(8,1000) CYL,VD,NUMV,RC,B,S,PLUG,CREVVOL,VO,TCOOL,RELSPRKO,
     & EGR*100,IVALDIA,EVALDIA,IMAXLIF,EMAXLIF
      WRITE(8,*)
```

```
      WRITE(8,*)
      WRITE(8,1007)
      WRITE(8,1008)
      WRITE(8,1015) POSTOXI(J)*100,XR2(J)*100,EXHMOD2(J)*C6*100
      WRITE(8,1020) FASBPO(J),FSBRES(J),FASAPO(J),FSBRES(J),FASARES(J)
     &  ,FSARES(J),FASOUT(J),FS(J),UHCI(J)
      WRITE(8,3000)
      END IF
      ELSE
C
CCCCCCCCCCCCCCCCCCCCCCCCCCCCCCCCCCCCCCCCCCCCCCCCCCCCCCCCCCCCCCCCCCCCCCCCCCC
C
C     MODEL INPUT VARIATION SECTION
C     ONE OF TEN INPUT PARAMETERS CAN BE VARIED
C           1 - COMPRESSION RATION
C           2 - CREVICE VOLUME (cubic centimeters)
C           3 - COOLANT TEMPERATURE (Kelvin)
C           4 - EXHAUST GAS RECIRCULATION (fraction)
C           5 - SPARK TIMING (spark - MBT) where minus is spark retard
C           6 - VALVE OVERLAP (crank angles)
C           7 - INLET VALVE DIAMETER  (mm)
C           8 - EXHAUST VALVE DIAMETER (mm)
C           9 - INLET VALVE MAXIMUM LIFT (mm)
C          10 - EXHAUST VALVE MAXIMUM LIFT (mm)
C
CCCCCCCCCCCCCCCCCCCCCCCCCCCCCCCCCCCCCCCCCCCCCCCCCCCCCCCCCCCCCCCCCCCCCCCCCCC
C
      WRITE (*,2000)
      WRITE(*,*)'INPUT THE NUMBER CORRESPONDING TO THE PARAMETER'
      READ(*,*) PARA
      WRITE(*,*)'ENTER NUMBER OF TEST POINTS'
      READ(*,*) TESTPT
C
CCCCCCCCCCCCC  THIS SECTION TESTS TO DETERMINE  CCCCCCCCCCCCCCCCCCCCC
CCCCCCCCCCCCC  WHICH PARAMETER TO VARY.         CCCCCCCCCCCCCCCCCCCCC
C
C     VAR(J) = PARAMETER IS SET TO THIS VARAIBLE
C     TESTPT = NUMBER TEST POINTS
C     EXHMOD2(J) = DUMMY VARIABLE USED FOR COMPUTING EASE
C     XR2(J) = DUMMY VARIBLE FOR USED COMPUTING EASE
C     FLAG = DETERMINES IF THE PROGRAM HAS GONE THRU THIS SECTION
C
C     SUBROUTINE BREAKDOWN - BREAKSDOWN THE MODEL TO OBSERVE THE
C           BEHAVIOR OF THE INDIVIDUAL HC MECHANISMS.
C     SUBROUTINE MODEL - PERFOMRS HC MODEL CALULATIONS
C
100   IF (PARA .EQ. 1) THEN
            IF (FLAG .EQ. 1) THEN
                  DO J=1,TESTPT
                        RC = VAR(J)
                        CALL MODEL
                        EXHMOD2(J)=EXHMOD
                        XR2(J) = XR
                        CALL BREAKDOWN
                  END DO
            ELSE
                  WRITE(*,*) 'ENTER COMPRESSION RATIO POINTS'
                  READ(*,*) (VAR(J),J=1,TESTPT)
                  VARNAM1 = ' COMPRESSION RATIO'
                  VARNAM2 = '  RC'
            ENDIF
      ELSEIF (PARA .EQ. 2) THEN
            IF (FLAG .EQ. 1) THEN
                  DO J=1,TESTPT
```

```
                    CREVVOL = VAR(J)
                    CALL MODEL
                    EXHMOD2(J)=EXHMOD
                    XR2(J) = XR
                    CALL BREAKDOWN
              END DO
       ELSE
       WRITE(*,*) 'ENTER CREVICE VOLUME IN CUBIC CENTIMETERS'
       READ(*,*) (VAR(J),J=1,TESTPT)
       VARNAM1 = 'CREVICE VOLUME (cc)'
       VARNAM2 = 'CREVV'
       ENDIF
ELSEIF (PARA .EQ. 3) THEN
       IF (FLAG .EQ. 1) THEN
             DO J=1,TESTPT
                    TCOOL = VAR(J)
                    CALL MODEL
                    EXHMOD2(J)=EXHMOD
                    XR2(J) = XR
                    CALL BREAKDOWN
             END DO
       ELSE
       WRITE(*,*) 'ENTER COOLANT TEMPERATURE IN KELVIN'
       READ(*,*) (VAR(J),J=1,TESTPT)
       VARNAM1 = 'COOLANT TEMPERATURE (K)'
       VARNAM2 = 'TCOOL'
       ENDIF
ELSEIF (PARA .EQ. 4) THEN
       IF (FLAG .EQ. 1) THEN
             DO J=1,TESTPT
                    EGR = VAR(J)
                    CALL MODEL
                    EXHMOD2(J)=EXHMOD
                    XR2(J) = XR
                    CALL BREAKDOWN
             END DO
       ELSE
       WRITE(*,*) 'ENTER EGR - 0.10 FOR 10% EGR'
       READ(*,*) (VAR(J),J=1,TESTPT)
       VARNAM1 = 'EXHAUST GAS RECIRCULATION'
       VARNAM2 = ' EGR'
       ENDIF
ELSEIF (PARA .EQ. 5) THEN
       IF (FLAG .EQ. 1) THEN
             DO J=1,TESTPT
                    RELSPRKO = VAR(J)
                    CALL MODEL
                    EXHMOD2(J)=EXHMOD
                    XR2(J) = XR
                    CALL BREAKDOWN
             END DO
       ELSE
             WRITE(*,*) 'ENTER RELATIVE SPARK TIMING (SPARK - MBT)'
       WRITE(*,*) 'IN CRANK ANGLE DEGREES'
       READ(*,*) (VAR(J),J=1,TESTPT)
       VARNAM1 = 'SPARK TIMING (SPARK - MBT)'
       VARNAM2 = 'SPARK'
       ENDIF
ELSEIF (PARA .EQ. 6) THEN
       IF (FLAG .EQ. 1) THEN
             DO J=1,TESTPT
                    VO = VAR(J)
                    CALL MODEL
                    EXHMOD2(J)=EXHMOD
```

```
                XR2(J) = XR
                CALL BREAKDOWN
            END DO
      ELSE
      WRITE(*,*) 'ENTER VALVE OVERLAP IN CRANK ANGLE DEGREES'
      WRITE(*,*) 'WITH VALVE EVENTS DEFINED AT 0.15mm LIFT'
      READ(*,*) (VAR(J),J=1,TESTPT)
      VARNAM1 = 'VALVE OVERLAP (CA)'
      VARNAM2 = ' VO'
      ENDIF
ELSEIF (PARA .EQ. 7) THEN
      IF (FLAG .EQ. 1) THEN
            DO J=1,TESTPT
                IVALDIA = VAR(J)
                CALL MODEL
                EXHMOD2(J)=EXHMOD
                XR2(J) = XR
                CALL BREAKDOWN
            END DO
      ELSE
      WRITE(*,*) 'ENTER INLET VALVE DIAMETER IN MILLIMETERS'
      READ(*,*) (VAR(J),J=1,TESTPT)
      VARNAM1 = 'INLET VALVE DIAMETER (mm)'
      VARNAM2 = ' IVD'
      ENDIF
ELSEIF (PARA .EQ. 8) THEN
      IF (FLAG .EQ. 1) THEN
            DO J=1,TESTPT
                EVALDIA = VAR(J)
                CALL MODEL
                EXHMOD2(J)=EXHMOD
                XR2(J) = XR
                CALL BREAKDOWN
            END DO
      ELSE
      WRITE(*,*)'ENTER EXHAUST VALVE DIAMETER IN MILLIMETERS'
      READ(*,*) (VAR(J),J=1,TESTPT)
      VARNAM1 = 'EXHAUST VALVE DIAMETER (mm)'
      VARNAM2 = ' EVD'
      ENDIF
ELSEIF (PARA .EQ. 9) THEN
      IF (FLAG .EQ. 1) THEN
            DO J=1,TESTPT
                IMAXLIF = VAR(J)
                CALL MODEL
                EXHMOD2(J)=EXHMOD
                XR2(J) = XR
                CALL BREAKDOWN
            END DO
      ELSE
         WRITE(*,*)'ENTER INLET VALVE MAXIMUM LIFT IN MILLIMETERS'
      READ(*,*) (VAR(J),J=1,TESTPT)
      VARNAM1 = 'INLET VALVE MAX. LIFT (mm)'
      VARNAM2 = ' IVML'
      ENDIF
ELSEIF (PARA .EQ. 10) THEN
      IF (FLAG .EQ. 1) THEN
            DO J=1,TESTPT
                EMAXLIF = VAR(J)
                CALL MODEL
                EXHMOD2(J)=EXHMOD
                XR2(J) = XR
                CALL BREAKDOWN
            END DO
```

```
            ELSE
           WRITE(*,*) 'ENTER EXHAUST VALVE MAXIMUM LIFT IN MILLIMETERS'
            READ(*,*) (VAR(J),J=1,TESTPT)
            VARNAM1 = 'EXHAUST VALVE MAX. LIFT (mm)'
            VARNAM2 = ' EVML'
            ENDIF
       END IF
       IF (FLAG .EQ. 1) THEN
C
CCCCCCCCCCCCC  INPUT VARIATION OUTPUT  CCCCCCCCCCCCCCCCCCCCCCCCCCCCCC
C
       WRITE(*,1000) CYL,VD,NUMV,RC,B,S,PLUG,CREVVOL,VO,TCOOL,RELSPRKO,
      & EGR*100,IVALDIA,EVALDIA,IMAXLIF,EMAXLIF
       WRITE(*,1390) VARNAM2
       DO J = 1,TESTPT
       WRITE(*,1400) VAR(J),FASBPO(J),FASAPO(J),FASARES(J),FASOUT(J)
      & ,FSBRES(J),FSARES(J),FS(J),POSTOXI(J),XR2(J),EXHMOD2(J)*C6
      & ,UHCI(J)
       END DO
       WRITE(*,3000)
       WRITE(*,1310)
       WRITE(*,1300) VARNAM2,VARNAM1
C
CCCCCCCCCCCCC  WRITE TO OUTPUT FILE OPTION  CCCCCCCCCCCCCCCCCCCCCCCCC
C

       WRITE(*,*) 'DO YOU WANT TO WRITE THE OUTPUT TO A FILE'
       WRITE(*,*) 'TYPE "1" FOR YES OR "2" FOR NO'
       READ(*,*) ANS3
       IF (ANS3 .EQ. 1) THEN
       WRITE(*,*) 'ENTER FILE NAME MAXIMUM OF 8 CHARACTERS'
       READ(*,'(A8)') FILEOUT
       OPEN (UNIT = 8, STATUS = 'UNKNOWN', FILE = FILEOUT)
       WRITE(8,1000) CYL,VD,NUMV,RC,B,S,PLUG,CREVVOL,VO,TCOOL,RELSPRKO,
      & EGR*100,IVALDIA,EVALDIA,IMAXLIF,EMAXLIF
       WRITE(8,1390) VARNAM2
       DO J = 1,TESTPT
       WRITE(8,1400) VAR(J),FASBPO(J),FASAPO(J),FASARES(J),FASOUT(J)
      & ,FSBRES(J),FSARES(J),FS(J),POSTOXI(J),XR2(J),EXHMOD2(J)*C6
      & ,UHCI(J)
       END DO
       WRITE(8,3000)
       WRITE(8,1310)
       WRITE(8,1300) VARNAM2,VARNAM1
       END IF
       GOTO 200
       END IF
       FLAG = 1
       GOTO  100
       END IF
200    CONTINUE

1000     FORMAT ((10X,'*************** ENGINE SET-UP ****************')
      & //(13X,F3.0,' - CYLINDER',5X,F3.1,' LITER')/
      &   (13X,F3.0,' - VALVES PER CYLINDER')/
      &   (14X,'  COMPRESSION RATIO = ',F4.1)/
      &   (14X,'              BORE = ',F4.1,' mm')/
      &   (14X,'            STROKE = ',F4.1,' mm')/
      &   (14X,'  SPARK PLUG OFFSET = ',F4.1,' mm')/
      &   (14X,'     CREVICE VOLUME = ',F5.3,' cc')/
      &   (14X,'      VALVE OVERLAP = ',F4.1,' CA')/
      &   (14X,'COOLANT TEMPERATURE = ',F5.1,' K')/
      &   (14X,'                EGR = ',F4.1,' % ')/
      &   (5X,'SPARK TIMING RELATIVE TO MBT = ',F4.1)/
```

```
     &       (17X,'                    INTAKE VALVE      EXHAUST VALVE ')/
     &       (5X,'INNER SEAT DIAMETER (mm) ',8x,F5.2,13x,F5.2)/
     &       (5X,'       MAXIMUM LIFT (mm) ',8x,F5.2,13X,F5.2)/)

1300      FORMAT(15X,'    ',A5,' -> ',A35)
1310   FORMAT((/,15X,'************** FUEL - AIR SOURCE HC *************')
     &     (/,15X,'    FASBO -> BEFORE IN-CYLINDER OXIDATION')
     &     (/,15X,'    FASAO -> AFTER IN-CYLINDER OXIDATION')
     &     (/,15X,'    FASAR -> AFTER FRACTION RETAINED IN RESIDUAL GAS')
     &     (/,15X,'     FASO -> AFTER EXHAUST OXIDATION (ENGINE-OUT)')
     &     (/,15X,'***************** FUEL SOURCE HC *****************')
     &     (/,15X,'     FSBR -> BEFORE FRACTION RETAINED')
     &     (/,15X,'     FSAR -> AFTER FRACTION RETAINED IN RESIDUAL GAS')
     &     (/,15X,'      FSO -> AFTER EXHAUST OXIDATION (ENGINE-OUT)')
     &     (/,15X,'**************************************************')
     &     (/,15X,'      OXI -> FRACTION OXIDIZED IN THE CYLINDER')
     &     (/,15X,'      RES -> FRACTION RETAINED IN THE CYLINDER')
     &     (/,15X,'     EOXI -> FRACTION OXIDIZED IN THE EXHAUST')
     &     (/,15X,'     UHCI -> TOTAL ENGINE-OUT HC EMISSIONS'))

1390   FORMAT(/(3X,A5,1X,'FASBO',1X,'FASAO',1X,'FASAR',2X)
     & ('FASO',2X,'FSBR',2X,'FSAR',2X,'FSO',4X,'OXI',3X,'RES',2X)
     & ('EOXI',2X,'UHCI'))
1400    FORMAT((1X,F7.3,1X,F5.3,1X,F5.3,1X,F5.3,1X,F5.3,1X,F5.3,1X)
     &   (F5.3,1X,F5.3,1X,F5.3,1X,F5.3,1X,F5.3,1X,F5.3))
1003   FORMAT ((15X,'*********************************************'))
1005   FORMAT ((15X,'*******',32X,'*******'))
1007   FORMAT ((15X,'*******','     HYDROCARBON EMISSIONS',6X,'*******'))
1008   FORMAT ((15X,'*******','        MODEL BREAKDOWN   ',6X,'*******'))
1015   FORMAT ((/,20X,'IN-CYLINDER OXIDATION = ',F5.2,'%')//
     &             (20X,' HYDROCARBON RETAINED = ',F5.2,'%')//
     &             (20X,'    EXHAUST OXIDATION = ',F5.2,'%'))


1020   FORMAT((//18X,'      FUEL-AIR SOURCE             FUEL SOURCE')//
     &(1X,'BEFORE IN-CYLINDER OXID.     ',F5.3,'%',21X,F5.3,'%')/
     &(1X,' AFTER IN-CYLINDER OXID.     ',F5.3,'%',21X,F5.3,'%')/
     &(1X,'          AFTER RESIDUAL    ',F5.3,'%',21X,F5.3,'%')/
     &(1X,'AFTER EXHAUST OXIDATION      ',F5.3,'%',21X,F5.3,'%')//
     &(1X,'TOTAL ENGINE-OUT HYDROCARBON EMISSIONS = ', F5.3,'%')/)
2000    FORMAT((/,10X,'             INPUT WHICH INPUT PARAMETER TO VARY')
     &         (/,10X,'                  CHOICE FROM THE LIST BELOW')
     &     (/,10X,'                   1 - COMPRESSION RATIO')
     &         (/,10X,'                     2 - CREVICE VOLUME')
     &         (/,10X,'                     3 - COOLANT TEMPERATURE')
     &         (/,10X,'                     4 - EXHAUST GAS RECIRCULATION')
     &         (/,10X,'                     5 - SPARK TIMING')
     &         (/,10X,'                     6 - VALVE OVERLAP')
     &         (/,10X,'                     7 - INLET VALVE DIAMETER')
     &         (/,10X,'                     8 - EXHAUST VALVE DIAMETER')
     &         (/,10X,'                     9 - INLET VALVE MAXIMUM LIFT')
     &     (/,10X,'                    10 - EXHAUST VALVE MAXIMUM LIFT',/))

3000   FORMAT(/(' note: HC emissions are expressed as a percentage of')
     &         /('       the mass of fuel per cylinder per cycle'))

      STOP
      END

CCCCCCCCCCCCCCCCCCCCCCCCCCCCCCCCCCCCCCCCCCCCCCCCCCCCCCCCCCCCCCCCCCCCCCCCCC
C
C     SUBROUTINE ---> HYDROCARBON EMISSIONS MODEL
C
CCCCCCCCCCCCCCCCCCCCCCCCCCCCCCCCCCCCCCCCCCCCCCCCCCCCCCCCCCCCCCCCCCCCCCCCCC
```

```
      SUBROUTINE MODEL
      IMPLICIT REAL (A-Z)
      REAL UHCI(50)
      COMMON/GEOM/B,VD,CYL,RC,CREVVOL,PLUG
      COMMON/VALVE/IVALDIA,EVALDIA,IMAXLIF,EMAXLIF,VO,NUMV
      COMMON/OPER/SPEED,TCOOL,EGR,RELSPRKO
      COMMON/MOD/FASMOD,FSMOD,XR,OXIMOD,EXHMOD,UHCI
C
C     THIS MODEL WAS DEVELOPED FOR ONE OPERATION CONDITION
C     IMEP = 380 kPa, and SPEED 1600 rpm
C
      IMEP = 380
      SPEED = 1600
C
CCCCCCCCCCCCCCCCCC NORMALIZED RELATIONSHIPS FOR SPARK ADVANCE CCCCCC
C
C     NORMALIZED RELATIONSHIPS FOR SPARK ADVANCE WERE DEVELOPED USING
C     THE MIT CYCLE SIMULATION. SPARK ADVANCE WAS NORMALIZED TO
C     MBT SPARK TIMING (SPARK - MBT SPARK TIMING).  SPARK LOOPS
C     WERE PERFORMED AT CONSTANT BMEP.  1600 RPM, BMEP = 241 KPA,
C     STOICHIOMETRIC OPERATION.
C
C     PINS = NORMALIZED INLET PRESSURE FOR SPARK ADVANCE
C     MFNS = NORMALIZED MASS OF FUEL PER CYCLE FOR SPARK ADVANCE
C     PMAXNS = NORMALIZED MAX. PRESSURE PER CYCLE FOR SPARK ADVANCE
C     T70NS = NORMALIZED TEMP. AT 70 CA ATC FOR SPARK ADVANCE
C     P70NS = NORMALIZED PRESS. AT 70 CA ATC FOR SPARK ADVANCE
C
      PINS = 1.001552+0.00061*RELSPRKO+0.000241*RELSPRKO**2
      MFNS = 0.9998 + 8.78909e-4*RELSPRKO + 3.14829E-4*RELSPRKO**2
      PMAXNS = 0.992477+0.0207557*RELSPRKO+0.733852E-4*RELSPRKO**2
      T70NS = 1.00118-5.53215E-3*RELSPRKO+8.83453e-5* RELSPRKO**2
      P70NS = 1.00302-4.83915E-3*RELSPRKO+3.5337E-4* RELSPRKO**2
C
CCCCCCCCCCCCCCCCCC NORMALIZED RELATIONSHIPS FOR EGR CCCCCCCCCCCCCCCC
C
C     NORMALIZED RELATIONSHIPS OF EGR WERE DEVELOPED USING THE MIT
C     CYCLE SIMULATION.  THE RELATIONSHIPS WERE NORMALIZED TO ZERO
C     EGR AT MBT SPARK TIMING FOR CONSTANT BMEP SPARK LOOPS
C     1600 RPM, BMEP = 241 KPA, STOICHIOMETRIC OPERATION.
C
C     PINEGR = NORMALIZED INLET PRESSURE FOR EGR
C     T70NEGR = NORMALIZED TEMP. AT 70 CA ATC FOR EGR
C     P70NEGR = NORMALIZED PRESS. AT 70 CA ATC FOR EGR

      PINEGR = 1.6*EGR + 1.00
      T70NEGR = 1.000-EGR*0.57
      P70NEGR = 0.1621*EGR + 1.000

CCCCCCCCCCCCCCCCCC NORMALIZED RELATIONSHIPS FOR COMP. RATIO  CCCCCCC
C
C     NORMALIZED RELATIONSHIPS FOR COMPRESSION RATIO CHANGES WERE
C     DEVELOPED USING THE MIT CYCLE SIMULATION.  THE RELATIONSHIPS
C     WERE NORMALIZED TO A 9.3 COMPRESSION RATIO AT MBT SPARK
C     TIMING FOR CONSTANT BMEP SPARK LOOPS; SPEED = 1600 RPM,
C     BMEP = 241 KPA, STOICHIOMETRIC OPERATION.
C
C     T70NRC = NORMALIZED TEMP. AT 70 CA ATC FOR COMPRESSION RATIO
C     P70NRC = NORMALIZED PRESS. AT 70 CA ATC FOR COMPRESSION RATIO
C     PINRC = NORMALIZED INLET PRESSURE FOR COMPRESSION RATIO
C     MFNRC = NORMALIZED MASS OF FUEL PER CYCLE FOR COMP. RATIO
C     PMAXNRC = NORMALIZED MAXIMUM CYLINDER PRESSURE FOR COMP. RATIO
C
      T70NRC = -0.02073*(RC-9.3)+1.00
```

```
      P70NRC = -0.02362*(RC-9.3)+1.00
      PINRC = -0.02589*(RC-9.3)+1.00
      MFNRC = -0.02481*(RC-9.3)+1.00
      PMAXNRC = 0.11547*(RC-9.3)+1.00

CCCCCCCCCCCCCCCCCCC NORMALIZED RELATIONSHIPS FOR COMP. RATIO  CCCCCCC
C
C     NORMALIZED RELATIONSHIPS FOR COOLANT TEMPERATURE CHANGES WERE
C     DEVELOPED USING THE MIT CYCLE SIMULATION.  THE RELATIONSHIPS
C     WERE NORMALIZED TO A COOLANT TEMPERATURE OF 365 K AT MBT SPARK
C     TIMING FOR CONSTANT BMEP SPARK LOOPS; SPEED = 1600 RPM,
C     BMEP = 241 KPA, STOICHIOMETRIC OPERATION.
C
C     T70NTCOOL = NORMALIZED TEMP. AT 70 CA ATC FOR COOLANT TEMP.
C     P70NTCOOL = NORMALIZED PRESS. AT 70 CA ATC FOR COOLANT TEMP.
C     PINTCOOL = NORMALIZED INLET PRESSURE FOR COOLANT TEMP.
C     MFNTCOOL = NORMALIZED MASS OF FUEL PER CYCLE FOR COOLANT TEMP.
C
      T70NTCOOL = 0.000276*(TCOOL-365)+ 1.00
      P70NTCOOL = 0.000101*(TCOOL-365)+1.00
      PINTCOOL = 0.000183*(TCOOL-365)+1.00
      MFNTCOOL = -0.00014*(TCOOL-365)+1.00

CCCCCCCCCCCCCCCCCCC FUNCTIONS OF IMEP CCCCCCCCCCCCCCCCCCCCCCCCCCCCCCC
C
C     THESE RELATIONSHIPS WERE DEVELOPED USING THE MIT CYCLE
C     SIMULATION.  CONSTANT BMEP (IMEP GROSS) SPARK LOOPS WERE
PERFORMED.
C     MBT SPARK TIMING WAS DETERMINED FOR EACH LOAD AND FITTED.
C     THESE MODELS ARE MULTIPLIED BY THE CORRESPONDING NORMALIZED
C     MODELS TO ADJUST FOR SPARK ADVANCE FROM MBT TIMING AND EGR
C     OPERATING CONDITIONS
C
C     PIOVPE = PI/PE AS A FUNCTION OF IMEP USED IN RESIDUAL MODEL
C     PE_PI = PE-PI AS A FUNCTION OF IMEP USED IN RESIDUAL MODEL
C     PMAX = MAXIMUM PRESSURE AS A FUNCTION OF IMEP
C     T70 = TEMPERATURE AT 70 CA ATC AS A FUNCTION OF IMEP
C     P70 = PRESSURE AT 70 CA ATC AS A FUNCTION OF IMEP
C
      PIOVPE=(0.098745 + 0.000986*IMEP)*PINS*PINEGR*PINRC*PINTCOOL
      PE_PI = 1-PIOVPE
      PMAX=(0.05677*IMEP+1.2276)*PMAXNS*PMAXNRC
      T70=(1599.362+0.758767*IMEP-0.00051*IMEP**2)*T70NS*
     &     T70NEGR*T70NRC*T70NTCOOL
      P70=(0.20933 +0.010186*IMEP)*P70NS*P70NEGR*P70NRC*P70NTCOOL
      MF=MFNRC*MFNTCOOL*MFNS
C
CCCCCCCCCCCCCCCCCCC RESIDUAL GAS MODEL   CCCCCCCCCCCCCCCCCCCCCCCCCCCCC
C
C     J.W. FOX RESIDUAL GAS MODEL (SAE 931025)
C
C     TRE RESIDUAL GAS MODEL USED WAS SET FOR STOICHIOMETRIC
C     OPERATION WITH INLET AND EXHAUST PRESSURE RELATIONSHIPS
C     MODELED AS FUNCTIONS OF IMEP,EGR, AND SPARK TIMING.
C
C     PHI = FUEL-AIR EQUIVALANCE RATIO
C     LVMAX = AVERAGE INTAKE AND EXHAUST VALVE MAXIMUM LIFT
C     DV = AVERAGE INTAKE AND EXHAUST VALVE INNER SEAT DIAMETER
C     OF = OVERLAP FACTOR
C     XR = RESIDUAL GAS FRACTION
C
      PHI=1.0
      LVMAX = (IMAXLIF+EMAXLIF)/2
      DV = (IVALDIA+EVALDIA)/2
```

```
      OF=NUMV/2.*(1.45/B*(107+7.8*VO+VO*VO)*(LVMAX*DV)/(B*B))
      XR=1.266*OF/(SPEED/60)*(PIOVPE**(-0.87))*PE_PI**0.5+0.632*PHI
     &    *(PIOVPE**(-0.74))/RC
C
CCCCCCCCCCCCCCCCCC FUEL-AIR SOURCE MODEL CCCCCCCCCCCCCCCCCCCCCCCCCCCC
C
C     FPLUG = NORMALIZED RELATIONSHIP FOR SPARK PLUG LOCATION
C     VD = DISPLACEMENT VOLUME (liters)
C     CYL = NUMBER OF CYLINDERS
C     VDC = DISPLACEMENT VOLUME PER CYLINDER (liters)
C     FASCON = FUEL-AIR SOURCE CONSTANT
C     FASMOD = TOTAL FUEL-AIR SOURCE MODEL
C     PMAX = MAXIMUM CYLINDER PRESSURE MODELED AS A FUNCTION OF IMEP
C     CREVVOL = CREVICE VOLUME (cc)
C     FPLUG = SPARK PLUG OFFSET FROM BORE CENTER (mm)
C
      FA=0.0685
      FPLUG=-0.429*(2*PLUG/B)+1.0
      VDC=VD/CYL
       FASMOD = 5442.8*(PMAX/IMEP)*CREVVOL/(VDC*TCOOL)*(1-XR-egr)*FPLUG
     &  *1/(1+1/FA)/MF
C
CCCCCCCCCCCCCCCCCC FUEL SOURCE MODEL CCCCCCCCCCCCCCCCCCCCCCCCCCCCCCCC
C
C     FA = FUEL-TO-AIR RATIO - STOICHIOMETRIC
C     B = ENGINE BORE (mm)
C     RC = COMPRESSION RATIO
C     TCOOL = COOLANT TEMPERATURE (Kelvin)
C
      FSMOD = 888579*FA*PIOVPE*(1+RC**1.3)/(IMEP*10**(0.0082*TCOOL)
     &  *B*MF)
C
C
CCCCCCCCCCCCCCCCCC IN-CYLINDER OXIDATION CCCCCCCCCCCCCCCCCCCCCCCCCCCC
C
C     TAVE = AVERAGE TEMPERATURE OF TEMP AT 70 CA ATC AND COOLANT TEMP.
C     TTHRES = THRESHOLD TEMPERATURE - FIXED AT 980 K
C     PTHRES = THRESHOLD PRESSURE
C     OXIMOD = FUEL-AIR SOURCE IN-CYLINDER OXIDATION MODEL
C
      TAVE=(T70-TCOOL)/(LOG(T70/TCOOL))
      TTHRES=980.
      PTHRES = P70*(TTHRES/TAVE)**3.0
      OXIMOD = (1-PTHRES/PMAX)
C
C
CCCCCCCCCCCCCCCCCC EXHAUST PORT OXIDATION CCCCCCCCCCCCCCCCCCCCCCCCCCCC
C
C     EXHAUST PORT OXIDATION MODEL WAS DEVELOPED BY REGRESSING
C     AGAINST EXHAUST PORT OXIDATION DATA FROM DROBOT.
C
C     EGRSP = ADJUSTED SPARK TIMING FOR EGR OPERATING CONDITIONS
C

      IF (EGR .NE. 0) THEN
            EGRSP = EGR*82.9012
            EGRN = SPEED*EGR
      ELSE
            SPEED = 1600.
            EGRSP = 0.0
      END IF
C
CCCCCC   SPEED AND SPARK ADJUSTMENTS FOR COMPRESSION RATIO CHANGES CC
C
```

```
      RCSP = 3.323*(RC-9.0)
      RCN = SPEED*(-0.0245*(RC-9.0))
C
C
CCCCCC   CONSTANTS FROM EXHAUST PORT OXIDATION DATA REGRESSION
C
      CS = -0.000148
      CI = -0.000699
      CSP = -0.007908
      CTC = 2.55E-5
      INTER = 0.866143
C
CCCCCC      EXHAUST PORT OXIDATION MODEL     CCCCCC
C
      EXHMOD=CS*(SPEED+RCN+EGRN)+CI*IMEP+CSP*(RELSPRKO+EGRSP+RCSP)+
     &  CTC*TCOOL+INTER
C
CCCCCCCCCCCCCCCCCCCCCCCCCCCCCCCCCCCCCCCCCCCCCCCCCCCCCCCCCCCCCCCCCCCCCCCCCC
      RETURN
      END
CCCCCCCCCCCCCCCCCCCCCCCCCCCCCCCCCCCCCCCCCCCCCCCCCCCCCCCCCCCCCCCCCCCCCCCCCC
C
      SUBROUTINE BREAKDOWN
C
CCCCCCCCCCCCCCCCCCCCCCCCCCCCCCCCCCCCCCCCCCCCCCCCCCCCCCCCCCCCCCCCCCCCCCCCCC
C
C     THIS SECTION BREAKS DOWN THE MODEL INTO THE INDIVIDUAL
C     HYDROCARBON MECHANISMS.
C
CCCCCCCCCCCCCCCCCCCCCCCCCCCCCCCCCCCCCCCCCCCCCCCCCCCCCCCCCCCCCCCCCCCCCCCCCC
C
      IMPLICIT REAL (A-Z)
      REAL VAR(50),POSTOXI(50),XR2(50),EXHMOD2(50),FASBPO(50)
     & ,FSBRES(50),FASAPO(50),FASARES(50),FSARES(50),FASOUT(50)
     & ,FS(50),UHCI(50),FAS(50)
      INTEGER J
      COMMON/MOD2/XR2,EXHMOD2
      COMMON/MOD/FASMOD,FSMOD,XR,OXIMOD,EXHMOD,UHCI
      COMMON/CON/C1,C2,C3,C5,C6,C7
      COMMON/BREAK/FAS,FASOXI,FASOUT,FASAPO,FASARES,FASBPO,POSTOXI,
     &    FS,FSARES,FSBRES,J

CCCCCCCCCCCCCCCCCCCCCCCCCCCCCCCCCCCCCCCCCCCCCCCCCCCCCCCCCCCCCCCCCCCCCCCCCC
C
C     FUEL AND AIR SOURCE HC MECHANISM BREAKDOWN
C
CCCCCCCCCCCCCCCCCCCCCCCCCCCCCCCCCCCCCCCCCCCCCCCCCCCCCCCCCCCCCCCCCCCCCCCCCC
C
C     FAS(J) = HC STORED IN FUEL-AIR SOURCE
C     FASOXI(J) = AMOUNT OF FUEL-AIR SOURCE HC OXIDATION
C     FASOUT(J) = ENGINE-OUT FUEL-AIR SOURCE
C     FASBPO(J) = FUEL-AIR SOURCE HC REMAINING BEFORE IN-CYL OXIDAITON
C     FASAPO(J) = FUEL-AIR SOURCE HC REMAINING AFTER IN-CYL OXIDAITON
C     FASARES(J) = FUEL-AIR SOURCE HC REMAINING AFTER FRACTION RETAINED
C     POSTOXI(J) = FUEL-AIR SOURCE FRACTION OXIDIZED
C     CONSTANT = DUMMY VARIABLE USED TO AID IN COMPUTING
C
      CONSTANT = (1-XR2(J))*(1-C6*EXHMOD2(J))
      FAS(J)=C1*C5*FASMOD*CONSTANT*100
      FASOXI=-C2*C5*C7*FASMOD*OXIMOD*CONSTANT*100
      FASOUT(J)=FAS(J)+FASOXI
      FASAPO(J)=FASOUT(J)/CONSTANT
      FASARES(J)=FASOUT(J)/(1-C6*EXHMOD2(J))
      FASBPO(J)=FAS(J)/CONSTANT
```

```
      POSTOXI(J)=-FASOXI/FAS(J)
CCCCCCCCCCCCCCCCCCCCCCCCCCCCCCCCCCCCCCCCCCCCCCCCCCCCCCCCCCCCCCCCCCCCCCCCCC
C
C     FUEL SOURCE HC MECHANISM BREAKDOWN
C
CCCCCCCCCCCCCCCCCCCCCCCCCCCCCCCCCCCCCCCCCCCCCCCCCCCCCCCCCCCCCCCCCCCCCCCCCC
C
C     FS(J) = FUEL SOURCE ENGINE-OUT HC EMISSIONS
C     FSARES(J) = FUEL SOURCE HC AFTER FRACTION RETAINED IN RESIDUAL
C     FSBRES(J) = FUEL SOURCE HC BEFORE FRACTION RETAINED IN RESIDUAL
C     UHCI(J) = TOTAL ENGINE-OUT HC EMISSIONS
C
      FS(J)=C3*FSMOD*CONSTANT*100
      FSARES(J)=FS(J)/(1-C6*EXHMOD2(J))
      FSBRES(J)=FS(J)/CONSTANT
      UHCI(J) = FAS(J) + FASOXI + FS(J)
      RETURN
      end
```